

DOCTORAL THESIS

**Multimethod identification of “universal” patterns in biological, metallic, and ceramic materials: Chemical composition, elasticity, and hardness.**

submitted in satisfaction of the requirements for the degree of  
Doctor of Science  
of the TU Wien, Faculty of Civil Engineering

---

DISSERTATION

**Kombination vielfältiger experimenteller Methoden zwecks Identifikation „universellen” Mustern in biologischen, metallischen und keramischen Materialien: Chemische Zusammensetzung, Elastizität und Härte.**

ausgeführt zum Zwecke der Erlangung des akademischen Grades eines  
Doktors der technischen Wissenschaften  
eingereicht an der Technischen Universität Wien, Fakultät für  
Bauingenieurwesen

von

**Dipl.-Ing. Luis Zelaya-Lainez, MSc.**  
Matrikelnummer: 1328369

- Betreuer: Univ.Prof. Dipl.-Ing. Dr.Techn. **Christian Hellmich**  
Ko-Betreuer: Associate Prof. Dipl.-Ing. Dr.Techn. **Stefan Scheiner**  
Ko-Betreuer: Associate Prof. Dipl.-Ing. Dr.Techn. **Josef Füssl**  
Institut für Mechanik der Werkstoffe und Strukturen  
Technische Universität Wien  
Karlsplatz 13/202, A-1040 Wien, Österreich
- Gutachter: Univ. Prof. Dr. **Heinz Redl**  
Ludwig Boltzmann Institut für experimentelle und klinische Traumatologie  
AUVA Forschungszentrum  
Donauerschlingengasse 13, A-1200 Wien, Österreich
- Gutachter: Prof. Dr. **Kalpana S. Katti**  
Department of Civil and Environmental Engineering  
North Dakota State University  
1410 North 14th Avenue, ND-58102 Fargo, Vereinigte Staaten von Amerika

Wien, im Jänner 2021

---

# Abstract

The study of structure-property relations is a universal theme in contemporary materials science, providing an ever-growing stage for interdisciplinary research endeavors of engineers, physicists, chemist, and biologists. The challenge, however, lies in identifying the right levels throughout the pronounced hierarchical organizations of many biological and man-made materials, which are governing their various physical, and particular so, mechanical properties.

This requires a well-balanced blend of experimental methods set in a clear theoretical understanding; and the current thesis significantly extends the state-of-the-art exploitation of such methods, namely nanoindentation, ultrasonic testing, scanning probe microscopy, scanning electron microscopy, light microscopy, computed tomography, Mercury intrusion porosimetry, mass spectroscopy, dehydration and demineralization testing, and weighing in combination with Archimedes' principle.

It does so in two complementing ways: On the one hand (see Chapters 3 to 5), well-accepted structure-function relations are investigated up to a new level of completeness and through the addition of unusual perspectives. This essentially concerns structural entities which have not yet been at the focus of respective studies, such as micro cracks which significantly modulate elastic properties in seemingly perfectly plastic materials such as steel for railway engineering, or the multi- rather than uni-scale nature of the porosities found in a variety of different fired clay bricks. In the same sense, while bone mineral (an impure form of hydroxyapatite) and type I collagen have been known for some time to drive the extracellular matrix's elastic and hardness/strength properties, the very composition patterns which hydroxyapatite and collagen build up across tissues of the same organ, but different species, has hardly been investigated systematically. The somewhat surprising result obtained in the present thesis is that variations in mineral and collagen content of femoral tissues of different species are (much) less pronounced than such variations between different organs of the same organism (say femoral and vertebral tissues). Such virtual invariances become particularly stable in genetically more relative vertebrates, such as mammals.

On the other hand, the thesis provides, in its "main" chapter, labeled with 2, a basic framework for structure-property relations in a material class, which as compared to bone, steel, or brick, has remained almost untouched: namely jaw tissues harvested from different bristle worm (*Polychaeta*) species. For the first time ever, elasticity, hardness, and chemical characteristics of the extraskelton of *Platynereis dumerilii* have been tested. The again surprising results show a picture which is distinctively different from that known with bone, fired clay, or steel; namely one where, in an unexpected fashion, features of very distinct metallic and biological materials are combined. In more detail, a new level of nanoindentation miniaturization provided access to a hardness scaling law similar to those known for crystalline metals, with even similar strength and elasticity. However, in contrast to metals, the ion-spiked structure proteins making up *Polychaeta* jaws are produced at room temperature, thanks to an unsurpassed, super-precise

3D printing-type device in the form of particularly committed biological cells. The latter may inspire unprecedented technological progress in the 3D printing field.

These results are framed by a general introduction to hierarchical structures in materials (in Chapter 1), and rich perspectives for future research and development (see Chapter 6).

# Kurzfassung

Das Studium von Struktur-Eigenschafts-Beziehungen, einem allgegenwärtigen Thema in den modernen Materialwissenschaften, bietet eine stetig wachsende Bühne für interdisziplinäre Forschungsanstrengungen an den Schnittstellen von Ingenieurwissenschaft, Physik, Chemie und Biologie. Die Herausforderung dabei liegt auf der Identifikation der richtigen Ebenen innerhalb der hierarchischen Organisation vieler biologischer und menschengemachter Materialien, welche deren physikalische und vor allem mechanische Eigenschaften steuern.

Dies erfordert eine gut ausbalancierte Mischung experimenteller Methoden, basierend auf einem klaren theoretischen Verständnis; und die vorliegende Dissertation erweitert ganz wesentlich den Stand der Technik betreffend der Nutzung solcher Methoden, nämlich folgender: Nanoindentierung, Ultraschallversuche, Rastersondenmikroskopie, Rasterelektronenmikroskopie, Lichtmikroskopie, Computertomographie, Quecksilber-Intrusionsporosimetrie, Massenspektrometrie, Dehydratations- und Demineralisierungsversuche, sowie Wiegeversuche in Verbindung mit dem archimedischen Prinzip.

Dies passiert auf zwei, sich gegenseitig ergänzende Arten: Einerseits, und zwar in den Kapiteln 3 bis 6, werden wohlbekannte Struktur-Eigenschafts-Beziehungen in bisher unerreichter Vollständigkeit bzw. aus ungewöhnlichen Perspektiven untersucht. Das betrifft im Wesentlichen Strukturelemente, welche typischerweise nicht Teil einschlägiger Studien sind, nämlich Mikrorisse, welche die elastischen Eigenschaften in scheinbar perfekt plastischen Werkstoffen wie Schienenstahl modulieren; oder die mehrskalige Natur von Porenräumen in gebranntem Ton unterschiedlicher Provenienz. Im selben Sinne ist es wohlbekannt, dass das Knochenmineral (eine unreine Form von Hydroxyapatit) und Typ1-Kollagen die Härte- und Elastizitätseigenschaften der extrazellulären Knochenmatrix steuern, während die Dosierung dieser elementaren Bausteine im selben Organ unterschiedlicher Wirbeltierarten kaum einer systematischen Untersuchung unterzogen wurde. Dazu wird in der vorliegenden Dissertation ein durchaus überraschendes Ergebnis vorgelegt: Variationen im Mineral- und Kollagengehalt von Oberschenkelknochen verschiedener Wirbeltierarten sind (wesentlich) kleiner als solche zwischen verschiedenen Organen desselben Organismus (z.B. solche zwischen Oberschenkel- und Wirbelknochen). Solche praktisch invarianten Zusammensetzungsverhältnisse sind besonders stabil innerhalb genetisch näher verwandter Wirbeltiere, wie der Säugetiere.

Andererseits wird im „Hauptkapitel“, dem Kapitel 2 der Dissertation, ein fundamentaler Rahmen für Struktur-Eigenschaftsbeziehungen einer im Vergleich zu Knochen, gebranntem Ton oder Stahl bislang nahezu unerforschten Materialklasse vorgestellt: Exoskelett-Material, aus welchem die Kiefer verschiedener Borstenwurmarten bestehen. Dazu wurden, zum allerersten Mal überhaupt, die chemischen, elastischen und Härte-Eigenschaften des Kiefermaterials von *Platynereis dumerilii* untersucht. Die zugehörigen Ergebnisse zeigen ein überraschendes Bild, wo - ganz im Gegensatz zur Situation bei Knochen, Stahl oder gebranntem Ton - Merkmale biologischer und metallischer Materialien miteinander verbunden werden. Namentlich fördert eine Miniatur-Version von Nanoindentierungsversuchen ein Härte-Skalierungsgesetz zu Tage,

wie es bisher nur von kristallinen Metallen bekannt war, sogar mit ähnlichen Elastizitäts- und Festigkeitseigenschaften. Allerdings werden die die Polychaeta-Kiefer aufbauenden, mit Ionen angereicherten Strukturproteine, im Gegensatz zu Metallen, energieeffizient bei Raumtemperatur im Rahmen eines äußerst präzisen biologischen 3D-Druckverfahrens hergestellt. Letzteres könnte neue technologische Entwicklungen inspirieren.

Diese Ergebnisse werden von einer Einleitung betreffend hierarchische strukturierte Materialien (Kapitel 1) und einen Ausblick auf weiterführende Forschungs- und Entwicklungsschritte eingerahmt.

# Acknowledgments

This work could have been never accomplished without the help and contribution from many people who I meet along my stay at the Institute for Mechanics of Materials and Structures.

First, I would like to express my sincere gratitude to my adviser and supervisor, Prof. Christian Hellmich, for all his guidance, trust, and continuous support through all of these years working together. The great vision, knowledge, and creativity of Prof. Hellmich have been a source of inspiration not only for this work, but for my professional and personal life.

I would like to thank my examiners Prof. Heinz Redl and Prof. Kalpana Katti for taking time in their busy agenda.

I would also like to thank Prof. Stefan Scheiner, Prof. Josef Füssl, and Prof. Bernhard Pichler for all of your guidance during my research, and more importantly, the amazing talks we had together.

I would like to thank my office neighbor and research colleague Dr. Giuseppe Balduzzi for all the good times and amazing discussions.

I would like to thank Martina Pöll, Gabriele Ostrowski, and Astrid Schuh for all the administrative assistance you have given to me.

I would also like to thank all of my colleagues at the Institute for Mechanics of Materials and Structures for the help given, the discussions, and the best working environment I could ever wish for.

In addition, I would like to thank my family for giving me so much emotional support.

Finally, I would like to specially praise all the love and help given to me by my wife, Dr. Michaela Fraubaum. You have always encourage me to achieve every goal, or crazy idea, I set my mind on. You have been my rock, you have been my star, you have been my everything for all of these years. This work is for you.

# Contents

<b>1</b>	<b>Introduction</b>	<b>10</b>
1.1	Biological materials . . . . .	10
1.1.1	Bristle worms . . . . .	10
1.1.2	Halogen and metallic elements present at macromolecules . . . . .	16
1.1.3	Bones . . . . .	18
1.2	Man-made materials . . . . .	23
1.3	Outline of the thesis . . . . .	24
1.4	Contribution of the author . . . . .	25
<b>2</b>	<b>Metal-type hardness properties in jaws of <i>Platynereis dumerilii</i></b>	<b>27</b>
2.1	Introduction . . . . .	28
2.2	Materials and methods . . . . .	31
2.2.1	Sample selection and preparation . . . . .	31
2.2.2	Nanoindentation of <i>Platynereis dumerilii</i> jaw . . . . .	33
2.2.3	Chemical analysis of <i>Platynereis dumerilii</i> jaw . . . . .	33
2.2.4	Size effect-related re-evaluation of nanoindentation tests on jaws of <i>Nereis</i> and <i>Glycera</i> . . . . .	37
2.3	Results . . . . .	37
2.3.1	Mechanical and chemical property distributions in <i>Platynereis dumerilii</i> jaw . . . . .	37
2.3.2	Trans-species size effect law for hardness of jaws across different <i>Polychaeta</i> . . . . .	40
2.4	Discussion . . . . .	43
<b>3</b>	<b>“Variances” and “invariances” in porosity and composition in various femoral tissues</b>	<b>45</b>
3.1	Introduction . . . . .	46
3.2	Materials and Methods . . . . .	47
3.2.1	Sample Extraction . . . . .	47
3.2.2	Sample polishing and imaging by light microscopy - vascular and lacunar porosities . . . . .	49
3.2.3	Dehydration and re-hydration tests - partition of water between vascular, lacunar and extracellular pore spaces . . . . .	50
3.2.4	Demineralization tests - mineral, organic, and water concentrations within the extracellular matrix . . . . .	52
3.3	Results . . . . .	53
3.3.1	Vascular and lacunar porosities from light microscopy . . . . .	53
3.3.2	Dehydration and re-hydration kinetics - water partition between different pore spaces . . . . .	58

3.3.3	Composition of extracellular bone matrix - in terms of mineral and organic volume fractions . . . . .	62
3.4	Discussion . . . . .	67
3.4.1	“Invariant” chemical composition of extracellular bone matrix . . . . .	67
3.4.2	Intraspecies and inter-species variations in lacunar and vascular porosities . . . . .	68
3.4.3	Ultrastructural features of bone: crystals and intercrystalline porosity . . . . .	69
3.4.4	“Universal patterns” in the context biology, philosophy of science, and biomedical engineering . . . . .	70
3.5	Appendix . . . . .	72
<b>4</b>	<b>Multiscale elasticity of grooved rail steel</b>	<b>85</b>
4.1	Introduction . . . . .	86
4.2	Materials and Methods . . . . .	87
4.2.1	Sample selection and preparation . . . . .	87
4.2.2	Nanoindentation testing . . . . .	88
4.2.3	Ultrasonic testing . . . . .	91
4.2.4	Microscopic evaluation of sample surfaces . . . . .	92
4.2.5	Micromechanical modeling . . . . .	92
4.3	Results . . . . .	94
4.3.1	Nanoindentation results: topology, elasticity, hardness . . . . .	94
4.3.2	Young’s modulus distributions obtained from ultrasonic testing . . . . .	99
4.3.3	Crack density of steel obtained from micromechanics and validated by microscopy . . . . .	99
4.4	Discussion . . . . .	101
4.4.1	Chemical versus mechanical material phases . . . . .	101
4.4.2	Multitechnique investigations and reasons for stiffness outliers . . . . .	103
4.5	Conclusions . . . . .	106
4.6	Appendix . . . . .	107
4.6.1	Concept of statistical nanoindentation . . . . .	107
<b>5</b>	<b>Pore spaces of fired bricks used across the European industry</b>	<b>108</b>
5.1	Introduction . . . . .	109
5.2	Investigated materials, particle size analysis, X-ray fluorescence spectroscopy and powder X-ray diffraction . . . . .	110
5.3	Methods . . . . .	111
5.3.1	Mercury intrusion porosimetry . . . . .	111
5.3.2	Archimedes’ principle . . . . .	111
5.3.3	Helium pycnometry . . . . .	112
5.3.4	Micro-CT scanning . . . . .	112
5.3.5	Scanning electron microscopy . . . . .	114
5.4	Results . . . . .	115
5.4.1	Particle size distribution, XRF and PXRD analysis . . . . .	115
5.4.2	Total porosity distribution over sample thicknesses . . . . .	117
5.4.3	Porosity and true density measurements . . . . .	119
5.4.4	3D structure of coarse pores . . . . .	121
5.4.5	Pore size distributions determined by three independent methods . . . . .	122



---

5.5	Discussion . . . . .	129
5.5.1	Evolution of mineralogy during firing . . . . .	129
5.5.2	Investigation methods for porous space . . . . .	130
5.5.3	Comparison of fired bricks . . . . .	131
5.5.4	True density measurements . . . . .	133
5.6	Conclusion . . . . .	133
<b>6</b>	<b>Conclusions and outlook</b>	<b>135</b>
<b>7</b>	<b>Curriculum Vitae</b>	<b>163</b>

# Chapter 1

## Introduction

---

### 1.1 Biological materials

Through biomimetics, biological systems have served humanity as an inspiration source due to their unparalleled effectiveness [295]. The composition of biological materials such as bone, teeth, and sea shells have been studied for decades. These natural structures show surprisingly comparable or improved mechanical properties as to the man-made counterparts [200]. The organic macro-molecules which build these biological systems are primarily assembled from common elements such as carbon, hydrogen, nitrogen, and oxygen. However, the mechanical properties of these organic macro-molecules are commonly “poor” whenever they are isolated [55, 164]. Thus, most biological materials are composed not only of an organic part, but also an inorganic part, and these are assembled in hierarchical and complex structures [70].

#### 1.1.1 Bristle worms

*Polychaeta*, also known as bristle worms, are marine organisms living in pelagic habitats. *Platynereis Dumerilii* is a type of *Polychaeta* and part of the annelid phylum [245]. Since 1953, *Platynereis Dumerilii* has been considered a model organism for developmental research due to regular and controlled reproduction at a laboratory [97, 98]. *Platynereis Dumerilii* develops epidermal extracellular structures better known as *chaetae*. The *chaetae* formation model was first coined by [33] as chaetogenesis and describes how chaetoblast, a specialized follicular cell, forms an assembly of microvilli. These particular microvilli allow the growth by basal apposition of new chaetal material on its surface [219, 297]. Although the process of new chaetal material deposition remains largely unclear, it is known that there is no vesicular transport in between the microvilli and the chaetoblast. Therefore, new chaetal material should be formed by an ectodermal sac called chaetal follicle, which is formed by the chaetoblast and other few follicle cells [277, 305, 306]. The beforementioned apposition of chaetal material reminds of the emerging technology of 3D printing. Thus, it can be considered a “biological 3D printing process”. Moreover, compared with the current status of man-made 3D printing techniques, the *Platynereis Dumerilii* can 3D print complex and precise structures in a remarkable fast manner.

*Chaetae* are composed of beta-chitin and are extremely well-tailored beam-like structures that exhibit different morphologies [126]. According to [97], *chaetae* first appears after approximately

2 days of development, also called the late trochophore development stage. Nevertheless, trochophore stage individuals swim exclusively by means of multiciliated equatorial prototroch cells. Approximately 3 days after egg fertilization, also known as the nectochaetae development stage, as seen in Figure 1.1, parapodia aid larvae with mobilization. Until the nectochaetae stage, larvae have not developed the ability of ingesting food and use sacs for nutrition.

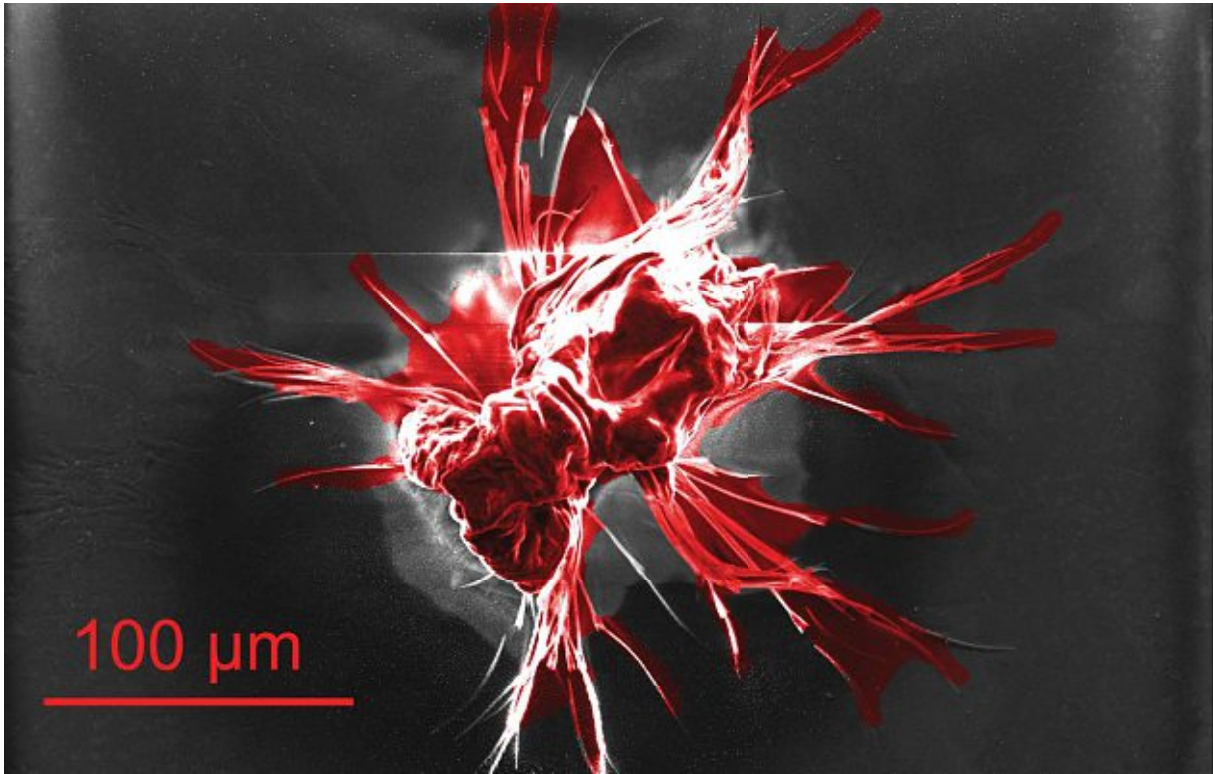


**Fig. 1.1:** Microcomputed tomography image of a *Platynereis Dumerilii* specimen at nectochaetae stage.

To understand better the external morphology of *chaetae*, adult and larvae *chaetae* were harvested and investigated by means of imaging techniques such as light microscopy and field emission gun scanning electron microscopy. Interestingly, four different types of *chaetae* were observed. This information has not been published before.

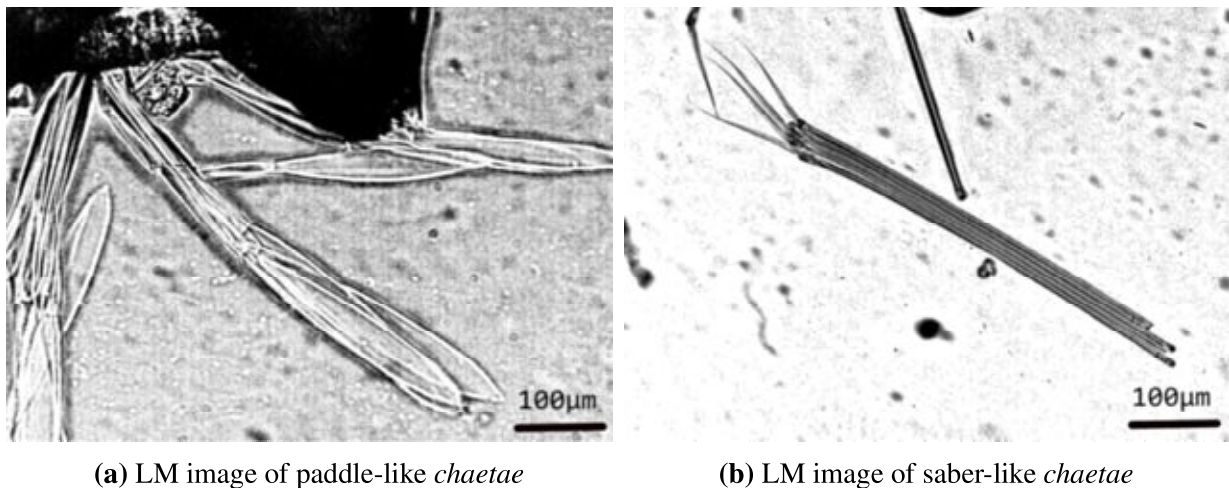
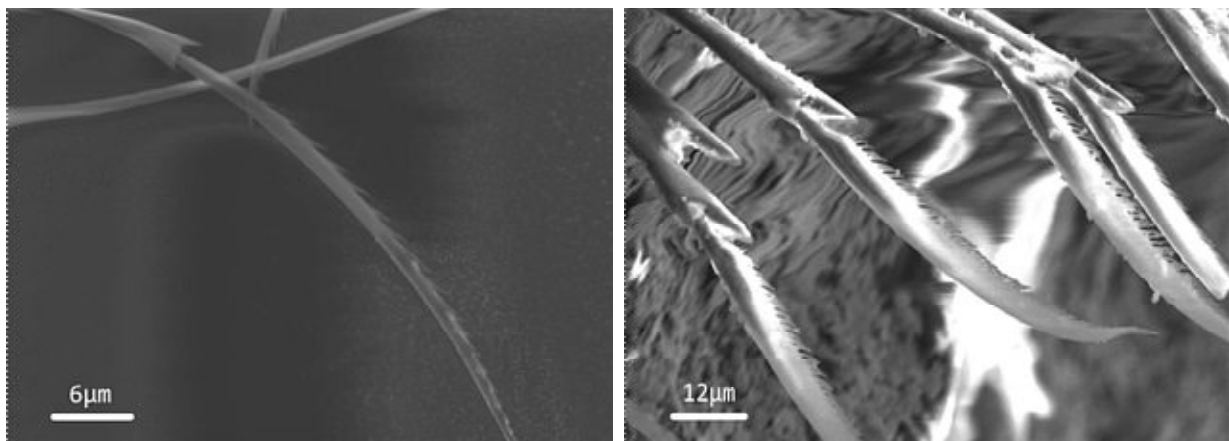


**Fig. 1.2:** Light microscopy (LM) images of different *chaetae* morphologies from an adult female *Platynereis Dumerilii* specimen.



**(a)** FEGSEM image of saber-like *chaetae* from a larva specimen of *Platynereis Dumerilii* **(b)** FEGSEM image of comb-like *chaetae* from a female adult specimen of *Platynereis Dumerilii*

**Fig. 1.3:** Types of *chaetae* observed through Field Emission Gun Scanning Electron Microscopy (FEGSEM) images of *Platynereis Dumerilii* specimen.

Additionally, internal morphology was investigated by means of state-of-the-art synchrotron based micro-computed tomography and x-ray phase contrast imaging (PCI) methods. The before-mentioned protocol was performed at the European Synchrotron Radiation Facility (ESRF). Synchrotron based micro computed tomography is a valuable new non-destructive tool and capable of imaging soft biological specimens [38]. This method was able to achieve resolutions of  $0.7 \mu\text{m}$ . The interaction in between x-rays from the radiation source and electrons of the *Platynereis Dumerilii* produces low-energy excitation of the system, resulting in different forms of x-ray scattering traveling to the detector, as seen in Fig.1.4. Phase contrast imaging techniques establish distributions of the scattering through the registration of the attenuation and the phase changes of the transmitted x-ray beam [52].

Chapter 2 explores further through light microscopy, micro-computed tomography, and nano-indentation techniques another interesting part of the *Platynereis Dumerilii*, the jaw. The jaws, as

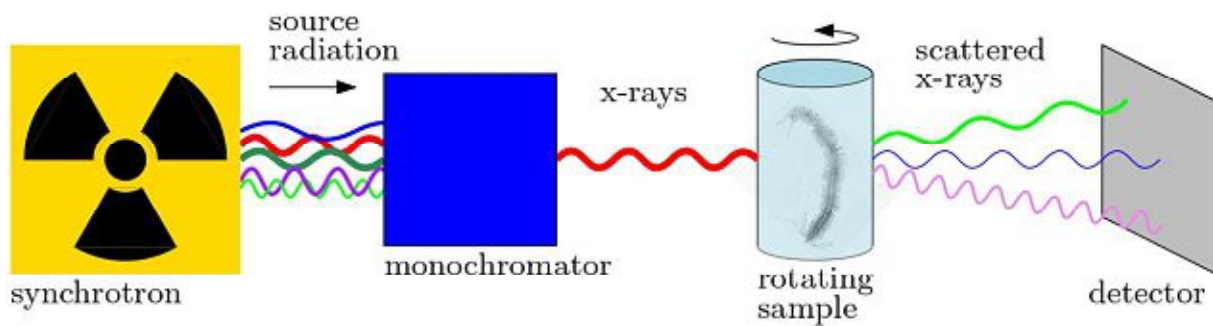


**Fig. 1.4:** Synchrotron based micro-computed tomography setup diagram.

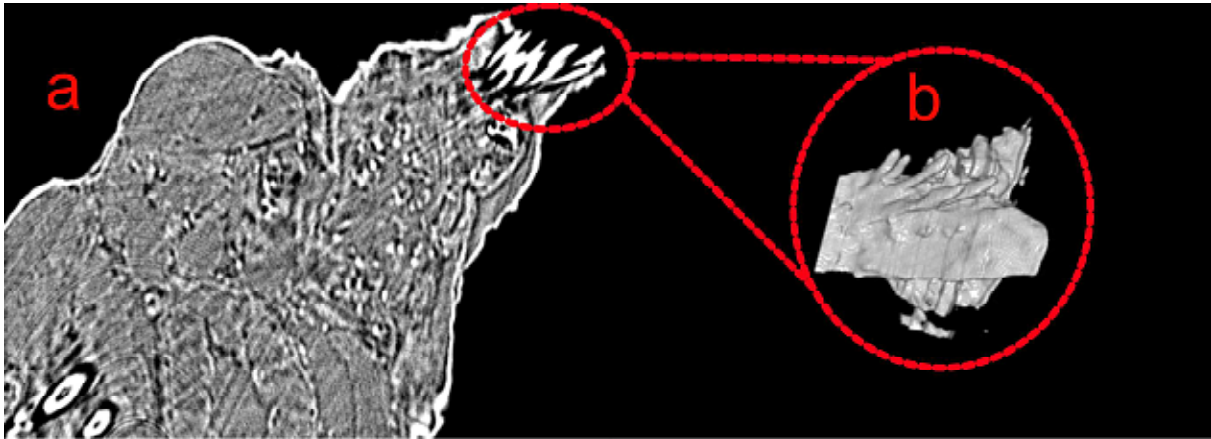


**Fig. 1.5:** Synchrotron-based computed tomography of an adult male *Platynereis Dumerilii* specimen (a) exemplary slice with parapodia highlighted; (b) 3D phase rendering of parapodia.

seen in Figure 1.6, contain a socket area which is where the body attaches to the jaw, a primary teeth and several other smaller ones, and two channels. The functionality of the channels is until the moment unknown. However, they could be used as a poison delivery system like in other *Glycera* species [210].

Several jaw were harvested from laboratory animals through a chemical process with perchloric acid. The jaws were then first embedded and later polished through a novel polishing protocol achieving a remarkable low roughness. The jaw was later probed by means of nanoindentation.

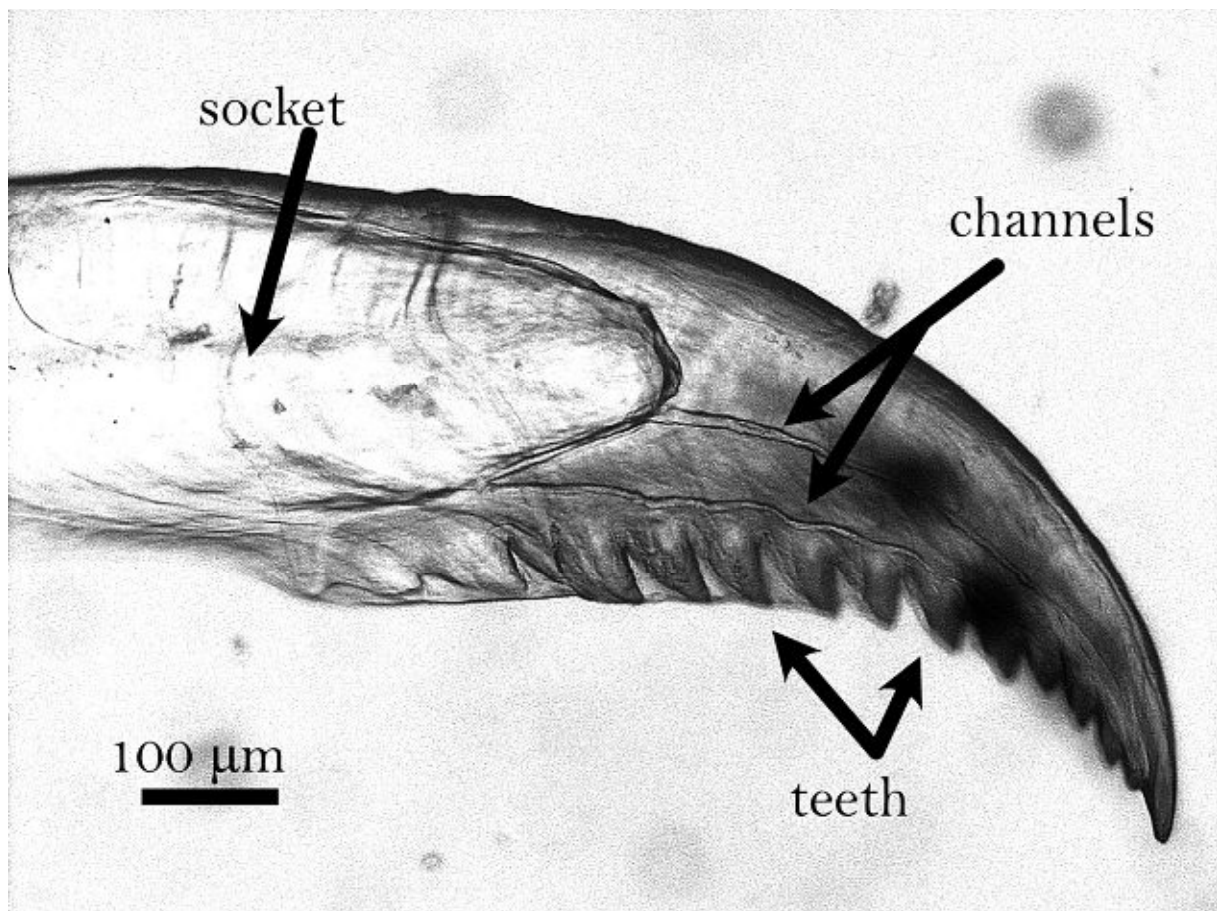


**Fig. 1.6:** Light microscopy image at 100 fold magnification of a *Platynereis Dumerilii*'s jaw.

The nanoindentation results were later compared to other studies performed in *Nereis* and *Glycera* specimens. The compared species can be seen in Figure 1.7.

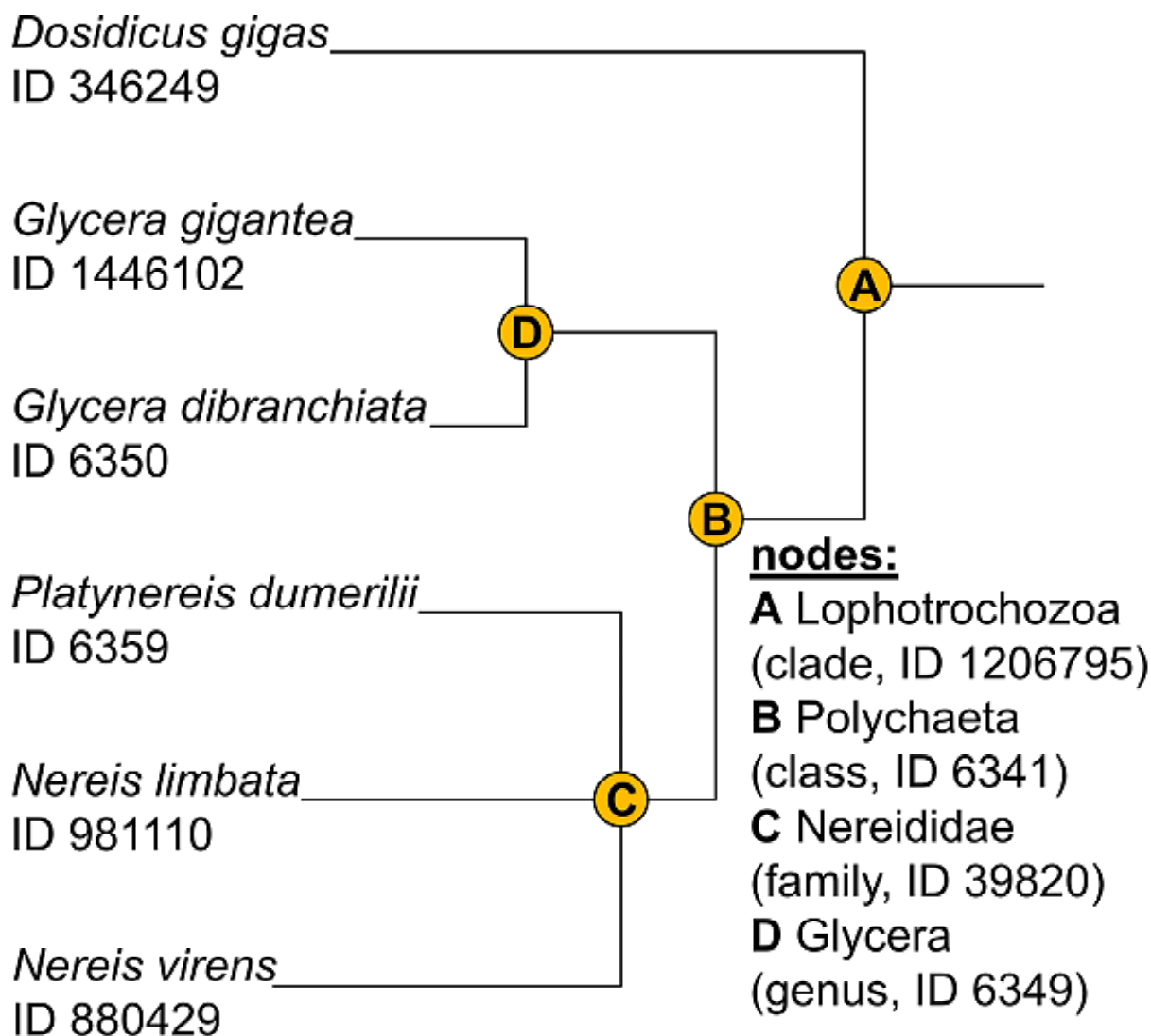


**Fig. 1.7:** Phylogenetic tree of *Polychaeta* and *Dosidicus gigas* specimens studied in Chapter 2.

The microscopy and nanoindentation protocols were further complemented by means of a novel chemical protocol (LA-ICP-MS) to detect the halogen elements within the jaw. The distribution of the halogens can be related to the existence of macromolecules, further described in Section 1.1.2.

The jaws of *Platynereis Dumerilii* exhibit an extremely precise complex geometry and have an extracellular structure with non-organic mineral inclusions. The literature in Chapter 2 remarks the predominant existence of proteins as the main building block of this structure. Studies performed in jumbo squid *Dosidicus gigas* beaks indicate that stiffness of around 9 GPa and hardness of around 0.7 GPa are comparable with the ones obtained from the jaws of *Polychaeta* worms [202]. Additionally, they agree with the rest of the community on the existence of histidine- and glycine-rich proteins, which accounts for 45% of its mass, but they also detected around 20% of chitin. This strongly supports the idea that chitin can also play an important role in the mechanical properties of the jaws from *Platynereis Dumerilii*.

### 1.1.2 Halogen and metallic elements present at macromolecules

The elemental  $WF$  results obtained in Chapter 2 by means of LA-ICP-MS, and images reconstructed through ImageLab-software version 2.99 (Epina GmbH, Austria) give access to the weight fraction maps of the element ions of interest distributed across the tested jaw. The total  $WF$  for each tested element ion in the jaw was obtained by color thresholding each elemental ion weight fraction map into three different color sections, the latter representing maximum  $WF$ , half the maximum  $WF$  and a third of the maximum  $WF$ , respectively, as seen in Fig. 1.8. Subsequently, to obtain the pixel-wise concentration, the  $P$  belonging to each of the color sections was divided by the total amount of  $P$  comprising the jaw. Next, the pixel-wise concentration was multiply by their respective  $WF$ . Finally, the weighted  $WF$  of the three different color sections were added to obtain the total  $WF^*$  for each element ion, given in percentage and computed as

$$WF_i^* = \left[ \left( WF_i^{max} \times \frac{P_i^{max}}{P_{total}} \right) + \left( \frac{WF_i^{max}}{2} \times \frac{P_i^{half}}{P_{total}} \right) + \left( \frac{WF_i^{max}}{3} \times \frac{P_i^{third}}{P_{total}} \right) \right] \times 100 \quad \text{for } i = Br, Cu, Fe, I, Zn \quad (1.1)$$

These weight fractions give access to element ion specific volume fractions  $f^*$  computed as follows

$$f_i^* = \rho^{jaw} \times \frac{WF_i^{total}}{\rho_i} \quad \text{for } i = Br, Cu, Fe, I, Zn \quad \text{with} \quad (1.2)$$

$$\rho_i = \frac{M_i}{V_i} \quad \text{for } i = Br, Cu, Fe, I, Zn \quad (1.3)$$

and the real mass densities of  $\rho_{Br} = 3.12 \frac{g}{cm^3}$ ,  $\rho_{Cu} = 8.94 \frac{g}{cm^3}$ ,  $\rho_{Fe} = 7.86 \frac{g}{cm^3}$ ,  $\rho_I = 4.93 \frac{g}{cm^3}$ ,  $\rho_{Zn} = 7.13 \frac{g}{cm^3}$ , and  $\rho_{jaw} = 2.00 \frac{g}{cm^3}$ .

**Tab. 1.1:** Weight fraction and volume fractions of element ions detected in all the jaw

	bromide	copper	iron	iodine	zinc
$WF^*$	10.69%	0.002%	2.48%	0.60%	0.49%
$f^*$	6.86%	0.0006%	0.63%	0.24%	0.14%



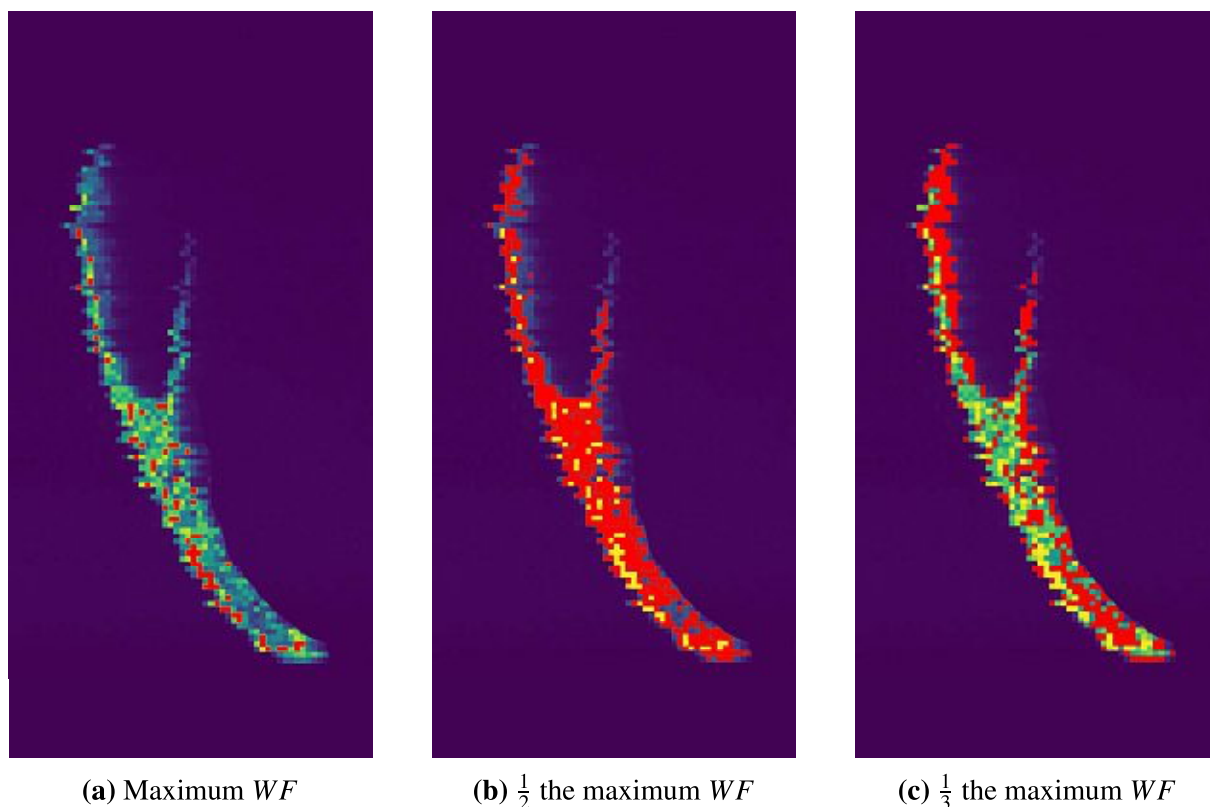


**Fig. 1.8:** Color thresholding determination, by example of weight fraction  $WF$  maps of bromide ions. The selected pixels are denoted as red.

The halogen ions tend to form self-assemble macro molecules [13, 226, 275, 299]. [181] suggests in *Polychaeta* jaws, the formation of  $Zn(His)_3Cl$  based protein matrix. Furthermore, bromiodohistidine  $C_6H_7BrIN_3O_2$  and bromotyrosine  $C_9H_{10}BrNO_3$  were reported by [27]. Besides proteinous macromolecules, [90] and [180] observed the formation of minerals from the cross-links with halogen ions in marine organism, atacamite  $Cu_2Cl(OH)_3$  and magnetite  $Fe_3O_4$  respectively.

The molecular weight fraction  $mWF$  of each element contained in macro-molecules, i.e.  $Zn(His)_3Cl$ ,  $C_6H_7BrIN_3O_2$ ,  $C_9H_{10}BrNO_3$ ,  $Cu_2Cl(OH)_3$ , and  $Fe_3O_4$ , can be computed from the molecular mass  $mm$  of each element contained in the macro-molecules and the sum of them as follows:

$$mWF_j = \frac{mm_j}{\sum mm_j} \quad \text{for } j = \text{elements in macromolecule} \quad (1.4)$$

The  $mWF$  from ions of interest i.e.  $Br^-$ ,  $Cu^-$ ,  $Fe^-$ ,  $I^-$ , and  $Z^-$  contained in each of the macro-molecules are the maximum weight fraction  $mWF_{max}$ . The amount of elements needed  $pn$  for 1 part of ion to form each macro-molecule can be computed as follows:

$$pn_j = \frac{mWF_j}{mWF_{max}} \quad (1.5)$$

The weight fraction of the macro-molecule in the jaw can be calculated from the addition of the weight fraction from the ion of interest contained in the macro-molecule and the sum of weighted  $WF$ .

$$WF_k = \sum WF_i \times pn_j \quad \text{for } i = Br, Cu, Fe, I, Zn \quad (1.6)$$

The volume fraction  $f$  of the macro-molecules was computed according to Eq.1.7, and together with the results of  $W$  can be observed in Table 1.2.

$$f_k = \rho^{jaw} \times \frac{WF_k}{\rho_k} \quad \text{for } k = C_9H_{10}BrNO_3, \\ Cu_2Cl(OH)_3, \\ Fe_3O_4, \\ C_6H_7BrIN_3O_2, \\ Zn(His)_3Cl \quad (1.7)$$

and the real mass densities of  $\rho_{C_9H_{10}BrNO_3} = 1.7 \frac{g}{cm^3}$ ,  $\rho_{Cu_2Cl(OH)_3} = 3.76 \frac{g}{cm^3}$ , and  $\rho_{Fe_3O_4} = 7.87 \frac{g}{cm^3}$ .

The density of bromiodohistidine  $\rho_{C_6H_7BrIN_3O_2}$  the macro-molecule  $Zn(His)_3Cl$   $\rho_{Zn(His)_3Cl}$  can be approximated by relating their molecular weight with the molecular weight and density of histidine for 1 unit of volume, as follows

$$\rho_k = mm_k \times \frac{\rho_{histidine}}{mm_{histidine}} \quad (1.8)$$

**Tab. 1.2:** Mass fraction and volume fractions of amino acids and minerals detected in the jaw

	tip		middle	
	$WF$	$f$	$WF$	$f$
$C_9H_{10}BrNO_3$	34.81%	40.95%	34.81%	40.95%
$Cu_2Cl(OH)_3$	0.005%	0.003%	0.005%	0.003%
$Fe_3O_4$	3.43%	0.87%	3.43%	0.87%
$C_6H_7BrIN_3O_2$	5.57%	3.41%	-	-
$Zn(His)_3Cl$	15.99%	5.65%	-	-

### 1.1.3 Bones

Bones specifically show an extraordinary variability and their optimization is mainly induced by biological evolution. Nevertheless, the probability of producing optimal bone material is quite low [218]. Meaning that the probable optimization happens at the whole organism level and not at the material level [105]. However, elementary organizational patterns can still be found inside the “chaotic” bone system, and this is due to “architectural constraints” [116]. These patterns can be observed over many length scales, and understanding the organization of the elementary building blocks can be the key to a more profound understanding of the mechanical

properties from bone. The main building blocks can be organized in the following hierarchical organization:

- The *macro-structure level* is the structural level where size and shape of whole bones are considered. At this observational length scale, you can classify bone into cortical and trabecular bone.
- The *micro-structure level* can be found at the length scale of approximately 100  $\mu\text{m}$ . It includes complex structures such as osteons, as seen in Fig.1.9.a. These osteons are constructed through substructures called lamellae. [196] classified these lamellae substructures as collagen rich (dense) and collagen poor (loose) lamellae, and can be observed in Fig.1.9.e.

The center of an osteon is composed of a vascular canal. Haversian and Volkmann canals conform the vascular porosity, enclose the vasculature, the nerves, and the bone fluid [336]. The lacunae porosity shelters the osteocytes, and is connected by a series of microscopic channels called canaliculi [132]. Due to diameters of around 100 nm [11], the canaliculi are also treated as part of ultra-structural porosity.

[214] called the fluid contained in the vascular porosity, “serum” and the fluid contained in the “smaller” pores i.e. lacunae pores and ultra-structure porosity, “extra-cellular fluid”. Both bone fluids have an equivalent composition, but are contained in different pressures. The pressure of the fluid within the “smaller” pores is high, meanwhile the pressure in the vascular canals is considered to be low [209], [336]. It is acknowledged that bone fluid is crucial for the transport of nutrients to the bone-forming cells (osteoblasts), and waste from the bone-resorbing cells (osteoclasts) [65, 238].

- The *ultra-structural level* includes the scale where several collagen type I fibrils form a “bundle”. [110] claimed that most of the mineral is located within the collagen fibrils or intrafibrillar spaces, while [129] claimed the majority of the mineral content is located outside the fibrils or extrafibrillar spaces. Studies using TEM [125], as seen in Fig.1.9.g, showed the clear division of organic and mineral components. This brought the thought of an impure hydroxyapatite ( $\text{Ca}_{10} [\text{PO}_4]_6 [\text{OH}]_2$ ) material coating the collagen “bundle” [241]. This way of calcification may be due to the extra-cellular matrix vesicles, although this can be only one of the ways that mineral component are formed.

The spaces found within ultra-structure level, where bone fluid can be located, are part of the ultra-structure porosity. The amount of bone fluid contained within ultra-structure porosity varies depending on the degree of mineralization in the bone [165, 167, 329]. The ultra-structure porosity is therefore considered the lowest characteristic lineal dimension porosity [65]. Additional division of spaces can be found at the intrafibrillar space and the extrafibrillar space. According to [129], most of the hydroxyapatite crystallites are located at the extrafibrillar spaces. Bone fluid can be located in the intrafibrillar or in the extrafibrillar spaces [329], [105]

- The *molecular level* is the scale at tens of nanometers. This level consists of the constituents or the so-called elementary components of mineralized tissue. These elementary components can be classified into organic or inorganic constituents.

The organic constituents are further divided into collagen type I proteins which account for 90% of the organic components [46], and over two hundred non-collagenous proteins (NPCs) which account for the remaining 10% of the total protein content [329]. The NPCs include also proteoglycans, phospholipids, glycoproteins, and phosphoproteins [318]. Proteoglycans have a regulatory effect, and phospholipids have a significant role in calcification. The degree of calcification is influenced by the NPCs [51].

The collagen type I fibrils with diameters of approximately 50-500 nm are assembled by tropocollagen macro-molecules [231]. Each tropocollagen is also composed of three equivalent helical polypeptide chains [45, 223]. Due to a certain variety of amino acid sequences, the tropocollagen may have some heterogeneity [190].

According to the two-dimensional model proposed by [231], the collagen type I is assembled by macro-molecules consisting of two  $\alpha_1$  chains and one  $\alpha_2$  chain [190]. Each of the two  $\alpha_1$  chains consists of a repeating five identical sub-units  $\sigma_1$  sequence, meanwhile the  $\alpha_2$  chain consists of a repeating seven identical sub-units  $\sigma_2$  sequence. The shifting of the tropocollagen macro-molecules create regions of gaps. The tropocollagen macro-molecules are stabilized by enzymatic and non-enzymatic cross-links. These cross-links are essential for the tensile strength of the collagen type I fibrils and the stiffening of the tissue [17, 125].

Recent findings by [223] showed that the theoretical two-dimensional model is considered too simplistic when describing the gap regions where the inorganic constituents are located [31]. Furthermore, [223] introduced a model that uses an electron density map to describe a more realistic three-dimensional structure as seen in Fig.1.9.h.

The inorganic constituents found within mineralized bone tissue are an impure form of hydroxyapatite [130, 165, 329] and water [255].

Bones also have a complex network of canals and pores, and contains porosity at different length scales. According to [46], the surface of the porosities together is 100 times larger than the combined inner and outer surface of cortical bone. From a composition point of view, the porosities are divided into:

- The *vascular porosity* has characteristic diameters of approximately 10-100  $\mu\text{m}$  and hosts the blood vessels, lymphatic vessels, and in some cases nerves. The canals that run longitudinally through the bone cortex are called Haversian canals, and the ones running transversely are the Volkmann canals.
- The *lacunae porosity* has characteristic diameters of approximately 0.1-10  $\mu\text{m}$  and each of them hosts an osteocyte cell. The osteocytes are connected with their neighboring osteocytes through tiny channels called canaliculi. However, the canaliculi are considered from a compositional point of view, a part of the ultra-structural porosity.
- The *ultra-structural porosity* includes the small canaliculi pores with diameters of approximately 100-500 nm and the smallest fluid-filled spaces which can not be detected via light microscopy.

The macro- and micro-structure of bone have been investigated through computed tomography, and this has led to important micro finite element models. However, in order to understand

the ultra-structure requires a deeper interpretation of its constituents and their physical interactions. Pioneering and ground-breaking experimental campaigns performed by Sidney Lees and coworkers [167–170, 172, 173, 175, 177, 179, 241] set the first stepping stone to determining the chemical composition of bony tissues by means of dehydration-demineralization protocols. Chapter 3 expands on this original idea, and combines it with light microscopy and scanning electron microscopy to assess the “universal” patterns of the main building constituents of bone, i.e. organic, mineral, and water, at the micro- and ultra-structural level of 7 different species, including mammalian, struthionine, and ranine specimens.

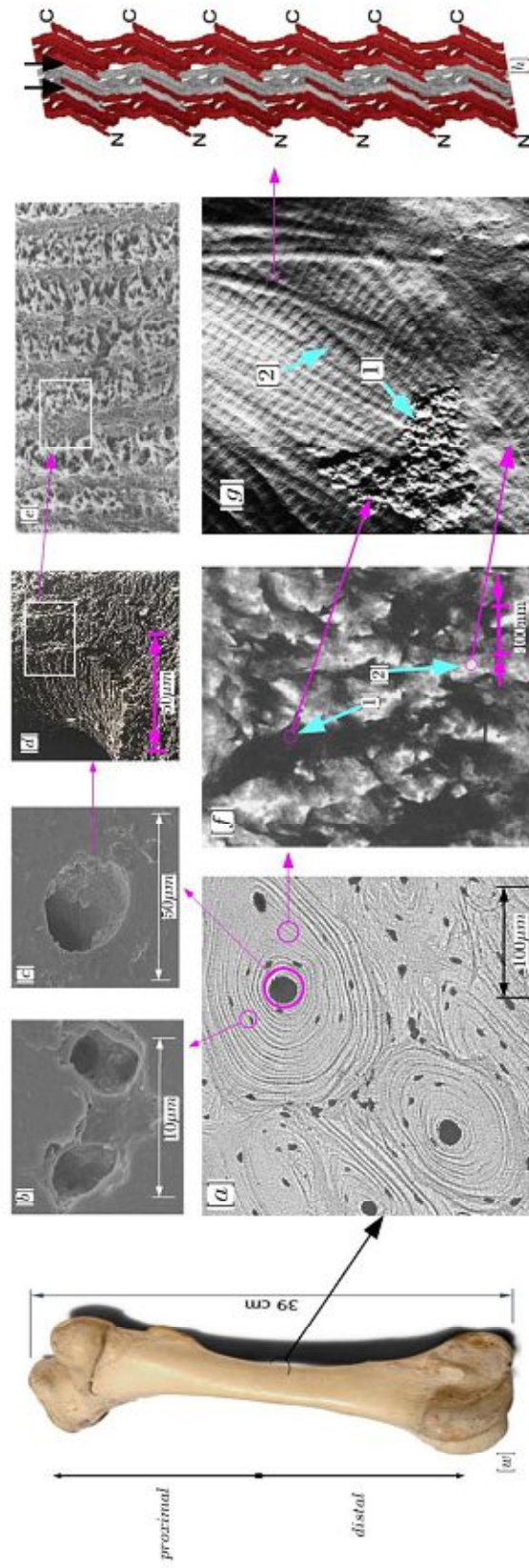


**Fig. 1.9:** [a] Micro-structural level of the axial face observed under the light microscopy at 100 fold magnification. [b] Lacunae pores observed with the FEGSEM at 12000 fold magnification and a voltage of 5kV at High Vacuum. [c] Haversian canal observed with the FEGSEM at 1600 fold magnification and a voltage of 5kV at High Vacuum. [d] With SEM and a voltage of 10 kV, [246] observed the lamellae structure near a haversian canal [e] With SEM (magnified 1965x), [195] observed and identified the alternating types of lamellae i.e. dense and loose lamellae. [f] TEM of cross section from a fully mineralized human bone. Arrow [1] points the mineral full extrafibrillar space and arrow [2] points the protein content or intrafibrillar space [241]. [g] A  $2 \times 2 \mu\text{m}^2$  tapping mode AFM protocol, arrow [1] points impure hydroxyapatite material and arrow [2] points collagen fibrils forming a “bundle” [125]. [h] Model of a collagen fibril by [223]. Three tropocollagen are shown side by side with a remark at the possible binding site. A N-terminal of a sub unit from a tropocollagen is bound to two other, while a C-terminal cross-links with only one. The banding seen in collagen fibrils is due to the 3D organization of these tropocollagens. [w] Bovine femur (public image from the University of New South Wales, Australia).

## 1.2 Man-made materials

The investigation of man-made materials intended for structures such as rail-way steel tracks are discussed in Chapter 4. The micro-structure of rail-way steel was investigated by means of nano-indentation and several microscopy techniques. Nano-indentation is a technique that allows the characterization of hardness and stiffness. Nano-indentation, specifically statistical nano-indentation protocols, have proven to be successful approaches to identify the mechanical properties of the micro-structure in biological materials such as bone [107] or cementitious materials such as Portland cement hydrates [59, 201, 317].

Steel for underground, tramway, and rail-way rails are commonly heat treated to improve the micro-structural characteristics such as toughness and hardness. Nevertheless, this process can create nanometer “imperfections”, which can be only observed through scanning electron microscopy, and affect the macroscopical characteristics of the material.

Interesting clay materials, such as bricks intended for construction, are discussed in Chapter 5. Although fired clay ceramics have been among the oldest building materials used by humanity, mechanical and thermal improvements of bricks or clay blocks are difficult due to the still prevailing lack of understanding of their micro-structure, as seen in Fig. 1.10. The micro-structure of bricks is influenced by chemical and mineral composition. However, the firing temperature also influences the mineral transformations and the porosity. The present work investigates the porosity depending on the chemical composition and firing temperature by means of different imaging techniques.

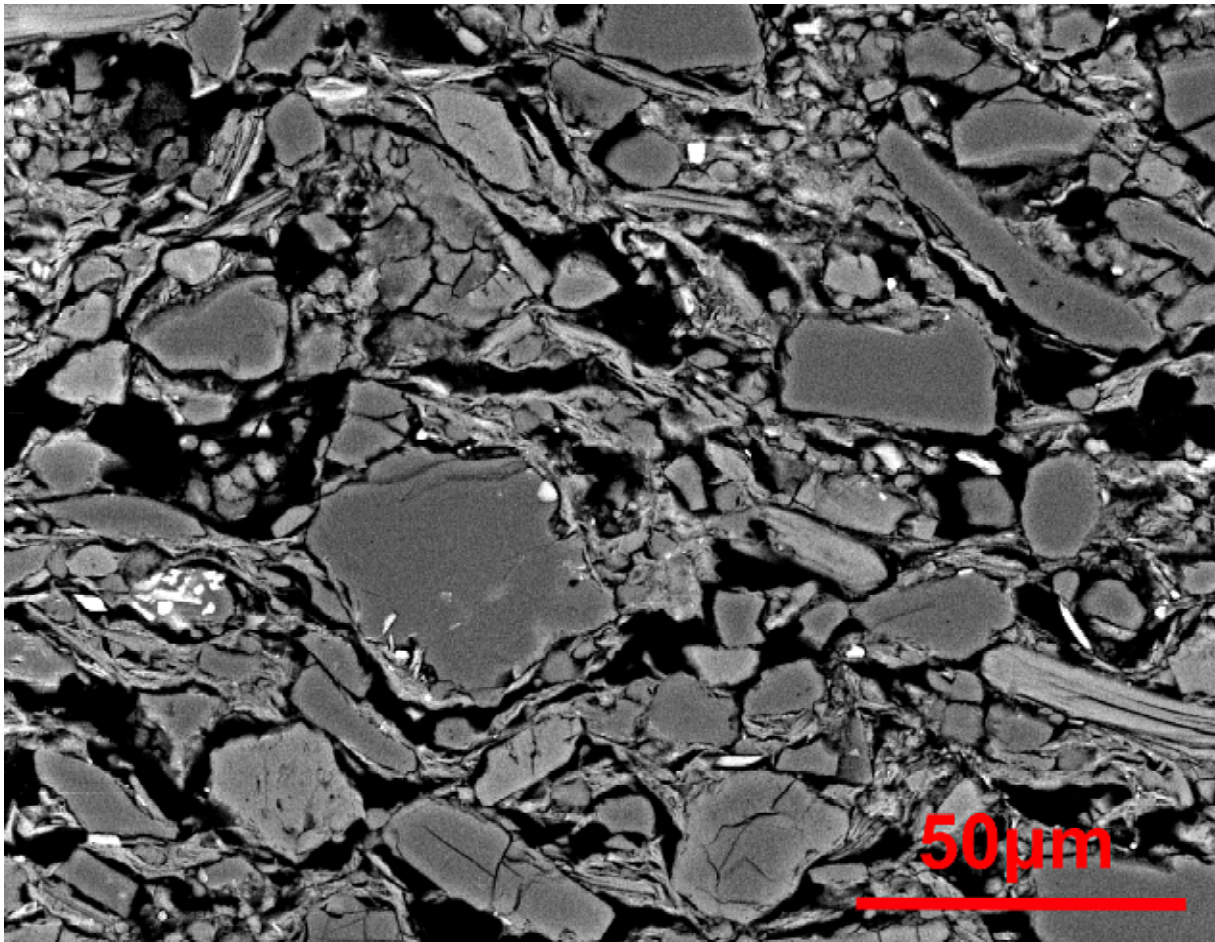


**Fig. 1.10:** Field emission gun scanning electron microscopy (FEGSEM) image of the polished surface from the microstructure of a brick sample.

### 1.3 Outline of the thesis

The aim of this work is to distinguish “universal” patterns in several biological and man-made materials. The investigation of these patterns could facilitate the understanding of their material constituents and their physical interactions. The work is distributed in different Chapters containing original work is presented in the form of scientific publications. The Chapters contents are the followings:

**Chapter 2** utilizes a nano-indentation protocol to obtain the stiffness and hardness of jaws from the marine organism *Platynereis dumerilii*. The protocol was crucially dependent on a new polishing protocol to obtain the lowest roughness possible and therefore, obtain the lowest indentation depth possible. The results were later compared to other nano-indentation protocols performed in genetically “related” *Polychaeta*. The extremely low roughness and the nanoindentation results brought to light some interesting patterns concerning the size effect whenever performing nanoindentation in *Polychaeta* specimens. Specifically, the hardness values differ from the lower values reported in other studies performed in *Nereis* and *Glycera*. This could be explained by the Nix-Gao type nanoindentation size effect normally observed in crystalline metals. The differing hardness values for *Platynereis*, *Nereis*, and *Glycera* jaws actually reflect



a “universal”, i.e. invariant, material property of the ion-spiked structural proteins used by all types of bristle worms (*Polychaeta*). Additionally, novel chemical protocol and analysis were performed by means of Laser Ablation Inductively Coupled Plasma Mass Spectrometry. The chemical analysis made it possible to obtain elemental ion concentrations of the jaw.

In **Chapter 3** a novel approach combining dehydration-rehydration-demineralization protocols and microscopy techniques, such as light microscopy and scanning electron microscopy, results in the quantification of the main building blocks of femora from bovine, equine, porcine, leporine, ranine, and struthionine specimens, and establishes by means of statistical tools relationships and “universal” patterns at the organ and species level. The demineralization protocol was possible through the use of several ethylenediaminetetraacetic acid treatments, which create chelates with the impure hydroxyapatite content. The acid contents, which were submitted to the bone demineralization, were further examined by means of a state-of-the-art Inductively Coupled Plasma Mass Spectrometry protocol.

Continuing with the application of nano-indentation protocols, **Chapter 4** exploited well established statistical indentation approaches to investigate and quantify patterns in the stiffness and hardness through the fitting of Gaussian curve distributions over the data. Chapter 4 investigates rail-way steel by means of an extensive nano-indentation campaign and compares it to the macroscopic stiffness results obtained by means of ultra-sound experiments. The differences were surprising results, and through scanning electron microscopy and a micro-mechanical model the contrast was explained by the observation of patterns found at the micrometer and nanometer scale.

**Chapter 5** identifies and quantifies the porosity of masonry obtained from five different clayey material sources. This was done by employing techniques commonly utilized in biomedical and material science fields, such as scanning electron microscopy, micro computed tomography, mercury intrusion porosimetry, helium pycnometry, and traditional techniques such as Archimedes’ principle. The results showed “universal” patterns in specific porosities dependent on the manufacturing process.

## 1.4 Contribution of the author

The present thesis consists of four publications. Three of them are already published or accepted in peer-reviewed journals, and one of them is a mature manuscript submitted for scientific publication. The author’s contributions to the respective scientific publications are as follows:

- **Chapter 2:** *Jaws of Platynereis Dumerilii: Biologically 3D printed miniature structures with hardness properties similar to those of crystalline metals* (submitted)

The author prepared and evaluated the jaws of *Platynereis dumerilii* examined during all the experimental campaign. The author elaborated all the standards used to calibrate the results obtained by means of Laser Ablation Inductively Coupled Plasma Mass Spectrometry. The author also performed all the data analysis of the nano-indentation and chemical campaign results, and finally, wrote the draft of the manuscript which was submitted in a peer-reviewed journal.

- **Chapter 3:** *“Variances” and “in-variances” in hierarchical porosity and composition, across femoral tissues from cow, horse, ostrich, emu, pig, rabbit, and frog* (Zelaya-Lainez et al, 2020)

The author harvested, prepared, and evaluated all the femur samples examined during all of the experimental campaign. Furthermore, the author designed and manufactured all specific tools used during the polishing protocols. The author also performed all the data and chemical analysis of the results, and wrote the draft of the manuscript which was later published in the peer-reviewed journal *Materials Science and Engineering C*.

- **Chapter 4:** *Multiscale and multitechnique investigation of the elasticity of grooved rail steel* (Jagsch et al, 2020)

The author contributed in the discussion of the experiments and interpretation of the results. The author also performed the scanning electron microscopy, the scanning probe microscopy, and several light microscopy protocols used during the experimental campaign. The contribution was reflected in the manuscript published in the peer-reviewed journal *Construction and Building Materials*.

- **Chapter 5:** *A multitechnique, quantitative characterization of the pore space of fired bricks made of five clayey raw materials used in European brick industry* (Buchner et al, 2020)

The author contributed by guiding and assisting during the sample preparation and the microscopy experimental campaigns. The contribution was reflected in the manuscript accepted in the peer-reviewed journal *Applied Clay Sciences*.

# Chapter 2

## Metal-type hardness properties in jaws of *Platynereis dumerilli*

### Jaws of *Platynereis dumerilli*: Biologically 3D printed miniature structures with hardness properties similar to those of crystalline metals

**Authored by:** Luis Zelaya-Lainez<sup>1</sup>, Giuseppe Balduzzi<sup>1</sup>, Olaf Lahayne<sup>1</sup>, Kyojiro N. Ikeda<sup>2</sup>, Florian Raible<sup>3</sup>, Christopher Herzig<sup>3</sup>, Winfried Nischkauer<sup>3</sup>, Andreas Limbeck<sup>4</sup>, and Christian Hellmich<sup>1</sup>

**Submitted:** *The Journal of The Minerals, Metals and Materials Society*

#### Abstract

*Platynereis dumerilli*, a bristle worm living almost ubiquitously in coastal environments, has become a model organism in the fields of genetics and marine biology. We complement the ever-growing knowledge on this species by the first set of mechanical and chemical tests on the material making up the animal's jaws, minutely designed sub-millimetric structures produced through a biological 3D printing process. Therefore, state-of-the-art nanoindentation protocols are further miniaturized, eventually operating at 15 nm surface roughness, 100 mN maximum indentation force, and 90 nm indentation depth. Laser ablation inductively coupled plasma mass spectroscopy (LA-ICP-MS) in combination with weighing and mixing of known ionic masses within an organic matrix standard reveal local concentration differences of metal and halogen ions built into the jaw's structural protein matrix. They imply slight, yet statistically significant, variations in local hardness and elastic modulus of the jaw material, between the tip and the central regions of the organ.

<sup>1</sup>Institute for Mechanics of Materials and Structures, Vienna University of Technology (TU Wien), Karlsplatz 13/E202, 1040 Vienna, Austria.

<sup>2</sup>Department of Microbiology, Immunobiology and Genetics, University of Vienna, Vienna, Austria

<sup>3</sup>Max Perutz Labs, Vienna BioCenter, Vienna, Austria

<sup>4</sup>Institute of Chemical Technologies and Analytics, Division of Instrumental Analytical Chemistry, Vienna University of Technology (TU Wien), Getreidemarkt 9/164, 1060 Vienna, Austria.

However, the mean of the herein measured hardness values, namely 0.8 GPa, differs pronouncedly from the lower values reported for jaws of much larger bristle worm species, such as *Glycera* or *Nereis*. This appears to be the result of a Nix-Gao-type nanoindentation size effect which is well known for crystalline metals: Due to indentation depth-dependent dislocation densities, the square of the hardness scales with the inverse of the indentation depth, tending towards a limit hardness for the indentation depth going to infinity. Conclusively, herein as well as earlier reported, mutually differing hardness values for *Platynereis*, *Nereis*, and *Glycera* jaws actually reflect a “universal”, i.e. invariant, material property of the ion-spiked structural proteins used by all types of bristle worms (*Polychaeta*). The corresponding limiting hardness amounts to 0.53 GPa. These smart extra-skeletal biomaterials exhibiting beneficial features normally found with highly energy consuming materials such as metals, are expected to become a major source of bioinspiration for future technological processes.

## 2.1 Introduction

The bristle worm *Platynereis dumerilii* is an almost ubiquitous annelid species inhabiting coastal environments. It is often considered as a model organism for evolutionary and neuro-biological research [9, 149, 245], due to its regular and easily controllable reproduction at laboratory conditions [97, 98]. In 1832, the worm was initially classified as a *Nereis* species [12], before being assigned, in 1914, to the genus *Platynereis* [91]. However, its taxonomy has remained somewhat controversial up to the 1970s [73], and it is still a matter of some debate [199, 260].

*Platynereis dumerilii* develops several extracellular structures, namely: (i) *chaetae*, external well-tailored beam-like structures used for locomotion (crawling and swimming), for anchoring, for stabilization during muscle activity such as peristalsis, and for sensing the environment [98, 199]; (ii) *acicula*, beam-like structures supporting the *chaetae* while being part of the protrusions called *parapodia*; and (iii) a pair of jaws, used for feeding and, in the case of danger, for biting [97].

The *chaetae* have been investigated by different research communities. It is well established that they are made up of  $\beta$ -chitin crosslinked with proteins [126, 261], and the study of their morphology allowed for identification of different species and their mutual relations within phylogenetic trees [199]. The *chaetae* formation model was first coined by [33] as chaetogenesis, and describes how a chaetoblast, a specialized follicular cell, forms an assembly of micro-villi. The latter allows, by basal apposition, for the growth of new chaetal material on its surface [219, 297]. In this context, it is noteworthy that new *chaetae* material may probably be formed by an ectodermal sac called chaetal follicle, arising itself from the chaetoblast as well as from adjacent follicle cells [126, 277, 305, 306].

This type of apposition is reminiscent of modern 3D printing technology – and in that sense, it may be called “biological 3D printing process”. The latter leads to astonishingly complex and precisely manufactured structures, outperforming the very latest technological developments [262] in terms of minuteness of produced structural details. In addition, current 3D printing technology is typically limited in terms of mechanical integrity, with material strength values in the order of tens of Mega-pascals [315]. On the other hand, *Platynereis dumerilii* structures have astonishingly adapted to the harsh environmental conditions under which they need to

mechanically function, so that these biological structures may indeed present themselves as an interesting source of bio-inspiration, potentially helping not only to overcome challenges in nano-fabrication, but also in mechanical integrity.

However, the tiny dimensions of the *chaetae* pose presently insurmountable challenges with respect to direct mechanical testing. Therefore, we turned our current interest to somewhat larger structures in the same organism: the jaws. Jaw development has been described by [98]: Jaws start forming during the the mid-nectochaetae development stage, lasting, at a temperature of 18°C, from 3 to 4 days post fertilization. At this point in time, the primary tooth of each jaw becomes visible, it will later define the anterior end of the jaw. The jaws continue to grow in the subsequent development stages, with additional teeth being continuously added; until the final number of one primary and nine secondary teeth, see Fig. 2.1(a) and (b), is reached in the tubicolous juvenile stage, where the worm finally possesses two completed jaws, with each of them typically spanning some 800  $\mu\text{m}$  in length, see Fig. 2.1(b). They are then used over the lifespan ranging from 6 to 18 months, which is normally terminated by the nuptial dance lasting for not more than a few hours.

The cell-driven jaw development process is somehow similar to that of the *chaetae*; hence, also the jaws may be regarded as a biologically 3D printed structures. However, chemical composition and mechanical properties of *Platynereis dumerilli* jaws have remained largely unexplored. We here enter the corresponding undiscovered scientific territory, by exploring the chemical and mechanical properties of *Platynereis dumerilli* jaws, seen as the product of a biological 3D printing process.

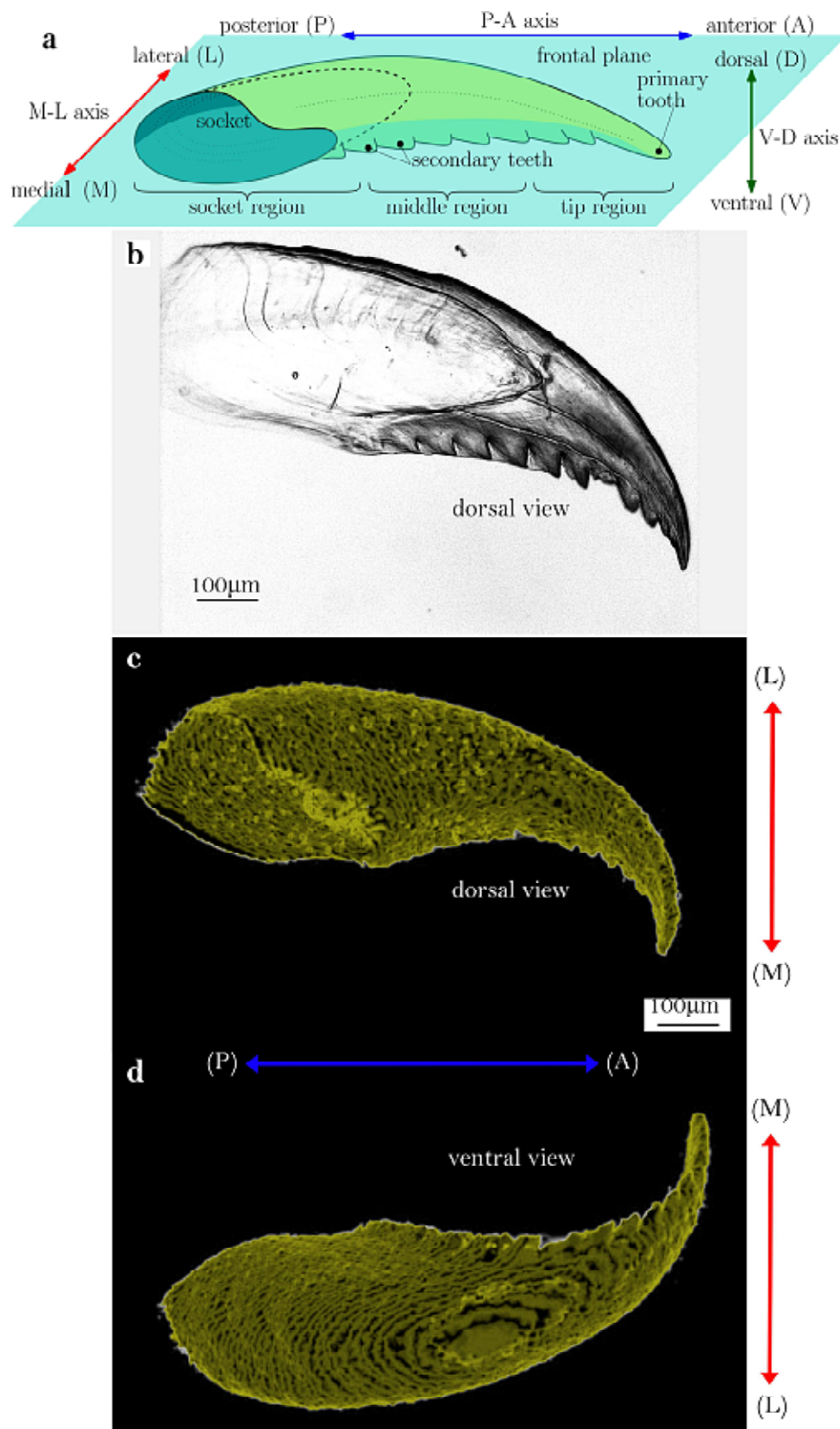


**Fig. 2.1:** Imaging of *Platynereis dumerilli* jaw: (a) axonometric sketch with indication of anatomical axes, (b) light micrograph of upper side (dorsal view), (c) volume rendered  $\mu$ CT image of upper side (dorsal view), (d) volume rendered  $\mu$ CT image of lower side (ventral view)

At the same time, the results of such an exploration can be beautifully set in context with the extensive scientific literature on mouth structures in various invertebrates, including those of other *Polychaeta* worms. It turns out that, in contrast to load-bearing *mineralized* structures in vertebrates [249], mineral phases are virtually absent in the chewing instruments of invertebrates. Instead, as a rule, it is a protein matrix which constitutes the backbone of such hard mouth parts. This protein matrix may be reinforced by chitin fibers, as it was shown for beaks of the jumbo squid *Dosidicus gigas* [202], and it may incorporate metal or halogen ions, such as zinc, chloride, or magnesium, as it was shown for the mandibles of six species from four families of *Isoptera* [66]. Intensive studies have been devoted to the deciphering of the relation between hardness properties and the presence of metal and halogen ions in the jaws of several bristle worm species. The scene was basically set by Lichtenegger and co-workers, and their studies of jaws from the genera *Glycera* [180] and *Nereis* [181]. They showed that nanoindentation-derived elastic and hardness properties are positively correlated with concentrations of metal ions, such as zinc quantified through X-ray absorption and fluorescence imaging of *Nereis* jaws, or copper quantified by means of electron microprobe experiments on *Glycera* jaws. Later on, partial peptide mapping and molecular cloning of a partial cDNA from a jaw pulp library [43] allowed for identification of *Nvjp-1* as the key protein making up the organic matrix of *Nereis* jaws. The latter matrix hosted not only zinc ions, but also halogen ions, such as chloride, bromide, and iodine. Corresponding ionic concentrations were quantified through energy dispersive X-ray spectroscopy (EDS) [27, 42, 44]. In the case of *Glycera* jaws [210, 239], EDS evidenced copper and chloride as the key ions incorporated into the structural protein matrix.

The present paper extends these studies towards the significantly smaller species *Platynereis dumerilii*, introducing unprecedented miniaturization steps to the nano-indentation protocol, including a refined polishing procedure; in this context, we do not only invest into the identification of metal and halogen ions as drivers of the mechanical properties, but we complement the current state of the art in bristle worm mechanics by the key topic of *size effects* – elucidating astonishing similarities between the nanoindenter-probed hardness of crystalline metals [216], and that of ion-enriched protein complexes making up *Polychaeta* jaws.

## 2.2 Materials and methods

### 2.2.1 Sample selection and preparation

Jaws were harvested from adult *Platynereis dumerilii* worms. The worms were first treated with perchloric acid, before being put into a centrifuge of type Heraeus Biofuge primo (Heraeus, Germany). Centrifuging with 10 000 rpm for ten minutes resulted in physical separation of the jaws from the rest of the bodies. In order to check the integrity and the intactness of the jaws, they were then observed by light microscopy; being mounted into a Zeiss Axio Imager Z1m (Carl Zeiss, Germany), with images taken by a Zeiss AxioCam MRc5 camera, as seen in Fig. 2.1(b). Afterwards, ninety jaws were embedded in a two component EpoFix resin (Struers, Denmark), ten each in 5 mL Eppendorf microtubes (Eppendorf, Germany). Air pockets within the resin were removed by means of a desiccator and a pump. Next, a micro-tomography device ( $\mu$ CT 100, Scanco, Switzerland) was employed at a resolution of 1.2  $\mu$ m, in order to identify the orientation of the jaw planes orthogonal to the dorsal-ventral axis, with the respect to the tube axis. The jaw with its dorsal-ventral axis lying perfectly parallel to the tube axis (within the

precision provided by the micro-tomography device) was further analyzed: Therefore, the jaw, together with a surrounding 3 mm thick slice with faces orthogonal to the tube axis, was cut out of the tube, by means of an Isomet low speed saw (Buehler, USA), see Fig. 2.2(a). This slice was attached, by means of resin, to a glass microscope slide. The latter was mounted into the circular polishing system Logitech PM5 (Logitech, Scotland), see Fig. 2.2(b). There, it was polished by means of a Microtex 300 mm polishing disc in a suspension of agglomerated polycrystals made of alpha aluminum oxide (Struers, Denmark). The individual polycrystalline agglomerates exhibited a particle size of initially 1  $\mu\text{m}$ , diminishing during the polishing process. The latter

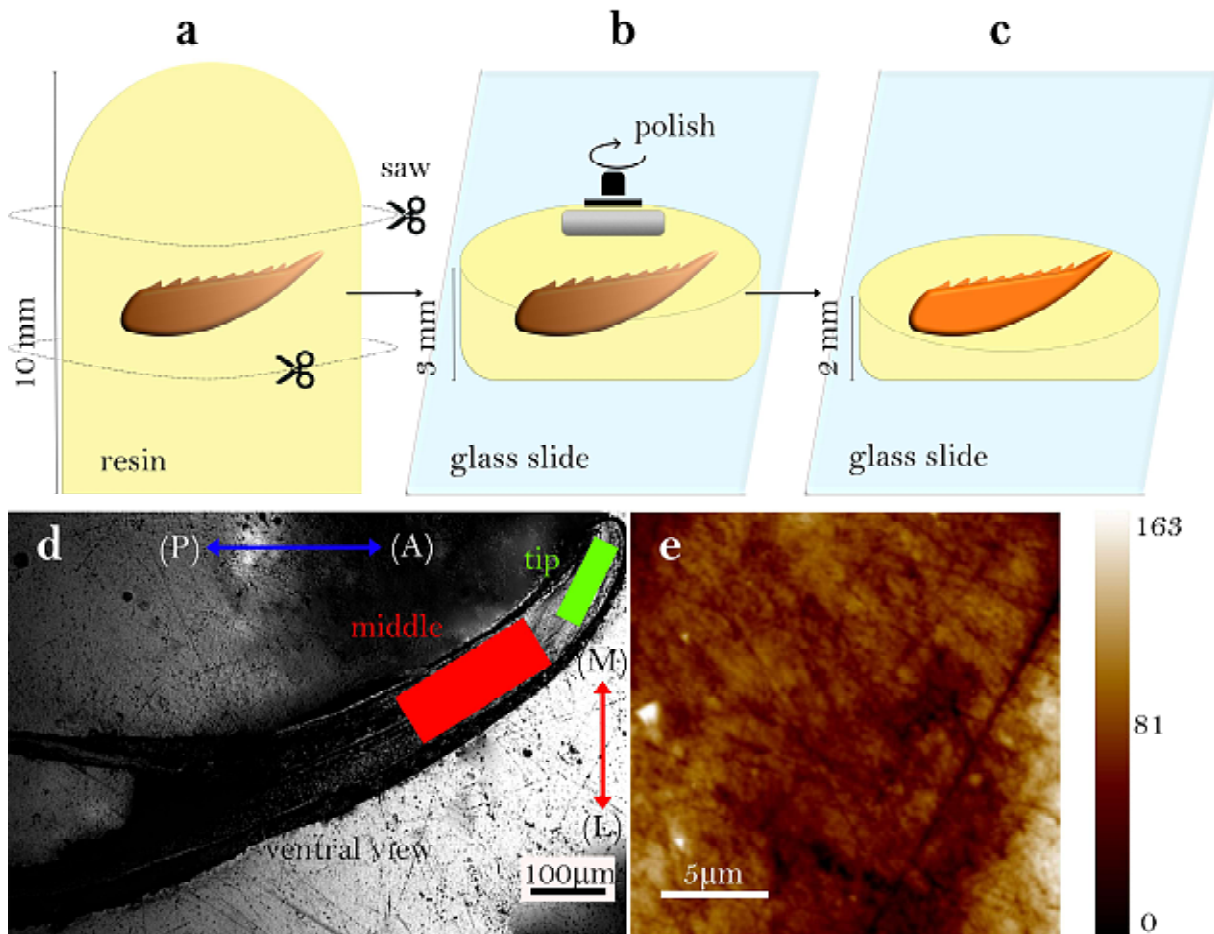


**Fig. 2.2:** Sample preparation steps and outcome: (a) cutting resin-embedded jaws out of micro-tube, (b) circular polishing of the indentation surface, (c) sample preparation completed, with (d) indentation areas “middle” and “tip” indicated in a light micrograph taken by nanoindenter-inbuilt microscope, and with (e) scanning probe-microscopic topography quantification of polished surface portion within the middle region, measuring  $400\mu\text{m}^2$ ; the pixel-wise heights are given in nanometers.

process was terminated once a surface roughness of 15 nm, as measured in a Triboindenter TI 900 device in scanning probe microscopy (SPM) mode, was reached, see Figure 2.2(c). In more detail, raster scanning the polished surface by means of the Berkovich diamond tip yields topographical images as the one seen in Fig. 2.2(e), and made up of pixels with a size of 6 nm.



Such images also allow for computing the root-mean-squared average (RMS) of the topography of the surface,  $R_q$ , according to [201]:

$$R_q = \sqrt{\frac{1}{P^2} \sum_{m=1}^P \sum_{n=1}^P z_{mn}^2} \quad (2.1)$$

where  $P$  is the number of scanned pixels from the image obtained by scanning probe microscopy, and  $z_{mn}$  is the height difference between the pixels and the mean scanned plane [141, 201].

### 2.2.2 Nanoindentation of *Platynereis dumerilii* jaw

The polished surface, with its outward normal pointing in the ventral direction, was indented by a Berkovich tip attached to a Hysitron Triboindenter TI900, according the following protocol for load control: At a rate of 0.01 mN/s, the load was increased up to 100  $\mu$ N maximum load; the latter was held for 5 s, before unloading took place, again at a rate of 0.01 mN/s. This indentation process was repeated 156 times, in order to realize two grids of  $6 \times 6$  and one grid of  $6 \times 5$  indents in the middle region of the jaw, depicted as red area in Fig. 2.2(d), and one grid of  $6 \times 9$  indents in the tip region of the jaw, depicted as green area in Fig. 2.2(d). Thereby, the spacing between the indents always amounted to 5  $\mu$ m. The corresponding maximum indentation depths ranged from 80 nm to 120 nm, hence, they were at least 2.5 to 5 times larger than the roughness of 15 nm, as is required for the experimental realization of an elasto-plastic half-space [82, 201]. For such an half-space, the recorded load-displacement curves were evaluated according to the method of [222]: The reduced modulus  $E$  and the hardness  $H$  were computed from the unloading stiffness  $S$  and the contact area  $A_c$  according to:

$$E = \frac{\sqrt{\pi}S}{2\sqrt{A_c}} \quad (2.2)$$

$$H = \frac{F_{max}}{A_c} \quad (2.3)$$

### 2.2.3 Chemical analysis of *Platynereis dumerilii* jaw

In order to quantify the spatial concentration distributions of halogen and metal ions in the *Platynereis dumerilii* jaw, the polished jaw surface was scanned, in line-mode, by a laser ablation inductively coupled plasma mass spectrometer (LA-ICP-MS). This device analyzed the uppermost twelve micrometers below the surface, while keeping the rest of the jaw sample virtually unaltered. The LA-ICP-MS set-up consisted of a New Wave 213 laser ablation system (Electro Scientific Industries Inc., USA) with a frequency quintupled neodymium-doped yttrium aluminum garnet laser operating at a wavelength of 213 nm, coupled, through a Polytetrafluoroethylene tubing, to a quadropole iCAPQ induced coupled plasma mass spectrometer (ICP-MS; ThermoFisher Scientific, USA). The laser spot size was set to 10  $\mu$ m, and the scan speed was chosen as 10  $\mu$ m/s. Helium was used as the ablation gas and argon was admixed as make-up gas before entering the ICP-MS. The measurements of the LA-ICP-MS provided intensities  $I$  of the isotopes of bromide, copper, iodine, iron, and zinc in counts per second. These counts needed to be related to the ionic ‘‘concentrations’’, which were approached here via weight fractions in

matrix-matched standards [30]. In more detail, a Mettler Toledo precision balance PGH403-S (Mettler-Toledo International Inc., Switzerland) was employed to define amounts of selected salts in terms of well defined weight, namely: ammonium bromide, copper(II) chloride, iron(II) chloride, potassium iodide, and zinc chloride. Then a certain weight-defined amount of the fluid organic compound N-Methyl-2-pyrrolidone (Merck KGaA, Germany) was put into 15 mL polycarbonate test tubes, together with the aforementioned salt portions. These components were then well mixed, in the sense that crystal formations could not be discerned any more by the pure eye. Thereafter, we added, again at a well-defined weight, the same two-compound acid which we had already used for the embedding of the worm jaws. The resulting fluid was then stirred by a vibrating mixer for 10 minutes and by a centrifuge for another 10 minutes. The weight fractions of the metal ions with respect to the weight of the overall mixture are given in the upper part of Table 2.1. Thereafter, our mixing products were cured, for two days, in the Duran Borosilicate Glass 3.3 Complete Vacuum Desiccator. Subsequently, all standards,

**Tab. 2.1:** Blank (ion-free) and ion-spiked calibration standards: weight fractions  $WF$  per weight of entire compound, LA-ICP-MS protocol-generated ionic intensities  $I^S$ , and weight-fraction-to-intensity conversion factors  $\beta$ ; for the ions of interest: bromide, copper, iron, iodine, and zinc

<b>standard</b>	$WF_{Br^-}$ [ $10^{-6}$ ]	$WF_{Cu^-}$ [ $10^{-6}$ ]	$WF_{Fe^-}$ [ $10^{-6}$ ]	$WF_{I^-}$ [ $10^{-6}$ ]	$WF_{Zn^-}$ [ $10^{-6}$ ]
blank	0	0	0	0	0
1	142	64	51	165	59
2	290	129	105	336	120
3	1322	590	477	1531	545
4	2721	1213	982	3151	1122
<b>standard</b>	$I_{Br^-}^S$ [cps]	$I_{Cu^-}^S$ [cps]	$I_{Fe^-}^S$ [cps]	$I_{I^-}^S$ [cps]	$I_{Zn^-}^S$ [cps]
blank	0	0	0	0	0
1	123	225	950	1890	99
2	208	385	1628	3193	156
3	1148	1752	7539	16564	722
4	2292	3088	13550	31581	1231
<b>slope</b>	$\beta_{Br^-}$ [ $10^{-6}$ cps $^{-1}$ ]	$\beta_{Cu^-}$ [ $10^{-6}$ cps $^{-1}$ ]	$\beta_{Fe^-}$ [ $10^{-6}$ cps $^{-1}$ ]	$\beta_{I^-}$ [ $10^{-6}$ cps $^{-1}$ ]	$\beta_{Zn^-}$ [ $10^{-6}$ cps $^{-1}$ ]
Eq. (3.15)	1.1774	0.3887	0.0718	0.0989	0.8981

the four spiked ones as well as the blank one, were cut by means of an Isomet low speed saw (Buehler, USA) into 3 mm thick circular slices, and then attached, by means of resin, to a glass slide. The free surfaces of these slices underwent a polishing protocol as described in [335]: They were machined by means of a Leica SM2500 heavy duty sectioning system and the Leica SP2600 ultramiller (Leica Biosystems GmbH, Germany), equipped with a diamond cutting edge rotating at 1000 rpm, at a feeding speed (i.e. a speed orthogonal to the surface) of 2 nm/polishing cycle, and an advancing speed (i.e. a speed within the plane of the surface) of 1.5 mm/s, until a roughness measure  $R_q$  according to Eq.(2.1), of around 15 nm was reached. Precautions were made to avoid cross contamination during the polishing process. Therefore, whenever a

sufficiently fine surface had been realized, the diamond blade was cleaned twice, 15 minutes in an ultrasonic bath containing 99% ethanol, followed by a rinse with distilled water.

The polished surfaces of the four spiked and the one blank standard then underwent the same LA-ICP-MS protocol as the *Platynereis dumerilli* jaw, yielding the intensities  $I^s$  given in the medium part of Table 2.1. The ionic intensities and ionic weight fractions turned out to be almost perfectly proportional to each other, so that the weight fractions could be expressed as a linear function, through the origin, of the intensities. Mathematically, this reads as

$$WF_i = \beta_i I_i^s \quad \text{for } i = Br^-, Cu^-, Fe^-, I^-, Zn^- \quad (2.4)$$

with ion-specific slope values  $\beta_i$  assembled in the lower portion of Table 2.1, representing the slopes seen in Fig. 2.3. These slope factors  $\beta$  were then used to convert the ionic intensity distributions measured on the jaws into corresponding weight fraction distributions, employed here as “concentration quantities”.

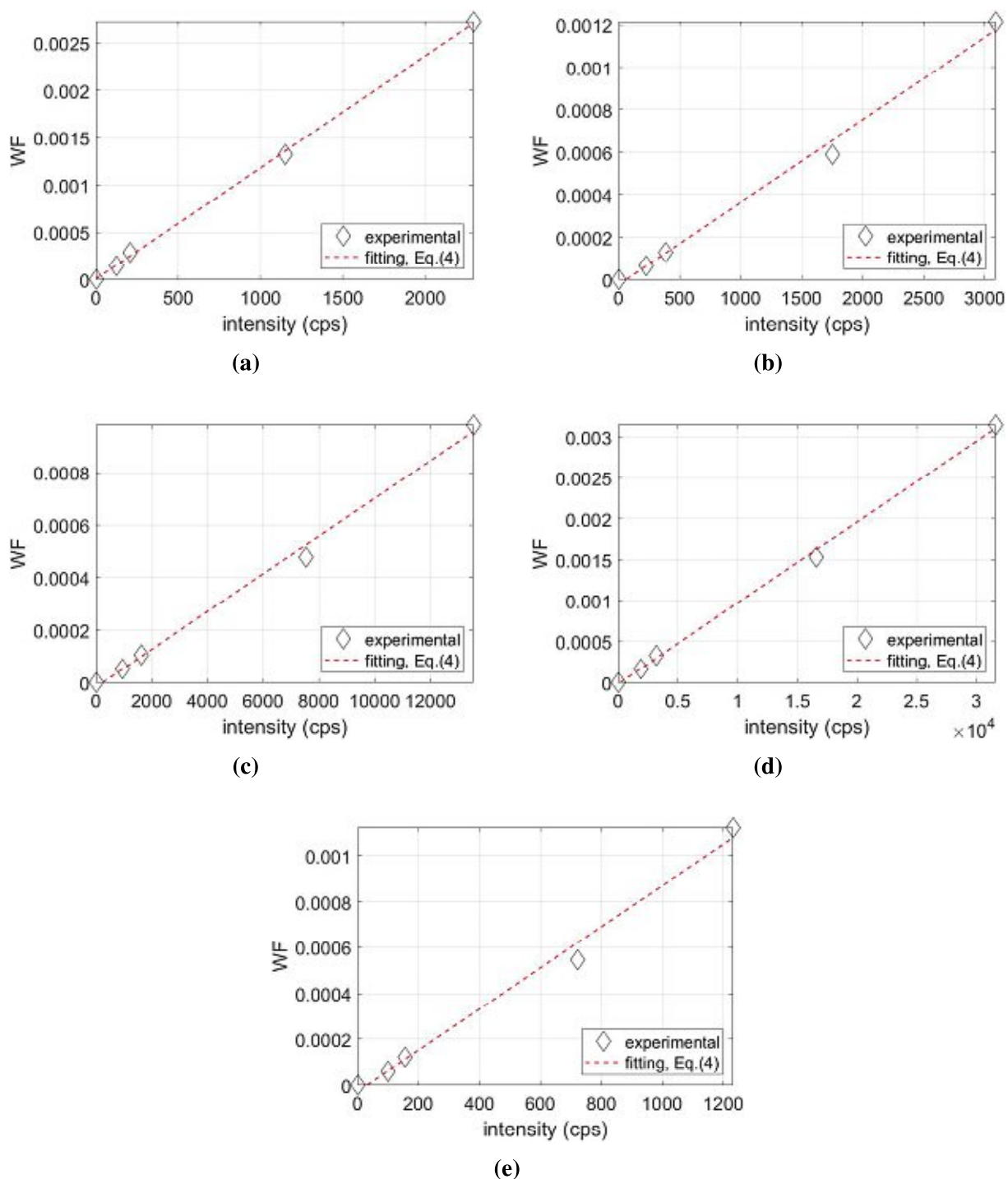


**Fig. 2.3:** Intensity-to-weight fraction conversion for the ions in the matrix-matched standards: (a) bromide, (b) copper, (c) iron, (d) iodine, and (e) zinc

## 2.2.4 Size effect-related re-evaluation of nanoindentation tests on jaws of *Nereis* and *Glycera*

Nanoindentation-tested hardness may not only depend on the chemical composition and the microstructure of the investigated material, but also on the indentation depths and the correspondingly tested three-dimensional domain below the indenting tip. Considering that the strength of the tested material is governed, according to Taylor [304], by the amount of dislocations in the aforementioned three-dimensional domain, Nix and Gao [216] derived the following relation between tested hardness and indentation depth

$$H^2 = H_0^2 \left( 1 + \frac{h^*}{h} \right) \quad (2.5)$$

with a size-independent hardness value  $H_0$  associated with infinitely large indentation depths, and a characteristic length  $h^*$  depending on indenter shape and material properties. Relation (2.5) was experimentally validated through tests on polycrystalline copper [197] and silver [187].

Herein, we check whether relation (2.5) may also hold for the material making up *Polychaeta* jaws. In this context, hardness values have been reported for *Glycera* and *Nereis* genera, by [42, 182, 210, 239]. These authors do not directly provide the indentation depths, however, they still give sufficient information from which the latter can be assessed. Namely, in case of a Berkovich indenter considered by Oliver and Pharr [222], the indentation depth is related to the maximum indentation force  $F_{max}$  via

$$h = \sqrt{\frac{F_{max}}{24.5H}} \quad (2.6)$$

and the maximum indentation forces applied to jaws of *Glycera* and *Nereis* have been reported in [42, 210, 239], see Table 2.7a. [182] do not provide explicit information on the maximum indentation force; however, the indenter contact area  $A_c$  can be assessed from the Fig.6(a) given in [182], and also this area gives access to the indentation depth, via [222],

$$h = \sqrt{\frac{A_c}{24.5}} \quad (2.7)$$

## 2.3 Results

### 2.3.1 Mechanical and chemical property distributions in *Platynereis dumerilii* jaw

The nanoindentation-probed hardness values according to Eq.(2.3) are only weakly correlated with the corresponding indentation depths, see Figure 4(a); and this holds true for the total set of all measurements, as it does for the subsets “middle” and “tip” according to Figure 2.2(d). This is even more the case for the reduced elastic modulus values according to Eq.(2.2), where hardly any correlation can be observed in Figure 4(a). Moreover, no significant correlation between reduced modulus and hardness values can be found, see Figure 4(c).

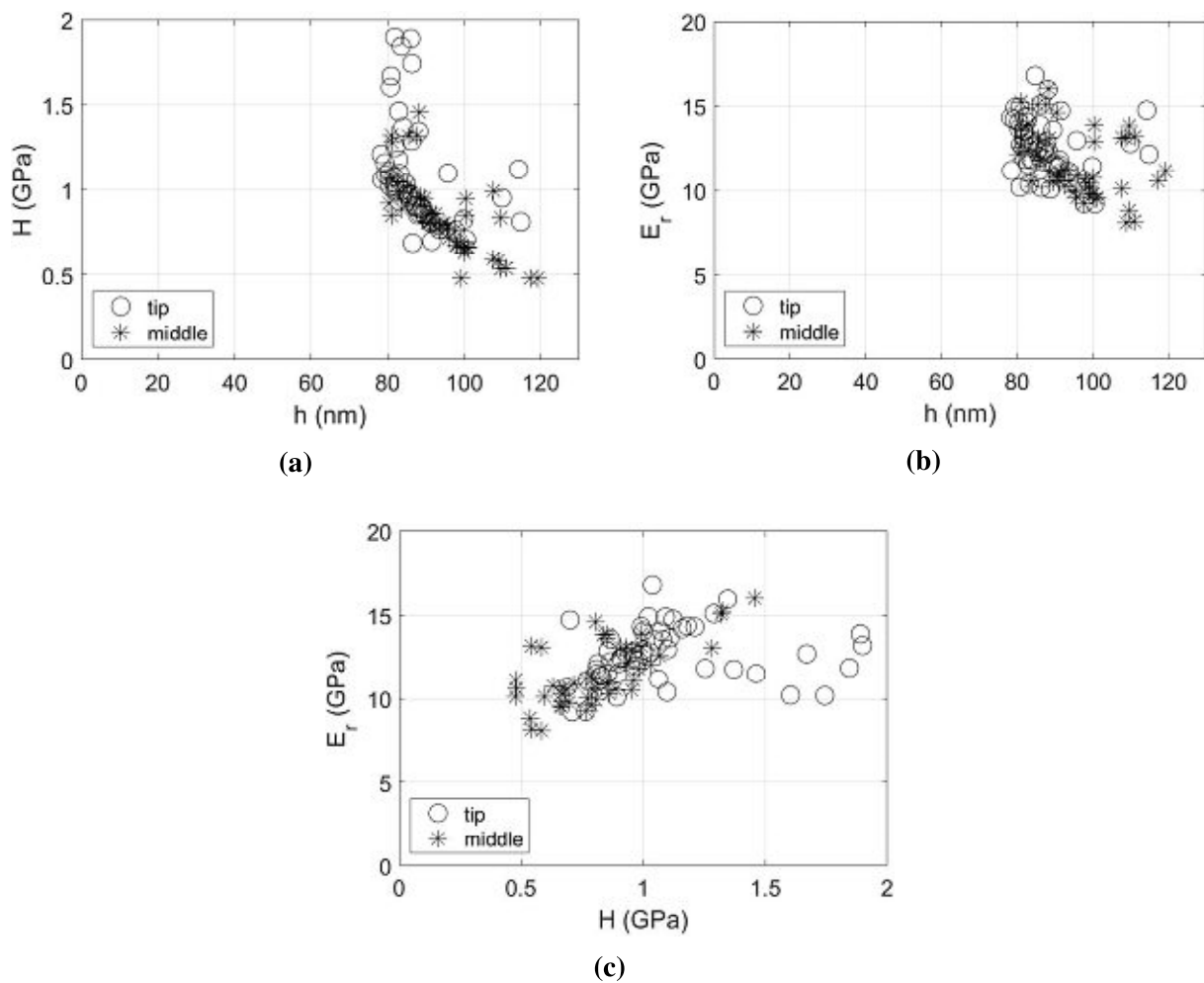


**Fig. 2.4:** Compilation of 156 nanoindentation-derived data sets: (a) Hardness versus indentation depth, (b) reduced elastic modulus versus indentation depth, and (c) reduced elastic modulus versus hardness values.

It is instructive to evaluate these nanoindentation-derived values in a statistical way, first by means of computing mean values and standard deviations, and of plotting histograms according to Scott's rule [280]: It turns out that the mean value over all 156 reduced elastic modulus values, 11.7 GPa, see Table 5(a), is slightly higher than the characteristic value of the most frequently inhabited histogram bin, amounting to 10.5 GPa, see Figure 5(b). The situation for the hardness values is different, where the mean value of 0.9 GPa does lie within the interval of the most inhabited histogram bin, see Figure 5(c).

Once we distinguish between the middle and the tip indentation regions, a slightly different picture emerges: As for the tip region, the mean value of the reduced modulus data, 12.7 GPa, see Table 5(a), lies within the most populated histogram bin, see Figure 5(d); while the mean value of the hardness data, 1.08 GPa, is slightly larger than the characteristic value of the most frequently inhabited histogram bin, amounting to 0.9 GPa, see Figure 5(e). As for the middle region, the mean values of both hardness and modulus data, 0.81 and 11.2 GPa, see Table 5(a), are slightly larger than the characteristic values of the most frequently populated histogram bins, which are 0.7 GPa and 10.5 GPa, see Figure 5(e) and Figure 5(d).

region	# of indents	$E$ (GPa)		$H$ (GPa)		$h$ (nm)	
		Eq. (2.2)	Eq. (2.2)	Eq. (2.3)	Eq. (2.3)	Eq. (2.6)	Eq. (2.6)
		$\bar{x}$	$\sigma$	$\bar{x}$	$\sigma$	$\bar{x}$	$\sigma$
all	156	11.68	1.80	0.90	0.27	93	9
tip	54	12.66	1.63	1.08	0.30	87	8
middle	102	11.17	1.68	0.81	0.20	95	9

(a)

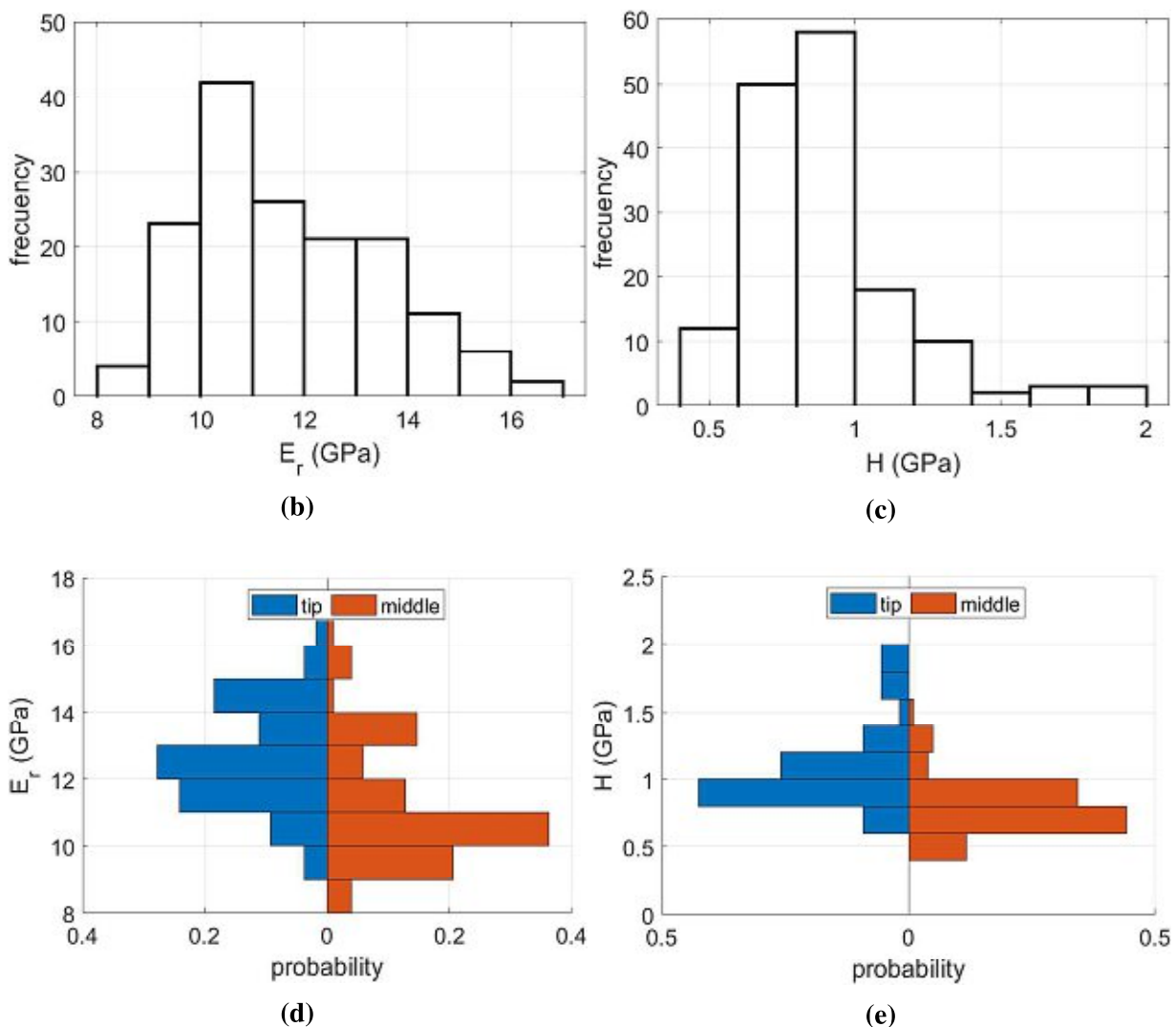


**Fig. 2.5:** Statistical evaluation of 156 nanoindentation experiments, 54 in the tip region and 102 in the middle region: (a) Mean values and standard deviations of reduced elastic modulus data and hardness data, (b) histogram over 156 reduced modulus values, (c) histogram over 156 hardness data values, (d) tip- and middle-related histograms of reduced modulus values, and (e) tip- and middle-related histograms of hardness values.

Deeper statistical analysis realized through software package IBM SPSS Statistics [140] concerns the question whether the data collected from the tip region may be significantly different from those collected in the middle region: Parametric tests, i.e. analysis of variance (ANOVA), cannot be applied due to the non-normal distribution nature of the data. Graphical interpretations of the data such as histograms are extremely helpful when judging normality. However, [203] recommends the combination of graphical interpretations with more rigorous numerical statistical test to conclude on the normal distribution of data. Thus, the Kolmogorov–Smirnov and the Shapiro-Wilk statistical tests were chosen to test further the normality of  $E$  and  $H$ , including the indentation data recollected from both the tip and the middle regions [286, 296]. Although [287] have found that the Shapiro-Wilk is the most powerful normality test, both performed test showed similar outcomes. The data sets turn out to be not normally distributed. Hence, non-parametric approaches are needed for finding out whether or not the data arising from the tip and middle indentation regions are similar. Accordingly, we resorted to the Mann-Whitney U and the Kruskal-Wallis H tests, which are non-parametric equivalents of parametric tests such as Student's t-test and ANOVA [64, 92, 162, 194, 291]. Our correspondingly tested null hypothesis was that there is no statistically significant difference between the indentation results obtained at the tip region and the middle region. However, after examining  $E$  and  $H$  results from both regions with the Mann-Whitney U and Kruskal–Wallis H tests showed that they both rejected our null hypothesis.

With this local differences in mind, it is instructive to study the ion distributions across the polished surface layer determined according to Section 2.2.3: Among all tested ions, zinc and iodine are much more concentrated in the jaw tip region than they are in the middle region, with maximum local weight fractions of up to almost 5% in the case of zinc, and up to more than 10% in the case of iodine, see Figures 6(d) and 6(e). Hence, the higher modulus and hardness values in the tip region when compared to the middle region, may well stem from the correspondingly higher concentrations of iodine and zinc. The situation is different when it comes to bromide, iron, and copper ions: Bromide ions are fairly uniformly distributed across the jaw and locally reach very high weight fractions of more than 20%, see Figure 6(a); copper ions are hardly present at all in the investigated *Platynereis dumerilli* jaw, see Figure 6(b); and iron ions, at weight fractions reaching almost 9%, are more frequently present in the middle region than they are in the tip region, see Figure 6(c).

### 2.3.2 Trans-species size effect law for hardness of jaws across different *Polychaeta*

The species-specifically averaged hardness values reported by [182] for *Nereis limbata*, by [42] for *Nereis virens*, by [239] and by [210] for *Glycera dibranchiata*, as well as by us, in Fig. 5(a), for *Platynereis dumerilli*, virtually perfectly follow Nix-Gao's size effect law Eq. (2.5), see Figure 7(b). This is underlined by an impressively large coefficient of determination amounting to  $R^2 = 99.7\%$ . The size-independent hardness and indentation quantities amount to  $H_0 = 0.53$  GPa and  $h^* = 0.13$   $\mu\text{m}$ .



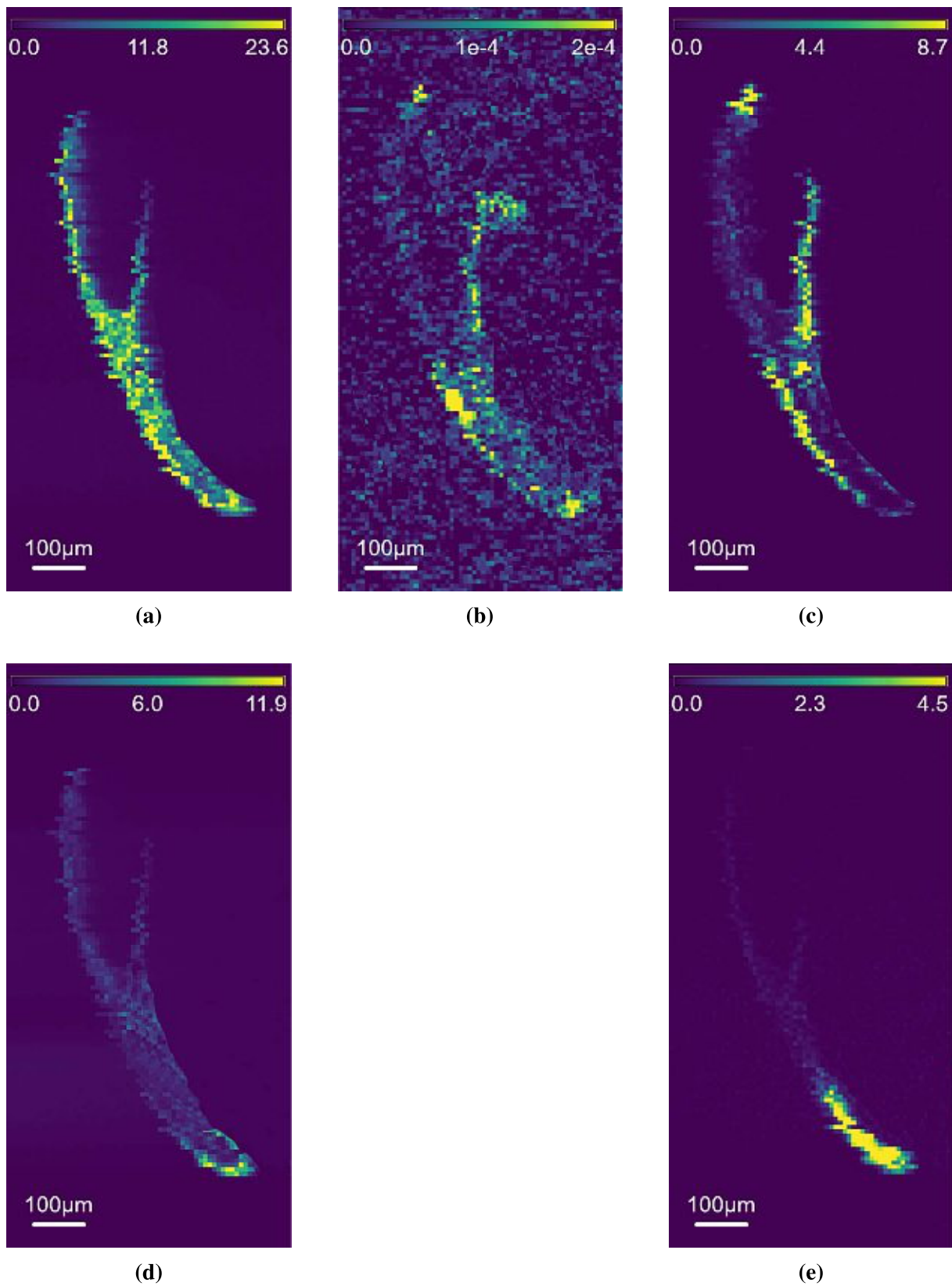
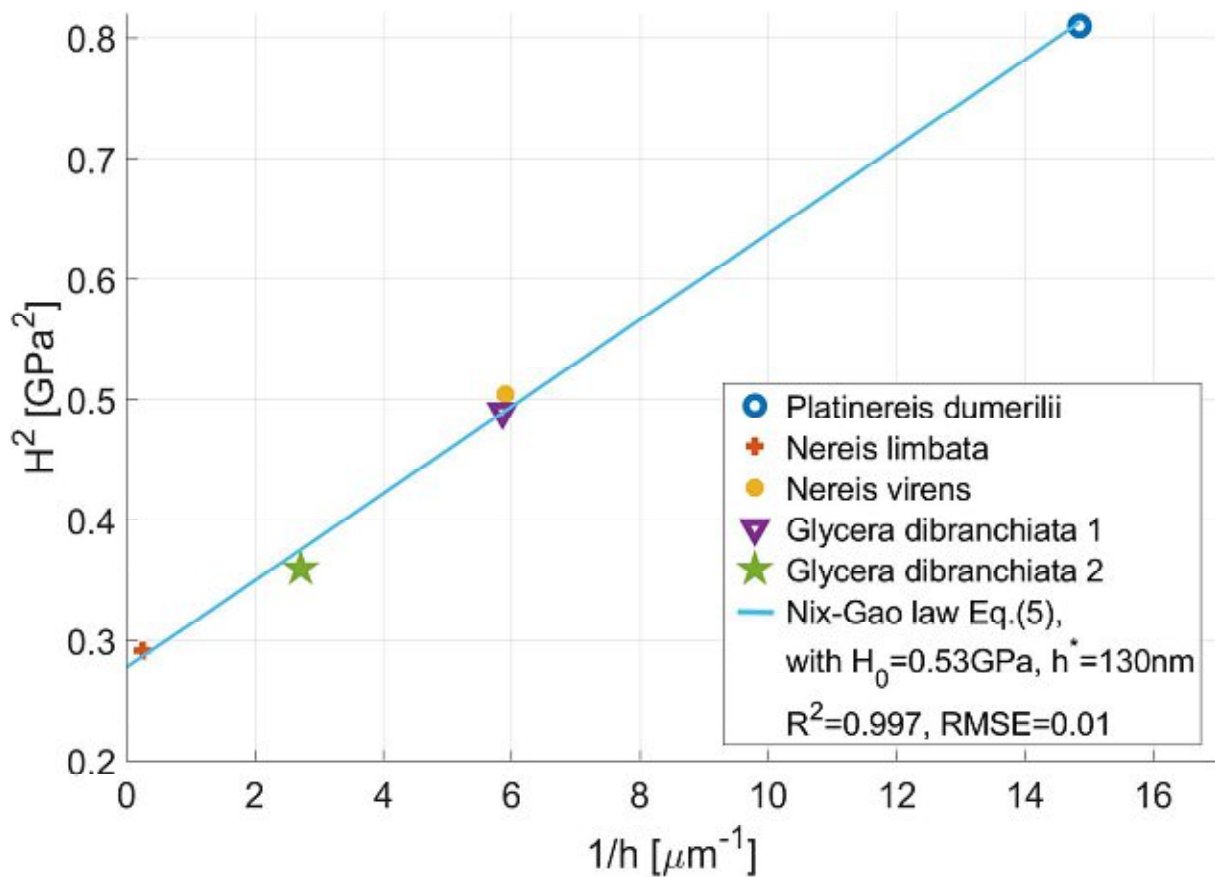


**Fig. 2.6:** Ion concentration distribution in *Platynereis dumerilli* jaw, in terms of ion weight fractions in %, resolved down to a pixel size of 10 microns: (a) bromide, (b) copper, (c) iron, (d) iodine, (e) zinc

species	source	indent direct	# indents	H [GPa]	$F_{max}$ [mN]	$A_c$ [ $\mu\text{m}^2$ ]	$h$ Eq.(2.6),(2.7) [ $\mu\text{m}$ ]
<i>P. dumerilii</i>	this study	D-V	156	0.90	0.1	0.1	0.07
<i>N. limbiata</i>	[182]	D-V	$\approx 50$	0.54	-	389.7	4.00
<i>N. virens</i>	[42]	A-P	$\approx 80$	0.71	0.5	-	0.17
<i>G. dibranchiata</i> 1	[239]	A-P	$\approx 40$	0.70	0.5	-	0.17
<i>G. dibranchiata</i> 2	[210]	A-P	$\approx 200$	0.60	2.0	-	0.37

(a)



(b)

**Fig. 2.7:** Nix-Gao size effect law across different species of *Polychaeta*:(a) tabular representation of experimental sources used for the determination of hardness and indentation depth; (b) graphical representation

## 2.4 Discussion

To the best knowledge of the authors, this is the first systematic experimental study on the chemical and mechanical properties, namely nanoindentation-probed hardness and reduced modulus as well as LA-ICP-MS- and calibration standard-derived ionic concentration distributions, across a jaw harvested from a bristle worm of species *Platynereis dumerilli*, a key model organism in marine biology.

The novel experimental results may be evaluated and discussed in terms of three major traditions found in the nanoindentation and applied material mechanics literature:

1. histogram representations
2. chemo-mechanical couplings
3. size effect laws for metals

With respect to histogram representations, distributions with only one peak were observed, see Figure 2.5, indicating that only one material phase was present at the observation scale tested by the nanoindentation device, which is about one half to one third of the indentation depth [141], i.e. around 33 to 50 nm.

With respect to chemo-mechanical couplings, larger zinc and iodine concentrations found in the tip region of the jaw are correlated with slightly, but still statistically significantly larger hardness and elasticity properties in the tip region; an effect which has been extensively in the literature on other bristle worm jaws [27, 42, 44, 180, 182, 210, 239].

However, the probably most remarkable original insight comes from setting our novel data in context with existing data on much larger bristle worm species tested at much larger indentation depths. The differences between the hardness tested herein, and the hardness values reported earlier, exceeding the variations having been reported as results from local ionic concentration variations, can be beautifully explained through the size effect law of [216], see Figure 7(b). This proposes that all species within the large *Polychaeta* class may share one basic architectural building block: ion-spiked structural proteins, with “universal”, i.e. species-invariant, hardness properties always following the Nix-Gao size effect law, hence sharing a mechanics-related hallmark with crystalline metals, i.e. with highly resistant and load-bearing material with high ductility. However, metals are produced at high temperatures with high energy consumption, while the ion-spiked high performance structural proteins are laid down in a biologically set, highly intricate 3D printing process. We regard this as very fascinating and inspiring for reaching out towards novel, unprecedented opportunities in the wide field of bioengineering. This is very remarkable also insofar as the aforementioned architectural building block is fundamentally different from those found in vertebrates. There, two main types of building blocks, structural proteins (such as collagen) and metal ions forming minerals (such as calcium being part of hydroxyapatite) are combined into nano-composites governing the mechanical properties of tissues such as bone [105]. The minerals, thereby, are much more brittle than the herein discussed ion-spiked proteins, with size effect properties far off the Nix-Gao law [150].

## Acknowledgements

This project was financially supported by the Austrian Academy of Sciences (OEAW), through the project Bio3DPrint.

# Chapter 3

## “Variances” and “invariances” in porosity and composition in various femoral tissues

### “Variances” and “in-variances” in hierarchical porosity and composition, across femoral tissues from cow, horse, ostrich, emu, pig, rabbit, and frog

**Authored by:** Luis Zelaya-Lainez<sup>1</sup>, Hawraa Kariem<sup>1</sup>, Winfried Nischkauer<sup>2</sup>,  
Andreas Limbeck<sup>2</sup>, and Christian Hellmich<sup>1</sup>

**Published in:** *Materials Science and Engineering: C*  
**DOI:** 10.1016/j.msec.2020.111234

#### Abstract

It is very well known that bone is a hierarchically organized material produced by bone cells residing in the fluid environments filling (larger) vascular pores and (smaller) lacunar pores. The extracellular space consists of hydroxyapatite crystals, collagen type I molecules, and water with non-collageneous organics. It is less known to which extent the associated quantities (mineral, organic, and water concentrations; vascular, lacunar, and extracellular porosities) vary across species, organs, and ages. We here investigate the aforementioned quantities across femoral shaft tissues from cow, horse, emu, frog, ostrich, pig, and rabbit; by means of light microscopy and dehydration-demineralization tests; thereby revealing interesting invariances: The extracellular volume fractions of organic matter turn out to be similar across all tested non-amphibian tissues; as do the extracellular volume fractions of hydroxyapatite across all tested mammals.

<sup>1</sup>Institute for Mechanics of Materials and Structures, Vienna University of Technology (TU Wien), Karlsplatz 13/E202, 1040 Vienna, Austria.

<sup>2</sup>Institute of Chemical Technologies and Analytics, Division of Instrumental Analytical Chemistry, Vienna University of Technology (TU Wien), Getreidemarkt 9/164, 1060 Vienna, Austria.

Hence, the chemical composition of the femoral extracellular bone matrix is remarkably “invariant” across differently aged mammals; while the water content shows significant variations, as does the partitions of water between the different pore spaces. The latter exhibit strikingly varying morphologies as well. This finding adds to the ample “universal patterns” in the sense of evolutionary developmental biology; and it provides interesting design requirements for the development of novel biomimetic tissue engineering solutions.

# Chapter 4

## Multiscale elasticity of grooved rail steel

### Multiscale and multitechnique investigation of the elasticity of grooved rail steel

**Authored by:** Valentin Jagsch<sup>1</sup>, Patricia Kuttke<sup>1</sup>, Olaf Lahayne<sup>1</sup>, Luis Zelaya-Lainez<sup>1</sup>, Stefan Scheiner<sup>1</sup>, Christian Hellmich<sup>1</sup>

**Published in:** *Construction and Building Materials*

**DOI:** 10.1016/j.conbuildmat.2019.117768

#### Abstract

Tramway rail steel is exposed to extreme temperature conditions both during production (e.g. in terms of heat treatment) and over its decades-to-century-long service life (e.g. in terms of welding operations in the course of maintenance). The question arises whether this induces local stiffness reductions and hence stiffness inhomogeneities at the half-millimeter level; i.e. the characteristic size governing the structural behavior of the rail. In order to address this question, a series of 16800 nanoindentation tests, with indentation depths ranging from 200 to 250 nm (characterizing 66- to 125 nm-sized material volumes), were performed on samples with less than 10 nm surface roughness, extracted from different locations of typical tramway rail cross sections at different time points during their service lives, and including both heat-affected and non-heat-affected zones. Thereby, each of these locations was probed through a grid of 20×20 nanoindentations, with a grid spacing of 500 microns. In very few cases, the indentation tip was probably moved into cracks of several microns width and tens-to-hundreds of microns length; as seen on light and electron micrographs. Zero-stiffness was assigned to the corresponding grid points. The probability distributions of the remaining, non-zero elastic moduli were fitted by one to four weighted Gaussians, representing all (non-zero) nanoindentation data as well as particular data subsets (namely data from each testing grid, data from each testing location across all rails, data from each rail, all data from heat-affected zones, and all data from non-heat-affected zones).

<sup>1</sup>Institute for Mechanics of Materials and Structures, Vienna University of Technology (TU Wien), Karlsplatz 13/E202, 1040 Vienna, Austria.

The aforementioned Gaussians refer to different solid elastic material phases, with expected Young's moduli ranging approximately from 100 to around 300 GPa, potentially reflecting different dislocation densities. On the other hand, at a larger material scale (i.e., that of 220 to 440 microns, tested through 2.25 MHz ultrasonics), the stiffness is reduced to approximately 213 GPa (from a mean nanoindentation-derived value of approximately 246 GPa). This reduction can be explained by a micromechanical model, with the intact steel stiffness as well as with crack sizes and crack numbers as input quantities.



# Chapter 5

## Pore spaces of fired bricks used across the European industry

### A multitechnique, quantitative characterization of the pore space of fired bricks made of five clayey raw materials used in European brick industry

**Authored by:** Thomas Buchner<sup>1</sup>, Thomas Kiefer<sup>1</sup>, Luis Zelaya-Lainez<sup>1</sup>, Wolfgang Gaggl<sup>2</sup>, Thomas Konegger<sup>3</sup>, and Josef Füssl<sup>1</sup>

**Published in:** *Applied Clay Science*

**DOI:** 10.1016/j.clay.2020.105884

#### Abstract

The development and improvement of brick materials is still based on empirical knowledge and large testing series. To enable a physically based optimization in terms of thermal and mechanical properties of clay bricks, detailed knowledge of their microstructure is required. We here present comprehensive investigations on the pore space of bricks made of five different clayey raw materials used in European brick production. Application and combination of micro-computed tomography and scanning electron microscopy delivered precise pore size distributions based on the real pore diameter and unaffected by the pore throat. The former also enabled to resolve the 3D pore structure down to a pore diameter of approximately 5.5 micrometers and gave access to porosity distributions over the sample's thickness. Furthermore, the brick's true densities were determined applying the Archimedes' principle and verified by helium pycnometry measurements. The extensive database generated in this work and the linking of results from different methods allow for new insights and a better understanding of these often used brick materials.

<sup>1</sup>Institute for Mechanics of Materials and Structures, Vienna University of Technology (TU Wien), Karlsplatz 13/E202, 1040 Vienna, Austria.

<sup>2</sup>Wienerberger AG, Wienerbergstraße 11, 1100 Vienna, Austria

<sup>3</sup>Institute of Chemical Technologies and Analytics, Vienna University of Technology (TU Wien), Getreidemarkt 9/164, 1060 Vienna, Austria.

# Chapter 6

## Conclusions and outlook

The optimization of the mechanical properties of materials depend undoubtedly in the systematic study of their micro-structure and composition. The present work expanded the morphological, chemical, and mechanical understanding of biological and man-made materials. The present work aims to fill the void in the literature and enables future research on the microstructure of *Polychaeta*, bone, steel, and bricks. Nevertheless, the newly developed protocols and methods are not limited to the materials targeted in Chapters 2, 3, 4, or 5. Detailed conclusions of the main findings are described in each of the Chapters. Nevertheless, summarized conclusions and a research outlook for each Chapter is presented in the following paragraphs.

In Chapter 2 we investigated an organ of a animal which mechanically and chemically was unknown until the present work. The jaws of the *Polychaeta Platynereis dumerilii* were polished by means of a novel polishing protocol resulting in low roughness in such a small scale. This made it possible to achieve low indentation depths and therefore, study the jaw at a level never achieved before. When compared to genetically “similar” *Polychaeta* at different indentation depths, the results show that studies performed on jaws from *Nereis* and *Glycera* specimens display a lower hardness than the jaws of *Platynereis dumerilii*. This surprising result can be attributed to the Nix-Gao-type indentation size effect [216]. This effect has been normally observed in crystalline metals. This outstanding mechanical behavior came as a surprise. *Platynereis dumerilii*, as well as other *Polychaeta*, 3D print or extrude jaws which demonstrate high performance, as well as intricate and complex designs by biological processes. Meanwhile, crystalline metals normally require high amounts of energy to achieve the same. This study was complemented by the chemical investigation of the jaw through a novel Laser Ablation Inductively Coupled Plasma Mass Spectrometry protocol. The chemical analysis showed the existence of halogen ions which can create macro-molecules. The macro-molecules are assumed to be proteins similar to the ones reported in other *Polychaeta* [27, 42, 44, 180, 182, 210, 239]. Although this assumption is based on published scientific data, our recent discoveries have preliminary showed that the halogen ions could also bind together into a “super” macromolecule, tentatively named *Platynereis dumerilii* JP1 (PladuJP1). Meaning the jaws of *Platynereis dumerilii* could further proof to be an important exception to biological “building blueprints” seen normally in organs from more studied animals as discussed in Chapter 3. Thus, the jaws of *Platynereis dumerilii* could be built by an organic mixture of the macro-molecule PladuJP1 and possibly chitin. The challenging polishing and indentation protocol together with the chemical analysis are a first stepping stone in describing the mechanical properties of such a “peculiar” animal. This opens a new frontier in the investigation of *Polychaeta*, and sets a new standard in testing biological materials which exhibit crystalline-metals-like behaviors.

In Chapter 3 we discussed the existence of “universal” patterns at the ultra-structural level of femoral bone. The cortical parts of femurs from bovine, equine, porcine, leporine, ranine, and struthionine specimens were studied by means of dehydration-demineralization protocols, and complemented by microscopy techniques. The results show that there is a quantitative similarity among the mammalian specimens at the ultra-structural level. Meaning the main building blocks of bone, i.e. organic, mineral, and water parts, were quantified as statistically similar at ultra-structural level. The similarities of the organic and mineral parts were only possible by the implementation of a demineralization protocol using ethylenediaminetetraacetic acid. The assurance of the level of demineralization was achieved by a novel Inductively Coupled Plasma Mass Spectrometry protocol. This protocol is quiet sensitive to contaminants and thus, special care is required whenever handling the samples. The main differences among the species appear at the larger micro-structural level, and to be more specific the vascular and the lacunar porosities. The quantification of porosities was only possible by the implementation of novel polishing protocols using a circular polishing system and an ultra-miller with an attached diamond blade. The polishing results were satisfactory when submitting the captured light microscope images to a threshold protocol and analysis. Now that we know through this experimental campaign the similarities and differences of one single organ, the femur, among several different species, we can expand the protocols to a different organ. At the macroscopic organ level, other bony organs such as vertebrae appear to be less mineralized than femoral tissues [115, 244, 325]. Meaning, the intra-species differences within an organism are greater than a inter-species comparison in-between species when comparing one individual organ. The implementation of the well defined protocol define in Chapter 3 can make further correlations of how bone is build at the ultra-structural level for different organs, and more importantly, translate it to understanding in more detail the human ultra structural bone. This could facilitate mathematical models and finite elements simulations, which can results in a better estimation of fracture risk determination, conveying possibly into a better patient specific assessment [244].

In Chapter 4, rail-way steel was investigated by means of nano-indentation and several microscopy techniques such as light microscopy and scanning electron microscopy. Steel used for rail-way applications is normally submitted to heat treatments to increase certain micro-mechanical properties of the material, such as wear resistance. Nevertheless, this process creates nano- and micro-structural “imperfections”, or cracks that can were observed by means of a scanning electron microscopy protocol. This explains the decrease in stiffness obtained by ultra-sound techniques (213 GPa) when compared to the results obtained by means of statistical nano-indentation on the intact areas of the structure (246 GPa). The belief that heat treated steel seems perfectly plastic is compromised by these surprising results, and in the future, railway engineering can be greatly improved by the discovery and consideration of these nanoscopical manufacturing imperfections.

Chapter 5 expands with bricks from five different clayey raw materials on the original work of [146]. This Chapter considered different microscopy techniques such as mercury intrusion porosimetry, Archimedes’ principle, microcomputed tomography, and scanning electron microscopy to characterize porosity at different scales, and therefore, expand the database on clayey raw materials for brick production in Central Europe. These pores and their morphology are introduced by different forming agents such as expanded polystyrene, paper sludge or sawdust. Mercury intrusion porosimetry and Archimedes’ principle provided true density of the different materials. This was additionally confirmed by findings through helium pycnometry. Furthermore,

the before-mentioned methods revealed a low degree of closed pores in all the investigated samples, confirming past finding of [146]. To obtain pore gradients across the volume of the microstructure of brick, samples of the bricks were investigated by means of microcomputed tomography. The latter also provided information about the influences of preparation and firing of the bricks on the porosity. However, the resolution limited the size of pores we could detect. Therefore, the samples had to carefully polished until achieving RMS roughness of around 20 nm or less, and later investigated by means of scanning electron microscopy to observe the structure of the smallest pores. Employing microcomputed tomography and scanning electron microscopy, we could characterize pores at different scales. Interestingly, we found out “universal” occurrences in the pore formation such as the low degree of collapsed or closed pores, and a higher porosity in the center of the samples in comparison to the edges. This information can be definitely useful for the optimization of brick production, due to the correlation between the brick’s preparation and firing with its porosity.

# Bibliography

- [1] T. Abdalrahman, S. Scheiner, and C. Hellmich. “Is the trabecular bone permeability governed by molecular ordering induced fluid viscosity gain? Arguments from re-evaluation of experimental data in the framework of homogenization theory.” In: *Journal of Theoretical Biology* 365 (2015), pp. 433–444.
- [2] T. Ahn, K. Um, J. Choi, D. Kim, K. Oh, M. Kim, and H. Han. “Small-scale mechanical property characterization of ferrite formed during deformation of super-cooled austenite by nanoindentation”. In: *Materials Science and Engineering A* 523 (2009), pp. 173–177.
- [3] O. Akkus, A. Polyakova-Akkus, F. Adar, and M. B. Schaffler. “Aging of microstructural compartments in human compact bone.” In: *Journal of Bone and Mineral Research* 18 (2003), pp. 1012–1019.
- [4] O. Akselsen, G. Rørvik, M. Onsjøien, and Ø. Grong. “Assessment and predictions of HAZ tensile properties of high-strength steels”. In: *Welding Research Supplement* (1989), 356s–362s.
- [5] I. Allegretta, G. Eramo, D. Pinto, and A. Hein. “The effect of mineralogy, microstructure and firing temperature on the effective thermal conductivity of traditional hot processing ceramics”. In: *Applied Clay Science* 135 (2017), pp. 260–270.
- [6] I. Allegretta, G. Eramo, D. Pinto, and A. Hein. “The effect of temper on the thermal conductivity of traditional ceramics: Nature, percentage and granulometry”. In: *Thermochimica Acta* 581 (2014), pp. 100–109.
- [7] R. Almany-Magal, N. Reznikov, R. Shahar, and S. Weiner. “Three-dimensional structure of minipig fibrolamellar bone: Adaptation to axial loading.” In: *Journal of Structural Biology* 186 (2014), pp. 253–264.
- [8] A. Ardizzoni. “Osteocyte lacunar size–lamellar thickness relationships in human secondary osteons.” In: *Bone* 28 (2001), pp. 215–219.
- [9] D. Arendt, K. Tessmar, M.-I. M. de Campos-Baptista, A. Dorresteijn, and J. Wittbrodt. “Development of pigment-cup eyes in the polychaete *Platynereis dumerilii* and evolutionary conservation of larval eyes in Bilateria”. In: *Development* 129.5 (2002), pp. 1143–1154.
- [10] A. Atkins, M. Dean, M. Habegger, P. Motta, L. Ofer, F. Repp, A. Shipov, S. Weiner, J. Currey, and R. Shahar. “Remodeling in bone without osteocytes Billfish challenge bone structure-function paradigms.” In: *Proceedings of the National Academy of Sciences* 111 (2014), pp. 16047–16052.
- [11] P. Atkinson and A. Hallsworth. “The Changing Pore Structure of Aging Human Mandibular Bone”. In: *Gerodontology* 2 (1983), pp. 57–66.

- [12] J. V. Audouin and H. Milne-Edwards. *Recherches pour servir à l'histoire naturelle du littoral de la France, ou Recueil de mémoires sur l'anatomie, la physiologie, la classification et les mœurs des animaux des nos côtes*. Vol. 1. Crochard, 1832.
- [13] P. Auffinger, F. A. Hays, E. Westhof, and P. S. Ho. "Halogen bonds in biological molecules". In: *Proceedings of the National Academy of Sciences* 101.48 (Nov. 2004), pp. 16789–16794. doi: 10.1073/pnas.0407607101.
- [14] J.-L. Auriault, C. Boutin, and C. Geindreau. *Homogenization of Coupled Phenomena in Heterogeneous Media*. Wiley-Iste, 2009.
- [15] Austrian Standards Institute. *ÖNORM EN 14811: Bahnanwendungen – Oberbau – Speziialschienen – Rillenschienen und zugehörige Konstruktionsprofile [Railway Applications – Superstructure – Special Rails – Grooved Rails and Related Construction Profiles]*. 2010.
- [16] B. Ay, K. Parolia, R. S. Liddell, Y. Qiu, G. Grasselli, D. M. Cooper, and J. E. Davies. "Hyperglycemia compromises Rat Cortical Bone by Increasing Osteocyte Lacunar Density and Decreasing Vascular Canal Volume." In: *Communications Biology* 3 (2020), p. 20.
- [17] A. Bailey. "Molecular mechanisms of ageing in connective tissues." In: *Mechanisms of Ageing and Development* 122 (2001), pp. 735–755.
- [18] R. Bartusch and F. Händle. *Extrusion in Ceramics*. Ed. by F. Händle. Springer-Verlag, 2007.
- [19] K. Begall and U. Vorwerk. "Artificial Petrous Bone Produced by Stereolithography for Microsurgical Dissecting Exercises." In: *ORL* 60 (1998), pp. 241–245.
- [20] R. Benedix. *Bauchemie–Einführung in die Chemie für Bauingenieure und Architekten*. Ed. by R. Hams. Vol. 6. Springer Vieweg, 2015. ISBN: 978-3-658-04143-4. doi: 10.1007/978-3-658-04144-1.
- [21] D. P. Bentz, D. A. Quenard, H. M. Kunze, J. Baruchel, F. Peyrin, N. S. Marty, and E. Garboczi. "Microstructure and transport properties of porous building materials. II: Three-dimensional X-ray tomographic studies". In: *Materials and Structures* 33 (2000), pp. 147–153. doi: 10.1007/bf02479408. url: <https://doi.org/10.1007/bf02479408>.
- [22] E. Bertrand and C. Hellmich. "Multiscale Elasticity of Tissue Engineering Scaffolds with Tissue-Engineered Bone: A Continuum Micromechanics Approach". In: *Journal of Engineering Mechanics* 135 (2009), pp. 395–412.
- [23] H. Bhadeshia and R. Honeycombe. *Steels: Microstructure and Properties*. 4th. Elsevier, Amsterdam, 2017.
- [24] R. Bhowmik, K. S. Katti, and D. R. Katti. "Mechanics of molecular collagen is influenced by hydroxyapatite in natural bone." In: *Journal of Materials Science*. 42 (2007), pp. 8795–8803.
- [25] R. Bhowmik, K. S. Katti, and D. R. Katti. "Mechanisms of Load-Deformation Behavior of Molecular Collagen in Hydroxyapatite-Tropocollagen Molecular System: Steered Molecular Dynamics Study." In: *Journal of Engineering Mechanics*. 135 (2009), pp. 413–421.

- [26] R. M. Biltz and E. D. Pellegrino. “The Chemical Anatomy of Bone”. In: *The Journal of Bone and Joint Surgery* 51 (1969), pp. 456–466.
- [27] H. Birkedal, R. K. Khan, N. Slack, C. Broomell, H. C. Lichtenegger, F. Zok, G. D. Stucky, and J. H. Waite. “Halogenated Veneers: Protein Cross-Linking and Halogenation in the Jaws of Nereis, a Marine Polychaete Worm”. In: *ChemBioChem* 7.9 (Aug. 2006), pp. 1392–1399. doi: 10.1002/cbic.200600160.
- [28] G. Boivin and P. Meunier. “The Degree of Mineralization of Bone Tissue Measured by Computerized Quantitative Contact Microradiography.” In: *Calcified Tissue International* 70 (2002), pp. 503–511.
- [29] L. Bonar, S. Lees, and H. Mook. “Neutron diffraction studies of collagen in fully mineralized bone.” In: *Journal of Molecular Biology* 181 (1985), pp. 265–270.
- [30] M. Bonta, H. Lohninger, V. Laszlo, B. Hegedus, and A. Limbeck. “Quantitative LA-ICP-MS imaging of platinum in chemotherapy treated human malignant pleural mesothelioma samples using printed patterns as standard”. In: *J. Anal. At. Spectrom.* 29.11 (2014), pp. 2159–2167. doi: 10.1039/c4ja00245h.
- [31] E. Bonucci. *Mechanical testing of bone and the bone-implant interface*. New York City, USA: CRC Press LLC, 2000.
- [32] E. Bossy, M. Talmant, F. Peyrin, L. Akrouf, P. Cloetens, and P. Laugier. “In vitro study of the ultrasonic axial transmission technique at the radius: 1 MHz velocity measurements are sensitive to both mineralization and intracortical porosity.” In: *Journal of Bone and Mineral Research* 19 (2004), pp. 1548–1556.
- [33] Y. Bouligand. “Les soies et les cellules associées chez deux Annélides Polychètes”. In: *Zeitschrift für Zellforschung und mikroskopische Anatomie* 79.3 (1967), pp. 332–363.
- [34] J. Bourret, N. Tessier-Doyen, R. Guinebretiere, E. Joussein, and D. S. Smith. “Anisotropy of thermal conductivity and elastic properties of extruded clay-based materials: Evolution with thermal treatment”. In: *Applied Clay Science* 116-117 (2015), pp. 150–157. doi: 10.1016/j.clay.2015.08.006. URL: <http://dx.doi.org/10.1016/j.clay.2015.08.006>.
- [35] V. Bousson, F. Peyrin, C. Bergot, M. Hausard, A. Sautet, and J. Laredo. “Cortical bone in the human femoral neck: Three dimensional appearance and porosity using synchrotron radiation.” In: *Journal of Bone and Mineral Research*. 19 (2004), pp. 794–801.
- [36] M. L. Bouxsein, S. K. Boyd, B. A. Christiansen, R. E. Guldberg, K. J. Jepsen, and R. Müller. “Guidelines for assessment of bone microstructure in rodents using micro-computed tomography.” In: *Journal of Bone and Mineral Research* 25 (2010), pp. 1468–1486.
- [37] A. Bracka and Z. Rusin. “Comparison of pore characteristics and water absorption in ceramic materials with frost resistance factor, Fc”. In: *Structure and Environment* 4.3 (2012), pp. 15–19.
- [38] A. Bravin, P. Coan, and P. Suortti. “X-ray phase-contrast imaging: from pre-clinical applications towards clinics”. In: *Physics in Medicine & Biology* 58.1 (2012), R1–R35.
- [39] S. Brenner. “Tensile strength of whiskers”. In: *Journal of Applied Physics* 27 (1956), pp. 1484–1491.

- [40] G. W. Brindley and G. Brown. “Crystal Structures of Clay Minerals and their X-ray Identification”. In: *Mineralogical Society of Great Britain and Ireland* 5 (1980), p. 495.
- [41] G. W. Brindley and M. Nakahira. “The Kaolinite-Mullite Reaction Series: II, Metakaolin”. In: *Journal of the American Ceramic Society* 42.7 (1959), pp. 314–318. doi: 10.1111/j.1151-2916.1959.tb14315.x. URL: <http://dx.doi.org/10.1111/j.1151-2916.1959.tb14315.x>.
- [42] C. Broomell, F. Zok, and J. Waite. “Role of transition metals in sclerotization of biological tissue”. In: *Acta Biomaterialia* 4.6 (2008), pp. 2045–2051.
- [43] C. C. Broomell, S. F. Chase, T. Laue, and J. H. Waite. “Cutting edge structural protein from the jaws of *Nereis virens*”. In: *Biomacromolecules* 9.6 (2008), pp. 1669–1677.
- [44] C. C. Broomell, M. A. Mattoni, F. W. Zok, and J. H. Waite. “Critical role of zinc in hardening of *Nereis* jaws”. In: *Journal of Experimental Biology* 209.16 (2006), pp. 3219–3225.
- [45] J. G. Bryan. “The Generalized Discriminant Function: Mathematical Foundations and Computational Routine”. In: *Harvard Educational Review* 21 (1951), pp. 90–95.
- [46] J. Buckwalter, M. Glimcher, R. Cooper, and R. Recker. “Bone biology. I: Structure, blood supply, cells, matrix, and mineralization.” In: *The Journal of Bone and Joint Surgery* 77.8 (1996), pp. 1256–1275.
- [47] B. Budiansky and R. O’Connell. “Elastic moduli of a cracked solid”. In: *International Journal of Solids and Structures* 12.2 (1976), pp. 81–97.
- [48] J. Burket, S. Gourion-Arsiquaud, L. M. Havill, S. P. Baker, A. L. Boskey, and M. C. van der Meulen. “Microstructure and nanomechanical properties in osteons relate to tissue and animal age.” In: *Journal of Biomechanics* 44 (2011), pp. 277–284.
- [49] C. M. Burns. “The effect of the continued ingestion of mineral acid on growth of body and bone and on the composition of bone and of the soft tissues”. In: *Biochemical Journal* 23 (1929), pp. 860–867.
- [50] A. Busch, K. Schweinar, N. Kampman, A. Coorn, V. Pipich, A. Feoktystov, L. Leu, A. Amann-Hildenbrand, and P. Bertier. “Determining the porosity of mudrocks using methodological pluralism”. In: *Geological Society, London, Special Publications* 454.1 (2017), pp. 15–38.
- [51] W. Butler. “Matrix macromolecules of bone and dentin”. In: *Collagen and Related Research* 297.6 (1984), pp. 297–307.
- [52] M. de Castro Fonseca, B. H. S. Araujo, C. S. B. Dias, N. L. Archilha, D. P. A. Neto, E. Cavalheiro, H. Westfahl, A. J. R. da Silva, and K. G. Franchini. “High-resolution synchrotron-based X-ray microtomography as a tool to unveil the three-dimensional neuronal architecture of the brain”. In: *Scientific Reports* 8.1 (Aug. 2018). doi: 10.1038/s41598-018-30501-x.
- [53] Z. Cheng, Z. Ning, H. Zhao, Q. Wang, Y. Zeng, X. Wu, R. Qi, and S. Zhang. “A comprehensive characterization of North China tight sandstone using micro-CT, SEM imaging, and mercury intrusion”. In: *Arabian Journal of Geosciences* 12 (2019), p. 407. doi: 10.1007/s12517-019-4568-9. URL: <https://doi.org/10.1007/s12517-019-4568-9>.



- [54] A. Cho, S. Suzuki, J. Hatakeyama, N. Haruyama, and A. B. Kulkarni. “A method for rapid demineralization of teeth and bones.” In: *The Open Dentistry Journal* 4 (2010), pp. 223–229.
- [55] D. L. Christiansen, E. K. Huang, and F. H. Silver. “Assembly of type I collagen: fusion of fibril subunits and the influence of fibril diameter on mechanical properties”. In: *Matrix Biology* 19.5 (Sept. 2000), pp. 409–420. doi: 10.1016/s0945-053x(00)00089-5.
- [56] C. Coletti, G. Cultrone, L. Maritana, and C. Mazzoli. “Combined multi-analytical approach for study of pore system in bricks: How much porosity is there?” In: *Materials Characterization* 121 (2016), pp. 80–92.
- [57] C. Coletti, G. Cultrone, L. Maritana, and C. Mazzoli. “How to face the new industrial challenge of compatible, sustainable brick production: Study of various types of commercially available bricks”. In: *Applied Clay Science* 124-125 (2016), pp. 219–226.
- [58] G. Constantinides, K. Ravi Chandran, F.-J. Ulm, and K. Van Vliet. “Grid indentation analysis of composite microstructure and mechanics: Principles and validation”. In: *Materials Science & Engineering A* 430 (2006), pp. 189–202.
- [59] G. Constantinides and F.-J. Ulm. “The effect of two types of C-S-H on the elasticity of cement-based materials: Results from nanoindentation and micromechanical modeling”. In: *Cement and Concrete Research* 34 (2004), pp. 67–80.
- [60] G. Constantinides and F.-J. Ulm. “The nanogranular nature of C-S-H”. In: *Journal of the Mechanics and Physics of Solids* 55 (2007), pp. 64–90.
- [61] G. Constantinides, F.-J. Ulm, and K. Van Vliet. “On the use of nanoindentation for cementitious materials”. In: *Materials and Structures* 36 (2003), pp. 191–196.
- [62] D. Cooper, J. Matyas, M. Katzenberg, and B. Hallgrímsson. “Comparison of Microcomputed tomographic and microradiographic measurements of cortical bone porosity.” In: *Calcified Tissue International*. 74 (2004), pp. 437–447.
- [63] D. Cooper, D. Thomas, J. Clement, A. Turinsky, C. Sensen, and B. Hallgrímsson. “Age-dependent change in the 3D structure of cortical porosity at the human femoral midshaft.” In: *Bone*. 40 (2007), pp. 957–965.
- [64] G. W. Corder and D. I. Foreman. *Nonparametric Statistics for Non-Statisticians: A Step-By-Step Approach*. John Wiley & Sons, May 1, 2009. 247 pp. ISBN: 047045461X.
- [65] S. C. Cowin. “Bone poroelasticity”. In: *Journal of Biomechanics* 32.1999 (1999), pp. 217–238.
- [66] B. W. Cribb, A. Stewart, H. Huang, R. Truss, B. Noller, R. Rasch, and M. P. Zalucki. “Insect mandibles—comparative mechanical properties and links with metal incorporation”. In: *Naturwissenschaften* 95.1 (2008), pp. 17–23.
- [67] G. Cultrone, E. Molina, and A. Arizzi. “The combined use of petrographic, chemical and physical techniques to define the technological features of Iberian ceramics from the Canto Tortoso area (Granada, Spain)”. In: *Ceramics International* 40 (2014), pp. 10803–10816. doi: 10.1016/j.ceramint.2014.03.072. URL: <http://dx.doi.org/10.1016/j.ceramint.2014.03.072>.

- [68] G. Cultrone, C. Rodriguez-Navarro, E. Sebastian, O. Cazalla, and M. J. de la Torre. “Carbonate and silicate phase reactions during ceramic firing”. In: *European Journal of Mineralogy* 13 (2001), pp. 621–634. doi: 10.1127/0935-1221/2001/0013-0621.
- [69] G. Cultrone, E. Sebastian, K. Elert, M. J. de la Torre, O. Cazalla, and C. Rodriguez-Navarro. “Influence of mineralogy and firing temperature on the porosity of bricks”. In: *Journal of the European Ceramic Society* 24 (2004), pp. 547–564.
- [70] J. D. Currey. “The structure and mechanics of bone”. In: *Journal of Materials Science* 47.1 (Sept. 2011), pp. 41–54. doi: 10.1007/s10853-011-5914-9.
- [71] A. Czenek, R. Blanchard, A. Dejaco, Ó. E. Sigurjónsson, G. Örylgsson, P. Gargiulo, and C. Hellmich. “Quantitative intravoxel analysis of micro-CT-scanned resorbing ceramic biomaterials – Perspectives for computer-aided biomaterial design”. In: *Journal of Materials Research* 29.23 (2014).
- [72] M. D’Orazio, S. Lenci, and L. Graziani. “Relationship between fracture toughness and porosity of clay brick panels used in ventilated façades: Initial investigation”. In: *Engineering Fracture Mechanics* 116 (2014), pp. 108–121.
- [73] J. M. Daly. “Behavioural and secretory activity during tube construction by *Platynereis dumerilii* Aud & M. Edw.[Polychaeta: Nereidae]”. In: *Journal of the Marine Biological Association of the United Kingdom* 53.3 (1973), pp. 521–529.
- [74] W. De Boever, H. Derluyn, D. Van Loo, L. Van Hoorebeke, and V. Cnudde. “Data-fusion of high resolution X-ray CT, SEM and EDS for 3D and pseudo-3D chemical and structural characterization of sandstone”. In: *Micron* 74 (2015), pp. 15–21. ISSN: 0968-4328.
- [75] A. Dejaco, V. S. Komlev, J. Jaroszewicz, W. Swieszkowski, and C. Hellmich. “Micro CT-based multiscale elasticity of double-porous (pre-cracked) hydroxyapatite granules for regenerative medicine.” In: *Journal of Biomechanics* 45 (2012), pp. 1068–1075.
- [76] V. Deude, L. Dormieux, D. Kondo, and S. Maghous. “Micromechanical approach to nonlinear poroelasticity: application to cracked rocks”. In: *Journal of Engineering Mechanics (ASCE)* 128.8 (2002), pp. 848–855.
- [77] S. Deville, E. Saiz, and A. P. Tomsia. “Freeze casting of hydroxyapatite scaffolds for bone tissue engineering.” In: *Biomaterials* 27 (2006), pp. 5480–5489.
- [78] C. Dhand, S. T. Ong, N. Dwivedi, S. Marrero Diaz, J. R. Venugopal, B. Navaneethan, M. H. Fazil, S. Liu, V. Seitz, E. Wintermantel, R. W. Beuerman, S. Ramakrishna, N. K. Verma, and R. Lakshminarayanan. “Bio-inspired in situ crosslinking and mineralization of electrospun collagen scaffolds for bone tissue engineering.” In: *Biomaterials* 104 (2016), pp. 323–338.
- [79] S. Diamond. “Mercury porosimetry: An inappropriate method for the measurement of pore size distributions in cement-based materials”. In: *Cement and Concrete Research* 30 (2000), pp. 1517–1525.
- [80] M. Dondi, G. Ercolani, B. Fabbri, and M. Marsigli. “An approach to the chemistry of pyroxenes formed during the firing of Ca-rich silicate ceramics”. In: *Clay Minerals* 33 (1998), pp. 443–452.

- [81] P. Dong, S. Hauptert, B. Hesse, M. Langer, P.-J. Gouttenoire, V. Bousson, and F. Peyrin. “3D osteocyte lacunar morphometric properties and distributions in human femoral cortical bone using synchrotron radiation micro-CT images”. In: *Bone* 60 (2014), pp. 172–185.
- [82] E. Donnelly, S. P. Baker, A. L. Boskey, and M. C. van der Meulen. “Effects of surface roughness and maximum load on the mechanical properties of cancellous bone measured by nanoindentation”. In: *Journal of Biomedical Materials Research Part A* 77A.2 (2006), pp. 426–435. doi: 10.1002/jbm.a.30633.
- [83] L. Dormieux, E. Lemarchand, D. Kondo, and E. Fairbairn. “Elements of poro-micromechanics applied to concrete”. In: *Materials and Structures / Concrete Science and Engineering* 37.265 (2004), pp. 31–42.
- [84] W. Drugan and J. Willis. “A micromechanics-based nonlocal constitutive equation and estimates of representative volume element size for elastic composites”. In: *Journal of the Mechanics and Physics of Solids* 44.4 (1996), pp. 497–524.
- [85] P. Duminuco, B. Messiga, and M. P. Riccardi. “Firing process of natural clays. Some microtextures and related phase compositions”. In: *Thermochimica Acta* 321 (1998), pp. 185–190.
- [86] L. Eberhardsteiner, C. Hellmich, and S. Scheiner. “Layered Water in Crystal Interfaces as Source for Bone Viscoelasticity: Arguments from a Multiscale Approach”. In: *Computer Methods in Biomechanics and Biomedical Engineering* 17 (2014), pp. 48–63.
- [87] K. Elert, G. Cultrone, C. R. Navarro, and E. S. Pardo. “Durability of bricks used in the conservation of historic buildings – influence of composition and microstructure”. In: *Journal of Cultural Heritage* 4 (2003), pp. 91–99.
- [88] J. Eshelby. “The determination of the elastic field of an ellipsoidal inclusion, and related problems”. In: *Proceedings of the Royal Society London, Series A* 241 (1957), pp. 376–396.
- [89] European Directorate for the Quality of Medicines and HealthCare. *European pharmacopoeia 7.0 vol. 1*. European pharmacopoeia 7.0 vol. 1, 2011.
- [90] D. Faivre and T. U. Godec. “From Bacteria to Mollusks: The principles underlying the biomineralization of iron oxide materials”. In: *Angewandte Reviews* (2015).
- [91] P. Fauvel. *Annélides Polychètes non pélagiques provenant des campagnes de l’Hirondelle et de la Princesse-Alice (1885-1910)*. Imprimerie de Monaco, 1914.
- [92] M. P. Fay and M. A. Proschan. “Wilcoxon-Mann-Whitney or t-test? On assumptions for hypothesis tests and multiple interpretations of decision rules”. In: *Statistics Surveys* 4.0 (2010), pp. 1–39. doi: 10.1214/09-ss051.
- [93] N. E. Fedorovich, J. R. De Wijn, A. J. Verbout, J. Alblas, and W. J. Dhert. “Three-Dimensional Fiber Deposition of Cell-Laden, Viable, Patterned Constructs for Bone Tissue Printing.” In: *Tissue Engineering Part A* 14 (2008), pp. 127–133.
- [94] S. Feik, C. Thomas, and J. Clement. “Age-related changes in cortical porosity of the midshaft of the human femur.” In: *Journal of Anatomy*. 191 (1997), pp. 407–416.

- [95] L. Feng and I. Jasiuk. “Multi-scale characterization of swine femoral cortical bone.” In: *Journal of Biomechanics* 44 (2011), pp. 313–320.
- [96] M. A. Fernández-Seara, S. L. Wehrli, and F. W. Wehrli. “Diffusion of Exchangeable Water in Cortical Bone Studied by Nuclear Magnetic Resonance”. In: *Biophysical Journal* 82 (2002), pp. 522–529.
- [97] A. Fischer and A. Dorresteijn. “The polychaete *Platynereis dumerilii* (Annelida): a laboratory animal with spiralian cleavage, lifelong segment proliferation and a mixed benthic/pelagic life cycle”. In: *Bioessays* 26.3 (2004), pp. 314–325.
- [98] A. H. Fischer, T. Henrich, and D. Arendt. “The normal development of *Platynereis dumerilii* (Nereididae, Annelida)”. In: *Frontiers in zoology* 7.1 (2010), p. 31.
- [99] L. Fischer, A. Valentinitzsch, M. D. DiFranco, C. Schueller-Weidekamm, D. Kienzl, H. Resch, T. Gross, M. Weber, P. Jaksch, W. Klepetko, B. Zweytick, P. Pietschmann, F. Kainberger, G. Langs, and J. M. Patsch. “High-Resolution Peripheral Quantitative CT Imaging: Cortical Porosity, Poor Trabecular Bone Microarchitecture, and Low Bone Strength in Lung Transplant Recipients.” In: *Radiology* 274 (2015), pp. 473–481.
- [100] P. Fischer. “Formation of the ceramic body in heavy clay products in firing - Part 2: Formation of the ceramic body structure”. In: *Ziegeleitechnisches Jahrbuch* (1987), pp. 96–108.
- [101] A. Fontes-Pereira, P. Rosa, T. Barboza, D. Matusin, A. Soares Freire, B. Ferreira Braz, C. Bittencourt Machado, M. A. von Krüger, S. A. Lopes de Souza, R. Erthal Santelli, and W. C. de Albuquerque Pereira. “Monitoring bone changes due to calcium, magnesium, and phosphorus loss in rat femurs using Quantitative Ultrasound.” In: *Nature Scientific Reports* 8 (2018), p. 11963.
- [102] W. Franus, A. Halicka, K. Lamorski, and G. Jozefaciuk. “Microstructural Differences in Response of Thermoresistant (Ceramic) and Standard (Granite) Concretes on Heating. Studies Using SEM and Nonstandard Approaches to Microtomography and Mercury Intrusion Porosimetry Data”. In: *Materials* 11.7 (2018), p. 1026.
- [103] S. Freyburg and A. Schwarz. “Influence of the clay type on the pore structure of structural ceramics”. In: *Journal of the European Ceramic Society* (2007).
- [104] A. Fritsch, C. Hellmich, and L. Dormieux. “The role of disc-type crystal shape for micromechanical predictions of elasticity and strength of hydroxyapatite biomaterials.” In: *Philosophical Transactions of the Royal Society A* 368 (2010), pp. 1913–1935.
- [105] A. Fritsch and C. Hellmich. ““Universal” microstructural patterns in cortical and trabecular, extracellular and extravascular bone materials: Micromechanics-based prediction of anisotropic elasticity.” In: *Journal of Theoretical Biology* 244.4 (2007), pp. 597–620.
- [106] A. Fritsch, C. Hellmich, and L. Dormieux. “Ductile sliding between mineral crystals followed by rupture of collagen crosslinks: Experimentally supported micromechanical explanation of bone strength”. In: *Journal of Theoretical Biology* 260 (2009), pp. 230–252.
- [107] I. Furin, M. Pastrama, H. Kariem, K. Luczynski, O. Lahayne, and C. Hellmich. “A new nanoindentation protocol for identifying the elasticity of undamaged extracellular bone tissue”. In: *MRS Advances* 1 (2016), pp. 693–704.

- [108] R. Furlong. “Electron diffraction and micrographic study of the high-temperature changes in illite and montmorillonite under continuous heating conditions”. In: *Clay and Clay Minerals: Proceedings of the Fifteenth Conference, Pittsburgh, PA. Pergamon Press* (1967).
- [109] K. Gadelrab, G. Li, M. Chiesa, and T. Souier. “Local characterization of austenite and ferrite phases in duplex stainless steel using MFM and nanoindentation”. In: *Journal of Materials Research* 27 (2012), pp. 1573–1579.
- [110] H. Gao, B. Ji, I. Jager, E. Arzt, and P. Fratzl. “Materials become insensitive to flaws at nanoscale: Lessons from nature”. In: *Proceedings of the National Academy of Sciences of the United States of America* 100 (2003), pp. 5597–5600.
- [111] J. Garcia-Ten, M. Orts, A. Saburit, and G. Silva. “Thermal conductivity of traditional ceramics Part II: Influence of mineralogical composition”. In: *Ceramics International* 36 (2010), pp. 2017–2024.
- [112] J. Garcia-Ten, M. Orts, A. Saburit, and G. Silva. “Thermal conductivity of traditional ceramics. Part I: Influence of bulk density and firing temperature”. In: *Ceramics International* 36 (2010), pp. 1951–1959.
- [113] H. Giesche. “Mercury Porosimetry: A General (Practical) Overview”. In: *Part. Part. Syst. Charact.* 23 (2006), pp. 9–19.
- [114] J. Glowacki, C. Cox, J. O’Sullivan, D. Wilkie, and L. Deftos. “Osteoclasts can be induced in fish having an acellular bony skeleton.” In: *Proceedings of the National Academy of Sciences* 83 (1986), pp. 4104–4107.
- [115] J. Gong, J. Arnold, and S. Cohn. “The density of organic and volatile and non-volatile inorganic components of the bone.” In: *The Anatomical Record* 149 (1964), pp. 319–324.
- [116] S. Gould and R. C. Lewontin. “The spandrels of San Marco and the Panglossian paradigm: A critique of the adaptationist programme.” In: *Proceedings of The Royal Society Series B* 205 (1979), pp. 581–598.
- [117] M. Granke, Q. Grimal, A. Saïed, P. Nauleau, F. Peyrin, and P. Laugier. “Change in porosity is the major determinant of the variation of cortical bone elasticity at the millimeter scale in aged women.” In: *Bone* 49 (2011), pp. 1020–1026.
- [118] R. E. Grim and W. F. Bradley. “Investigation of the effect of heat on the clay minerals illite and montmorillonite”. In: *Journal of the American Ceramic Society* (1940).
- [119] J. C. Groen, L. A. A. Peffer, and J. Pérez-Ramírez. “Incorporation of appropriate contact angles in textural characterization by mercury porosimetry”. In: *Studies in Surface Science and Catalysis* 144 (2002), pp. 91–98.
- [120] I. N. Grubeša, M. Vračević, V. Ducman, B. M. and I. Szenti 5, and Á. Kukovecz. “Influence of the Size and Type of Pores on Brick Resistance to Freeze-Thaw Cycles”. In: *Materials* 13.17 (2020).
- [121] I. N. Grubeša, M. Vračević, J. Ranogajec, and S. Vučetić. “Influence of Pore-Size Distribution on the Resistance of Clay Brick to Freeze–Thaw Cycles”. In: *Materials* 13.10 (2020).

- [122] M. L. Gualtieri, A. F. Gualtieri, S. Gagliardi, P. Ruffini, R. Ferrari, and M. Hanuskova. “Thermal conductivity of fired clays: Effects of mineralogical and physical properties of the raw materials”. In: *Applied Clay Science* 49 (2010), pp. 269–275.
- [123] C. Hall and A. Hamilton. “Porosity–density relations in stone and brick materials”. In: *Materials and Structures* 48 (2015), pp. 1265–1271.
- [124] T. Hassenkam, G. E. Fantner, J. A. Cutroni, J. C. Weaver, D. E. Morse, and P. K. Hansma. “High-resolution AFM imaging of intact and fractured trabecular bone.” In: *Bone* 35 (2004), pp. 4–10.
- [125] T. Hassenkam, H. L. Jørgensen, M. B. Pedersen, A. H. Kourakis, L. Simonsen, and J. B. Lauritzen. “Atomic force microscope on human trabecular bone from an old woman with osteoporotic fractures”. In: *Micron* 36 (2005), pp. 681–687.
- [126] H. Hausen. “*Chaetae* and chaetogenesis in *Polychaetes (Annelida)*”. In: *Developments in Hydrobiology*. In: Bartolomaeus T., Purschke G. (eds). Vol. 179. Springer-Verlag, 2005. Chap. Morphology, Molecules, Evolution and Phylogeny in Polychaeta and Related Taxa. Pp. 37–52. doi: 10.1007/1-4020-3240-4\_{\\_}4.
- [127] A. Hein, N. S. Müller, P. M. Day, and V. Kilikoglou. “Thermal conductivity of archaeological ceramics: The effect of inclusions, porosity and firing temperature”. In: *Thermochimica Acta* (2008).
- [128] C. Hellmich, J.-F. Berthelemy, and L. Dormieux. “Mineral–collagen interactions in elasticity of bone ultrastructure – a continuum micromechanics approach.” In: *European Journal of Mechanics* 23 (2004), pp. 783–810.
- [129] C. Hellmich and F. Ulm. “Average hydroxyapatite concentration is uniform in the extracollagenous ultrastructure of mineralized tissues: Evidence at the 1–10-micrometer scale”. In: *Biomechanics and Modeling in Mechanobiology* 2 (2003), pp. 21–36.
- [130] C. Hellmich, F.-J. Ulm, and L. Dormieux. “Can the diverse elastic properties of trabecular and cortical bone be attributed to only a few tissue-independent phase properties and their interactions? Arguments from a multiscale approach”. In: *Biomechanics and Modeling in Mechanobiology* 2 (2004), pp. 219–238.
- [131] B. Hernandez, S. Panda, M. Kuntz, and Y. Zhou. “Nanoindentation and microstructure analysis of resistance spot welded dual phase steel”. In: *Materials Letters* 64 (2010), pp. 207–210.
- [132] B. Hesse, P. Varga, M. Lagner, A. Pacureanu, S. Schrof, N. Männicke, H. Suhonen, P. Maurer, P. Cloetens, F. Peyrin, and K. Raum. “Canalicular Network Morphology is the Major Determinant of the Spatial Distribution of Mass Density in Human Bone Tissue: Evidence by Means of Synchrotron Radiation Phase-Contrast nano-CT”. In: *Journal of Bone and Mineral Research* 30 (2014), pp. 346–356.
- [133] R. Hill. “Continuum micro-mechanics of elastoplastic polycrystals”. In: *Journal of Mechanics and Physics of Solids* 13.2 (1965), pp. 89–101.
- [134] C. Hoffler, K. Moore, K. Kozloff, P. Zysset, and S. Goldstein. “Age, gender, and bone lamellae elastic moduli.” In: *Journal of Orthopedic Research* 18 (2000), pp. 432–437.
- [135] I. Hrivnak. *Theory of Weldability of Metals and Alloys*. Materials Science Monographs – Book 74. Elsevier, Amsterdam, 1991.

- [136] J. Hubbell. “Photon Mass Attenuation and Energy-Absorption Coefficients from 1 keV to 20 MeV”. In: *International Journal of Applied Radiation and Isotopes* 33.11 (1982), pp. 1269–1290.
- [137] J. Hubbell. “Photon Mass Attenuation and Mass Energy-Absorption Coefficients for H, C, N, O, Ar, and Seven Mixtures from 0.1 keV to 20 MeV”. In: *Radiation Research* 70 (1977), pp. 58–81.
- [138] J. Hubbell and S. Seltzer. “Tables of X-Ray Mass Attenuation Coefficients and Mass Energy-Absorption Coefficients from 1 keV to 20 MeV for Elements  $Z = 1$  to 92 and 48 Additional Substances of Dosimetric Interest”. In: (2004).
- [139] IBM Corp. *IBM SPSS Statistics for Windows, Version 25.0*. Released 2017. Armonk, NY, USA, 2017.
- [140] IBM Corp. *IBM SPSS Statistics for Windows, Version 26.0*. Released 2019. Armonk, NY, USA, 2019.
- [141] V. Jagsch, P. Kuttke, O. Lahayne, L. Zelaya-Lainez, S. Scheiner, and C. Hellmich. “Multiscale and multitechnique investigation of the elasticity of grooved rail steel”. In: *Construction and Building Materials* 238 (Mar. 2020), p. 117768. doi: 10.1016/j.conbuildmat.2019.117768.
- [142] D. Jones, H. Nolte, J. Scholübbbers, E. Turner, and D. Veltel. “Biochemical signal transduction of mechanical strain in osteoblast-like cells.” In: *Biomaterials* 12 (1991), pp. 101–110.
- [143] M. Jordan, M. Montero, M. Meseguer, and S. Sanfeliu. “Influence of firing temperature and mineralogical composition on bending strength and porosity of ceramic tile bodies”. In: *Applied Clay Science* 42 (2008), pp. 266–271.
- [144] S. J. Kalita, S. Bose, H. L. Hosick, and A. Bandyopadhyay. “Development of controlled porosity polymer-ceramic composite scaffolds via fused deposition modeling.” In: *Materials Science and Engineering: C* 23 (2003), pp. 611–620.
- [145] H. Kariem, J. Füssl, T. Kiefer, A. Jäger, and C. Hellmich. “The viscoelastic behaviour of material phases in fired clay identified by means of grid nanoindentation”. In: *Construction and Building Materials* 231 (2020), p. 117066.
- [146] H. Kariem, C. Hellmich, T. Kiefer, A. Jäger, and J. Füssl. “Micro-CT-based identification of double porosity in fired clay ceramics”. In: *Journal of Materials Science* 53.13 (2018), pp. 9411–9428.
- [147] H. Kariem, T. Kiefer, C. Hellmich, W. Gaggl, A. Steiger-Thirsfeld, and J. Füssl. “EDX/XRD-based identification of micrometer-sized domains inscanning electron micrographs of fired clay”. In: *Materials and Structures* 53.109 (2020).
- [148] H. Kariem, M. Pastrama, S. Roohani-Esfahani, P. Pivonka, H. Zreiqat, and C. Hellmich. “Micro-poro-elasticity of baghdadite-based bone tissue engineering scaffolds: A unifying approach based on ultrasonics, nanoindentation, and homogenization theory”. In: *Materials Science and Engineering C* 46 (2015), pp. 553–564.
- [149] P. Kerner, E. Simionato, M. Le Gouar, and M. Vervoort. “Orthologs of key vertebrate neural genes are expressed during neurogenesis in the annelid *Platynereis dumerilii*”. In: *Evolution & development* 11.5 (2009), pp. 513–524.

- [150] R. Khanna, K. S. Katti, and D. R. Katti. “Nanomechanics of Surface Modified Nanohydroxyapatite Particulates Used in Biomaterials”. In: *Journal of Engineering Mechanics* 135.5 (May 2009), pp. 468–478. doi: 10.1061/(asce)em.1943-7889.00000002.
- [151] T. Kiefer, J. Füssl, H. Kariem, J. Konnerth, W. Gaggl, and C. Hellmich. “A multi-scale material model for the estimation of the transversal isotropic thermal conductivity tensor of fired clay bricks”. In: *Journal of the European Ceramic Society* (2020).
- [152] V. Kilikoglou, G. Vekinis, Y. Maniatis, and P. M. Day. “Mechanical performance of quartz-tempered ceramics: Part I, strength and toughness”. In: *Archaeometry* 40.2 (1998), pp. 261–279.
- [153] S. Kim and W. Johnson. “Elastic constants and internal friction of martensitic steel, ferritic-pearlitic steel, and  $\alpha$ -iron”. In: *Materials Science and Engineering A* 452-453 (2007), pp. 633–639.
- [154] S.-S. Kim, M. S. Park, O. Jeon, C. Y. Choi, and B.-S. Kim. “Poly(lactide-co-glycolide) / hydroxyapatite composite scaffolds for bone tissue engineering.” In: *Biomaterials* 27 (2006), pp. 1399–1409.
- [155] I. Kiviranta, M. Tammi, R. Lappalainen, T. Kuusela, and H. Helminen. “The Rate of Calcium Extraction During EDTA Decalcification from Thin Bone Slices as Assessed with Atomic Absorption Spectrophotometry.” In: *Histochemistry* 68 (1980), pp. 119–127.
- [156] C. Kober, G. Kjeller, C. Hellmich, R. A. Sader, and B.-I. Berg. “Mandibular biomechanics after marginal resection: Correspondences of simulated volumetric strain and skeletal resorption.” In: *Journal of Biomechanics* 95 (2019), p. 109320.
- [157] C. Kohlhauser and C. Hellmich. “Ultrasonic contact pulse transmission for elastic wave velocity and stiffness determination: Influence of specimen geometry and porosity”. In: *Engineering Structures* 47 (2013), pp. 115–133.
- [158] H. Kolsky. *Stress Waves in Solids*. Oxford University Press, London, 1953.
- [159] H. Kolsky. “Stress waves in solids”. In: *Journal of Sound and Vibration* 1 (1964), pp. 88–110.
- [160] E. Köster. “Granulometrische und morphometrische Messmethoden an Mineralkörnern, Steinen und sonstigen Stoffen”. In: *Ferdinand Enke Verlag* (1964).
- [161] K. J. Krakowiak, P. B. Lourenco, and F.-J. Ulm. “Multitechnique Investigation of Extruded Clay Brick Microstructure”. In: *Journal of the American Ceramic Society* 94.9 (2011), pp. 3012–3022.
- [162] W. H. Kruskal and W. A. Wallis. “Use of Ranks in One-Criterion Variance Analysis”. In: *Journal of the American Statistical Association* 47.260 (Dec. 1952), pp. 583–621. doi: 10.1080/01621459.1952.10483441.
- [163] A. Kurfürst, P. Hernits, C. Morin, T. Abdalrahman, and C. Hellmich. “Bone Ultrastructure as Composite of Aligned Mineralized Collagen Fibrils Embedded Into a Porous Polycrystalline Matrix: Confirmation by Computational Electrodynamics.” In: *Frontiers in Physics* 6 (2018), p. 125.



- [164] W. J. Landis, J. J. Librizzi, M. G. Dunn, and F. H. Silver. “A study of the relationship between mineral content and mechanical properties of turkey gastrocnemius tendon”. In: *Journal of Bone and Mineral Research* 10.6 (June 1995), pp. 859–867. doi: 10.1002/jbmr.5650100606.
- [165] S. Lees. “Considerations regarding the structure of the mammalian mineralized osteoid from viewpoint of the generalized packing model.” In: *Connective Tissue Research* 16 (1987), pp. 281–303.
- [166] S. Lees. “Mineralization of type I collagen.” In: *Biophysical Journal* 85 (2003), pp. 204–207.
- [167] S. Lees. “Water content in type I collagen tissues calculated from the generalized packaging model.” In: *International Journal of Biological Macromolecules* 16 (1986), pp. 281–303.
- [168] S. Lees, J. Ahern, and M. Leonard. “Parameters influencing the sonic velocity in compact calcified tissues of various species.” In: *Journal of the Acoustical Society of America* 74 (1983), pp. 28–33.
- [169] S. Lees, L. Bonar, and H. Mook. “A study of dense mineralized tissue by neutron diffraction.” In: *International Journal of Biological Macromolecules* 6 (1984), pp. 321–326.
- [170] S. Lees, P. Cleary, J. Heeley, and E. Gariepy. “Distribution of sonic plesio- velocity in a compact bone sample.” In: *Journal of Acoustic Society of America* 66 (1979), pp. 641–646.
- [171] S. Lees and M. Escoubes. “Vapor Pressure Isotherms, Composition and Density of Hyperdense Bones of Horse, Whale and Porpoise”. In: *Connective Tissue Research* 16.4 (1987), pp. 305–322.
- [172] S. Lees, D. Hanson, and E. Page. “Some acoustical properties of the otic bones of a fin whale.” In: *Journal of the Acoustical Society of America*. 99 (1996), pp. 2421–2427.
- [173] S. Lees, D. Hanson, E. Page, and H. Mook. “Comparison of dosage-dependent effects of beta-aminopropionitrile, sodium fluoride, and hydrocortisone on selected physical properties of cortical bone.” In: *Journal of Bone and Mineral Research*. 9 (1994), pp. 1377–1389.
- [174] S. Lees and J. D. Heeley. “Density of a sample bovine cortical bone matrix and its solid constituent in various media”. In: *Calcified Tissue International* 33.1 (1981), pp. 499–504.
- [175] S. Lees, J. D. Heeley, and P. F. Cleary. “A study of some properties of a sample of bovine cortical bone using ultrasound”. In: *Calcified Tissue International* 29.1 (1979), pp. 107–117.
- [176] S. Lees and E. A. Page. “A study of some properties of mineralized turkey leg tendon”. In: *Connective Tissue Research* 28.4 (1992), pp. 263–287.
- [177] S. Lees, M. Pineri, and M. Escoubes. “A generalized packing model for type I collagen.” In: *International Journal of Biological Macromolecules* 6 (1984), pp. 133–136.

- [178] S. Lees and K. Probst. “The locus of mineral crystallites in bone.” In: *Connective Tissue Research* 18 (1988), pp. 41–54.
- [179] S. Lees, K. Probst, V. Ingle, and K. Kjoller. “The Loci of Mineral in Turkey Leg Tendon As Seen By Atomic Force Microscope and Electron Microscopy”. In: *Calcified Tissue International* 55 (1994), pp. 180–189.
- [180] H. C. Lichtenegger, T. Schöberl, M. H. Bartl, H. Waite, and G. D. Stucky. “High abrasion resistance with sparse mineralization: copper biomineral in worm jaws”. In: *Science* 298.5592 (2002), pp. 389–392.
- [181] H. C. Lichtenegger, T. Schöberl, J. T. Ruokolainen, J. O. Cross, S. M. Heald, H. Birkedal, J. H. Waite, and G. D. Stucky. “Zinc and mechanical prowess in the jaws of Nereis, a marine worm”. In: *Proceedings of the National Academy of Sciences* 100.16 (2003), pp. 9144–9149.
- [182] H. C. Lichtenegger, T. Schöberl, J. T. Ruokolainen, J. O. Cross, S. M. Heald, H. Birkedal, J. H. Waite, and G. D. Stucky. “Zinc and mechanical prowess in the jaws of Nereis, a marine worm”. In: *Proceedings of the National Academy of Sciences* 100.16 (2003), pp. 9144–9149.
- [183] C. Liu, B. Shi, J. Zhou, and C. Tang. “Quantification and characterization of microporosity by image processing, geometric measurement and statistical methods: Application on SEM images of clay materials”. In: *Applied Clay Science* (2011).
- [184] X. Liu, J. Wang, L. Ge, F. Hu, C. Li, X. Li, J. Yu, H. Xu, S. Lu, and Q. Xue. “Pore-scale characterization of tight sandstone in Yanchang Formation Ordos Basin China using micro-CT and SEM imaging from nm- to cm-scale”. In: *Fuel* 209 (2017), pp. 254–264.
- [185] B. Lubelli, D. de Winter, J. Post, R. van Hees, and M. Drury. “Cryo-FIB-SEM and MIP study of porosity and pore size distribution of bentonite and kaolin at different moisture contents”. In: *Applied Clay Science* 80-81 (2013), pp. 358–365.
- [186] K. Luczynski, A. Dejacó, O. Lahayne, J. Jaroszewicz, W. Swieszkowski, and C. Hellmich. “MicroCT/Micromechanics-Based Finite Element Models and Quasi-Static Unloading Tests Deliver Consistent Values for Young’s Modulus of Rapid-Prototyped Polymer-Ceramic Tissue Engineering Scaffold.” In: *CMES* 87 (2012), pp. 505–528.
- [187] Q. Ma and D. R. Clarke. “Size dependent hardness of silver single crystals”. In: *Journal of Materials Research* 10.4 (Apr. 1995), pp. 853–863. doi: 10.1557/jmr.1995.0853.
- [188] M. Maage. “Frost resistance and pore size distribution in bricks”. In: *Matériaux et Construction* 17 (1984), pp. 345–350.
- [189] I. C. Madsen, N. V. Y. Scarlett, and A. Kern. “Description and survey of methodologies for the determination of amorphous content via X-ray powder diffraction.” In: *Zeitschrift für Kristallographie – Crystalline Materials* 226.12 (2011), pp. 944–955.
- [190] P. Mahalanobis. “On the generalized distance in statistics”. In: *Proceedings of the National Institute of Science of India* 12 (1936), pp. 49–55.
- [191] J. Mahamid, A. Sharir, D. Gur, E. Zelzer, L. Addadi, and S. Weiner. “Bone mineralization proceeds through intracellular calcium phosphate loaded vesicles: A cryo-electron microscopy study.” In: *Journal of Structure Biology* 174 (2011), pp. 527–535.

- [192] A. Malandrino, A. Fritsch, O. Lahayne, K. Kropik, H. Redl, J. Noailly, D. Lacroix, and C. Hellmich. “Anisotropic tissue elasticity in human lumbar vertebra, by means of a coupled ultrasound-micromechanics approach.” In: *Material Letters* 78 (2012), pp. 154–158.
- [193] A. Malasoma, A. Fritsch, C. Kohlhauser, T. Brynk, C. Vitale-Brovarone, Z. Pakiela, J. Eberhardsteiner, and C. Hellmich. “Micromechanics of bioresorbable porous CEL2 glass ceramic scaffolds for bone tissue engineering.” In: *Advances in Applied Ceramics* 107 (2008), pp. 277–286.
- [194] H. B. Mann and D. R. Whitney. “On a Test of Whether one of Two Random Variables is Stochastically Larger than the Other”. In: *The Annals of Mathematical Statistics* 18.1 (Mar. 1947), pp. 50–60. DOI: 10.1214/aoms/1177730491.
- [195] G. Marotti. “A new theory of bone lamellation”. In: *Calcified Tissue International* 53 (1993), S47–S56.
- [196] G. Marotti, M. Muglia, C. Palumbo, and D. Zaffe. “The microscopic determinants of bone mechanical properties”. In: *Italian Journal of Mineral and Electrolyte Metabolism* 4 (1994), pp. 167–175.
- [197] K. W. McElhaney, J. J. Vlassak, and W. D. Nix. “Determination of indenter tip geometry and indentation contact area for depth-sensing indentation experiments”. In: *Journal of Materials Research* 13.5 (May 1998), pp. 1300–1306. DOI: 10.1557/jmr.1998.0185.
- [198] E. A. McNally, H. P. Schwarcz, G. A. Botton, and A. L. Arsenault. “TA Model for the Ultrastructure of Bone Based on Electron Microscopy of Ion-Milled Sections”. In: *PLoS ONE* 7 (2012), e29258.
- [199] R. A. Merz and S. A. Woodin. “Polychaete chaetae: function, fossils, and phylogeny”. In: *Integrative and comparative biology* 46.4 (2006), pp. 481–496.
- [200] M. A. Meyers, P.-Y. Chen, A. Y.-M. Lin, and Y. Seki. “Biological materials: Structure and mechanical properties”. In: *Progress in Materials Science* 53.1 (Jan. 2008), pp. 1–206. DOI: 10.1016/j.pmatsci.2007.05.002.
- [201] M. Miller, C. Bobko, M. Vandamme, and F.-J. Ulm. “Surface roughness criteria for cement paste nanoindentation”. In: *Cement and Concrete Research* 38.4 (Apr. 2008), pp. 467–476. DOI: 10.1016/j.cemconres.2007.11.014.
- [202] A. Miserez, Y. Li, J. H. Waite, and F. Zok. “Jumbo squid beaks: inspiration for design of robust organic composites”. In: *Acta Biomaterialia* 3.1 (2007), pp. 139–149.
- [203] P. Mishra, C. M. Pandey, U. Singh, A. Gupta, C. Sahu, and A. Keshri. “Descriptive statistics and normality tests for statistical data”. In: *Annals of Cardiac Anaesthesia* 22.1 (2019), p. 67. DOI: 10.4103/aca.aca\_157\_18.
- [204] D. M. Moore and R. C. Reynolds. “X-Ray Diffraction and the Identification and Analysis of Clay Minerals”. In: *Oxford University Press* (1997).
- [205] L. Morales-Rivas, A. González-Orive, C. Garcia-Mateo, A. Hernández-Creus, F. Caballero, and L. Vázquez. “Nanomechanical characterization of nanostructured bainitic steel: Peak Force Microscopy and Nanoindentation with AFM”. In: *Scientific Reports* 5 (2015), p. 17164.

- [206] C. Morin and C. Hellmich. “Mineralization-driven bone tissue evolution follows from fluid-to-solid phase transformations in closed thermodynamic systems.” In: *Journal of Theoretical Biology* 335 (2013), pp. 185–197.
- [207] C. Morin, C. Hellmich, and P. Henits. “Fibrillar structure and elasticity of hydrating collagen: A quantitative multiscale approach”. In: *Journal of Theoretical Biology* 317 (2013), pp. 384–393.
- [208] C. Morin, V. Vass, and C. Hellmich. “Micromechanics of elastoplastic porous polycrystals: Theory, algorithm, and application to osteonal bone”. In: *International Journal of Plasticity* 91 (2017), pp. 238–267.
- [209] M. Morris, J. Lopez-Curato, S. Hughes, K. An, J. Bassingthwaite, and P. Kelly. “Fluid spaces in canine bone and marrow”. In: *Microvascular Research* 23 (1982), pp. 188–200.
- [210] D. Moses, M. Mattoni, N. Slack, J. Waite, and F. Zok. “Role of melanin in mechanical properties of Glycera jaws”. In: *Acta biomaterialia* 2.5 (2006), pp. 521–530.
- [211] N. S. Müller, V. Kilikoglou, P. M. Day, and G. Vekinis. “The influence of temper shape on the mechanical properties of archaeological ceramics”. In: *Journal of the European Ceramic Society* 30 (2010), pp. 2457–2465.
- [212] N. S. Müller, G. Vekinis, P. Day, and V. Kilikoglou. “The influence of microstructure and texture on the mechanical properties of rock tempered archaeological ceramics”. In: *Journal of the European Ceramic Society* 35 (2015), pp. 831–843.
- [213] National Center for Biotechnology Information. *National Center for Biotechnology Information*. <https://www.ncbi.nlm.nih.gov/>. Last checked on Mar 13, 2020. Mar. 2020. URL: <https://www.ncbi.nlm.nih.gov/>.
- [214] W. F. Newman and M. W. Newman. *The Chemical Dynamics of Bone Mineral*. Vol. XI. 209. Chicago, USA: The University of Chicago Press, Oct. 1958.
- [215] J. K. Nielsen and J. Maiboe. “Epofix and vacuum: An easy method to make casts of hard substrates”. In: *Palaeontologia Electronica* 3.1 (2000).
- [216] W. D. Nix and H. Gao. “Indentation size effects in crystalline materials: a law for strain gradient plasticity”. In: *Journal of the Mechanics and Physics of Solids* 46.3 (1998), pp. 411–425.
- [217] L. Nodari, E. Marcuz, L. Maritan, C. Mazzoli, and U. Russo. “Hematite nucleation and growth in the firing of carbonate-rich clay for pottery production”. In: *Journal of the European Ceramic Society* 27 (2007), pp. 4665–4673.
- [218] N. C. Nowlan and P. J. Prendergast. “Evolution of mechanoregulation of bone growth will lead to non-optimal bone phenotypes”. In: *Journal of Theoretical Biology* 235.3 (Aug. 2005), pp. 408–418. DOI: 10.1016/j.jtbi.2005.01.021.
- [219] R. M. O’Clair and R. A. Cloney. “Patterns of morphogenesis mediated by dynamic microvilli: chaetogenesis in *Nereis vexillosa*”. In: *Cell and Tissue Research* 151.2 (1974), pp. 141–157.
- [220] S. E. Olesiak, M. L. Oyen, and V. L. Ferguson. “Viscous-elastic-plastic behavior of bone using Berkovich nanoindentation.” In: *Mechanics of Time-Dependent Materials* 14 (2010), pp. 111–124.

- [221] D. V. Oliveira, P. B. Lourenco, and P. Roca. “Cyclic Behaviour of Stone and Brick Masonry under Uniaxial Compressive Loading”. In: *Materials and Structures* 39.2 (2006), pp. 219–227.
- [222] W. C. Oliver and G. M. Pharr. “An improved technique for determining hardness and elastic modulus using load and displacement sensing indentation experiments”. In: *Journal of Materials Research* 7 (1992), pp. 1564–1583.
- [223] J. P. Orgel, T. Irving, A. Miller, and T. J. Wess. “Microfibrillar structure of type I collagen in situ”. In: *Proceedings of the National Academy of Sciences of the United States of America* 103.24 (2006), pp. 9001–9005.
- [224] N. Otsu. “A threshold selection method from gray-level histograms”. In: *EEE Trans. Sys., Man.* 9 (1979), pp. 62–66.
- [225] P. E. Palacio-Mancheno, A. I. Larriera, S. B. Doty, L. Cardoso, and S. P. Fritton. “3D Assessment of Cortical Bone Porosity and Tissue Mineral Density Using High-Resolution Micro-CT: Effects of Resolution and Threshold Method”. In: *Journal of Bone and Mineral Research* 29 (2014), pp. 142–150.
- [226] E. Parisini, P. Metrangolo, T. Pilati, G. Resnati, and G. Terraneo. “Halogen bonding in halocarbon–protein complexes: a structural survey”. In: *Chemical Society Reviews* 40.5 (2011), p. 2267. doi: 10.1039/c0cs00177e.
- [227] A. Parsa, N. Ibrahim, B. Hassan, A. Motroni, P. van der Stelt, and D. Wismeijer. “Influence of cone beam CT scanning parameters on grey value measurements at an implant site”. In: *Dentomaxillofacial Radiology* 42 (2013).
- [228] M. Pastrama, R. Blanchard, J. Clement, P. Pivonka, and C. Hellmich. “Modal analysis of nanoindentation data, confirming that reduced bone turnover may cause increased tissue mineralization/elasticity”. In: *Journal of the Mechanical Behavior of Biomedical Materials* 84 (2018), pp. 217–224.
- [229] M.-I. Pastrama, S. Scheiner, P. Pivonka, and C. Hellmich. “A mathematical multiscale model of bone remodeling, accounting for pore space-specific mechanosensation.” In: *Bone* 107 (2018), pp. 208–221.
- [230] G. Pelled, K. Tai, D. Sheyn, Y. Zilberman, S. Kumbar, L. Nair, C. Laurencin, D. Gazit, and C. Ortiz. “Structural and nanoindentation studies of stem cell-based tissue engineering bone.” In: *Journal of Biomechanics*. 40 (2007), pp. 399–411.
- [231] J. A. Pestruska and A. J. Hodge. “A subunit model for the tropocollagen macromolecule”. In: *Proceedings of the National Academy of Sciences of the United States of America* 51 (1964), pp. 871–876.
- [232] K. Pfefferkorn. “Ein Beitrag zur Bestimmung der Plastizität in Tonen und Kaolinen”. In: *Sprechaal* 57.25 (1924), pp. 297–299.
- [233] T. Pham, J. Kim, and S. Kim. “Estimating constitutive equation of structural steel using indentation”. In: *International Journal of Mechanical Sciences* 90 (2015), pp. 151–161.
- [234] T. Pham, J. Kim, and S. Kim. “Estimation of microstructural compositions in the weld zone of structural steel using nanoindentation”. In: *Journal of Constructional Steel Research* 99 (2014), pp. 121–128.

- [235] T. Pham and S. Kim. “Determination of mechanical properties in SM490 steel weld zone using nanoindentation and FE analysis”. In: *Journal of Constructional Steel Research* 114 (2015), pp. 314–324.
- [236] T. Pham and S. Kim. “Nanoindentation for investigation of microstructural compositions in SM490 steel weld zone”. In: *Journal of Constructional Steel Research* 110 (2015), pp. 40–47.
- [237] N. Phansalkar, S. More, A. Sabale, and M. Joshi. “Adaptive local thresholding for detection of nuclei in diversity stained cytology images”. In: *International Conference on Communications and Signal Processing* (2011), pp. 218–220.
- [238] P. Pivonka, P. R. Buenzli, S. Scheiner, C. Hellmich, and C. R. Dustan. “The influence of bone surface availability in bone remodelling — A mathematical model including coupled geometrical and biomechanical regulations of bone cells”. In: *Engineering Structures* 47 (2013), Pages 134–147.
- [239] M. G. Pontin, D. N. Moses, J. H. Waite, and F. W. Zok. “A nonmineralized approach to abrasion-resistant biomaterials”. In: *Proceedings of the National Academy of Sciences* 104.34 (2007), pp. 13559–13564.
- [240] K. Popper. *Conjectures and Refutations*. London, UK: Routledge., 1963.
- [241] K. Probst and S. Lees. “Visualization of crystal-matrix structure. In situ demineralization of mineralized turkey leg tendon and bone”. In: *Calcified Tissue International* 59 (1996), pp. 474–479.
- [242] T. Qu, D. Verma, M. Shahidi, and B. Pichler. “Mechanics of organic-inorganic biointerfaces—Implications for strength and creep properties.” In: *MRS Bulletin* 40 (2015), pp. 349–358.
- [243] M. el Quahabi, L. Daoudi, F. Hater, and N. Fagel. “Modified mineral phases during clay ceramic firing”. In: *Clay and Clay Minerals* 63.5 (2015), pp. 404–413.
- [244] r. “Patient-specific fracture risk assessment of vertebrae: A multiscale approach coupling X-ray physics and continuum micromechanics.” In: *International Journal for Numerical Methods in Biomedical Engineering* 32 (2016), e02760.
- [245] F. Raible, K. Tessmar-Raible, K. Osoegawa, P. Wincker, C. Jubin, G. Balavoine, D. Ferrier, V. Benes, P. De Jong, J. Weissenbach, et al. “Vertebrate-type intron-rich genes in the marine annelid *Platynereis dumerilii*”. In: *Science* 310.5752 (2005), pp. 1325–1326.
- [246] M. Raspanti, S. Guizzardi, R. Strocchi, and A. Ruggeri. “Different fibrillar architectures coexisting in haversian bone”. In: *Italian Journal of Anatomy and Embryology* 100 (1995), pp. 103–112.
- [247] G. M. Reeves, I. Sims, and J. C. Cripps. *Clay Materials Used in Construction*. Ed. by C. M. U. in Construction. The Geological Society, 2006.
- [248] G. A. P. Renders, L. Mulder, L. J. Van Ruijven, and T. M. G. J. Van Eijden. “Porosity of human mandibular condylar bone.” In: *Journal of Anatomy* 210 (2007), pp. 239–248.
- [249] G. Renders, L. Mulder, G. Langenbach, L. van Ruijven, and T. van Eijden. “Biomechanical effect of mineral heterogeneity in trabecular bone”. In: *Journal of Biomechanics* 41.13 (Sept. 2008), pp. 2793–2798. doi: 10.1016/j.jbiomech.2008.07.009.

- [250] J.-Y. Rho, L. Kuhn-Spearing, and P. Zioupos. “Mechanical properties and the hierarchical structure of bone.” In: *Medical Engineering and Physics* 20 (1998), pp. 92–102.
- [251] J. Rho, P. Zioupos, J. Currey, and G. Pharr. “Microstructural elasticity and regional heterogeneity in human femoral bone of various ages examined by nano-indentation.” In: *Journal of Biomechanics* 35 (2002), pp. 189–198.
- [252] M. P. Riccardi, B. Messiga, and P. Duminuco. “An approach to the dynamics of clay firing”. In: *Applied Clay Science* 15 (1999), pp. 393–409.
- [253] R. Riedl. “A Systems-Analytical Approach to Macro-Evolutionary Phenomena.” In: *The Quarterly Review of Biology* 52 (1977), pp. 351–370.
- [254] R. Riedl. *Order in Living Systems: A Systems Analysis of Evolution*. New York, USA: Wiley, 1978.
- [255] R. A. Robinson and S. R. Elliot. “The water content of Bone”. In: *The Journal of Bone and Joint Surgery* 39.1 (1957), pp. 167–188.
- [256] R. Rodriguez and I. Guitierrez. “Correlation between nanoindentation and tensile properties: Influence of the indentation size effect”. In: *Materials Science and Engineering A* 361 (2003), pp. 377–384.
- [257] E. Rokita, P. Chevallier, P. Mutsaers, Z. Tabor, and A. Wróbel. “Studies of crystal orientation and calcium distribution in trabecular bone.” In: *Nuclear Instruments and Methods in Physics Research Section B: Beam Interactions with Materials and Atoms* 240 (2005), pp. 69–74.
- [258] P. Roschger, H. S. Gupta, A. Berzlanovich, G. Ittner, D. W. Dempster, P. Fratzl, F. Cosman, R. Parisien M. and Lindsay, J. W. Nieves, and K. Klaushofer. “Constant mineralization density distribution in cancellous human bone.” In: *Bone* 32 (2003), pp. 316–323.
- [259] L. Roseti, V. Parisi, M. Petretta, C. Cavallo, G. Desando, I. Bartolotti, and B. Grigolo. “Scaffolds for Bone Tissue Engineering: State of the art and new perspectives.” In: *Materials Science and Engineering: C* 78 (2017), pp. 1246–1262.
- [260] G. Rouse and F. Pleijel. *Polychaetes*. Oxford university press, 2001.
- [261] K. Rudall. “The Chitin/Protein Complexes of Insect Cuticles”. In: *Advances in Insect Physiology*. Vol. 1. Elsevier, 1963, pp. 257–313. doi: 10.1016/s0065-2806(08)60177-0.
- [262] S. K. Saha, D. Wang, V. H. Nguyen, Y. Chang, J. S. Oakdale, and S.-C. Chen. “Scalable submicrometer additive manufacturing”. In: *Science* 366.6461 (Oct. 2019), pp. 105–109. doi: 10.1126/science.aax8760.
- [263] E. Sales, C. da Silva, S. Letichevsky, R. dos Santos, R. Leitao, C. dos Santos, L. de Oliveira, R. de Avelaz, M. Monteiro, R. Costa-Felix, S. Paciornik, and M. dos Anjos. “Chemical induced demineralization study in cortical bone.” In: *Journal of Instrumentation* 13 (2018), pp. C05010–C05010.
- [264] N. Sasaki, A. Tagami, T. Goto, M. Taniguchi, M. Nakata, and K. Hikichi. “Atomic force microscopic studies on the structure of bovine femoral cortical bone at the collagen fibril-mineral level”. In: *Journal of Materials Science: Materials in Medicine* 13 (2002), pp. 333–337.

- [265] J. Sauvola and M. Pietikäinen. “Adaptive document image binarization”. In: *Pattern Recognition* 33 (2000), pp. 225–236.
- [266] F. M. Savi, G. I. Brierly, J. Baldwin, C. Theodoropoulos, and M. A. Woodruff. “Comparison of Different Decalcification Methods Using Rat Mandibles as a Model.” In: *Journal of Histochemistry and Cytochemistry* 65 (2017), pp. 705–722.
- [267] H. Scheffé. *The analysis of variance*. New York, USA: John Wiley and Sons, INC., Oct. 1999.
- [268] S. Scheiner, V. Komlev, A. Gurin, and C. Hellmich. “Multiscale mathematical modeling in dental tissue engineering: towards computer-aided design of a regenerative system based on hydroxyapatite granules, focusing on early and mid-term stiffness recovery”. In: *Frontiers in Physiology* 7.383 (2016), pp. 1–18.
- [269] S. Scheiner, V. S. Komlev, and C. Hellmich. “Strength increase during ceramic biomaterial-induced bone regeneration: A micromechanical study.” In: *International Journal of Fracture* 202 (2016), pp. 217–235.
- [270] S. Scheiner, P. Pivonka, and C. Hellmich. “Poromechanics reveals that physiological bone strains induce osteocyte-stimulating lacunar pressure.” In: *Biomechanics and Modeling in Mechanobiology* 15 (2016), pp. 9–28.
- [271] S. Scheiner, R. Sinibaldi, B. Pichler, V. Komlev, C. Renghini, C. Vitale-Brovarone, F. Rustichelli, and C. Hellmich. “Micromechanics of bone tissue-engineering scaffolds, based on resolution error-cleared computer tomography.” In: *Biomaterials* 30 (2009), pp. 2411–2419.
- [272] C. Schneider, W. Rasband, and K. Eliceiri. “NIJ image to ImageJ: 25 years of image analysis”. In: *Nat Meth* 7 (2012), pp. 671–675.
- [273] P. Schneider, M. Meier, R. Wepf, and R. Müller. “Towards quantitative 3D imaging of the osteocyte lacuno-canalicular network.” In: *Bone* 47 (2010), pp. 848–858.
- [274] P. Schneider, M. Stauber, R. Voide, M. Stampanoni, L. R. Donahue, and R. Müller. “Ultrastructural Properties in Cortical Bone Vary Greatly in Two Inbred Strains of Mice as Assessed by Synchrotron Light Based Micro- and Nano-CT.” In: *Journal of Bone and Mineral Research* 22 (2007), pp. 1557–1570.
- [275] M. R. Scholfield, M. C. Ford, A.-C. C. Carlsson, H. Butta, R. A. Mehl, and P. S. Ho. “Structure–Energy Relationships of Halogen Bonds in Proteins”. In: *Biochemistry* 56.22 (Apr. 2017), pp. 2794–2802. doi: 10.1021/acs.biochem.7b00022.
- [276] R. Schröder. “Influences on development of thermal and residual stresses in quenched steel cylinders of different dimensions”. In: *Materials Science and Technology* 1 (1985), pp. 754–764.
- [277] P. G. Schroeder. *Chaetae*. Springer, 1984, pp. 297–309.
- [278] F. A. Schulte, F. M. Lambers, G. Kuhn, and R. Müller. “In vivo micro-computed tomography allows direct three-dimensional quantification of both bone formation and bone resorption parameters using time-lapsed imaging.” In: *Bone* 48 (2011), pp. 433–442.
- [279] L. G. Schultz. “Quantitative Interpretation of Mineralogical Composition from X-ray and Chemical Data for the Pierre Shale”. In: *Professional Paper* 391-C (1964).



- [280] D. W. Scott. “Scott’s rule”. In: *Wiley Interdisciplinary Reviews: Computational Statistics* 2.4 (June 2010), pp. 497–502. DOI: 10.1002/wics.103.
- [281] E. R. Segnit and C. A. Anderson. “Scanning electron microscopy of fired illite”. In: *Transactions and Journal of the British Ceramics Society* 71.3 (1972), pp. 85–88.
- [282] A. Seilacher. “Divaricate patterns in pelecypod shells.” In: *Lethaia* 5 (1972), pp. 325–343.
- [283] S. Seltzer. “Calculation of Photon Mass Energy-Transfer and Mass Energy-Absorption Coefficients”. In: *Radiation Research* 136 (1993), pp. 147–170.
- [284] K. M. Shah, J. C. H. Goh, R. Karunanithy, S. L. Low, S. Das De, and K. Bose. “Effect of Decalcification on Bone Mineral Content and Bending Strength of Feline Femur.” In: *Calcified Tissue International* 56 (1995), pp. 78–82.
- [285] R. Shahar and M. Dean. “The enigmas of bone without osteocytes.” In: *BoneKEY* 2 (2013).
- [286] S. S. Shapiro and M. B. Wilk. “An analysis of variance test for normality (complete samples)”. In: *Biometrika* 52.3-4 (Dec. 1965), pp. 591–611. doi: 10.1093/biomet/52.3-4.591.
- [287] S. S. Shapiro, M. B. Wilk, and H. J. Chen. “A Comparative Study of Various Tests for Normality”. In: *Journal of the American Statistical Association* 63.324 (Dec. 1968), pp. 1343–1372. doi: 10.1080/01621459.1968.10480932.
- [288] A. Shipov, P. Zaslansky, H. Riesemeier, G. Segev, A. Atkins, and R. Shahar. “Unremodeled endochondral bone is a major architectural component of the cortical bone of the rat (*Rattus norvegicus*).” In: *Journal of Structural Biology*. 183 (2013), pp. 132–140.
- [289] J. G. Skedros, T. R. Grunander, and M. W. Hamrick. “Spatial Distribution of Osteocyte Lacunae in Equine Radii and Third Metacarpals: Considerations for Cellular Communication, Microdamage, Detection and Metabolism.” In: *Cell Tissue Organs* 180 (2005), pp. 215–236.
- [290] P. Soille and L. M. Vincent. “Determining watersheds in digital pictures via flooding simulations”. In: *Proc. SPIE* 1360 (1990), pp. 240–250.
- [291] R. R. Sokal and F. J. Rohlf. *Biometry: The Principles and Practice of Statistics in Biological Research*. W. H. Freeman, 1981.
- [292] A. M. M. Soltan, K. Pöhler, F. Fuchs, F. A. El-Raouf, B. A.-H. El-Kaliouby, A. Koenig, and H. Pöllmann. “Clay-bricks from recycled rock tailings”. In: *Ceramics International* 42 (2016), pp. 16685–16696.
- [293] N. Soltan, C. E. Kawalilak, D. M. Cooper, S. A. Kontulainen, and J. D. Johnston. “Cortical porosity assessment in the distal radius: A comparison of HR-pQCT measures with Synchrotron-Radiation micro-CT-based measures.” In: *Bone* 120 (2019), pp. 439–445.
- [294] L. Sorelli, G. Constantinides, F.-J. Ulm, and F. Toutlemonde. “The nano-mechanical signature of Ultra High Performance Concrete by statistical nanoindentation techniques”. In: *Cement and Concrete Research* 38 (2008), pp. 1447–1456.

- [295] A. V. Srinivasan, G. K. Haritos, and F. L. Hedberg. “Biomimetics: Advancing Man-Made Materials Through Guidance From Nature”. In: *Applied Mechanics Reviews* 44.11 (Nov. 1991), pp. 463–482. doi: 10.1115/1.3119489.
- [296] M. A. Stephens. “EDF Statistics for Goodness of Fit and Some Comparisons”. In: *Journal of the American Statistical Association* 69.347 (Sept. 1974), pp. 730–737. doi: 10.1080/01621459.1974.10480196.
- [297] V. Storch. “Contributions of comparative ultrastructural research to problems of invertebrate evolution”. In: *American Zoologist* 19.2 (1979), pp. 637–646.
- [298] S. Stover, R. Pool, R. B. Martin, and J. Morgan. “Histological features of the dorsal cortex of the third metacarpal bone mid-diaphysis during postnatal growth in thoroughbred horses.” In: *Journal of Anatomy* 181 (1992), pp. 455–469.
- [299] R. J. Sundberg and R. B. Martin. “Interactions of histidine and other imidazole derivatives with transition metal ions in chemical and biological systems”. In: *Chemical Reviews* 74.4 (Aug. 1974), pp. 471–517. doi: 10.1021/cr60290a003.
- [300] P. Suquet. *Continuum Micromechanics*. Vol. 377. CISM Courses and Lectures. Springer Verlag, Wien New York, 1997.
- [301] M. Suzuki, Y. Ogawa, A. Kawano, A. Hagiwara, H. Yamaguchi, and H. Ono. “Rapid prototyping of temporal bone for surgical training and medical education.” In: *Acta Oto-Laryngologica* 124 (2004), pp. 400–402.
- [302] L.-E. Svensson. *Control of Microstructures and Properties in Steel Arc Welds*. CRC Press, Boca Raton, FL, 1994.
- [303] K. Szluzak, V. Vass, P. Hasslinger, J. Jaroszewicz, A. Dejaco, J. Idaszek, S. Scheiner, C. Hellmich, and W. Swieszkowski. “X-ray physics-based CT-to-composition conversion applied to a tissue engineering scaffold, enabling multiscale simulation of its elastic behavior.” In: *Materials Science and Engineering: C* 95 (2019), pp. 389–396.
- [304] G. I. Taylor. “The mechanism of plastic deformation of crystals. Part I.—Theoretical”. In: *Proceedings of the Royal Society of London. Series A, Containing Papers of a Mathematical and Physical Character* 145.855 (July 1934), pp. 362–387. doi: 10.1098/rspa.1934.0106.
- [305] E. Tilic and T. Bartolomaeus. “Structure, function and cell dynamics during chaetogenesis of abdominal uncini in Sabellaria alveolata (Sabellariidae, Annelida)”. In: *Zoological letters* 2.1 (2016), p. 1.
- [306] E. Tilic, J. von Döhren, B. Quast, P. Beckers, and T. Bartolomaeus. “Phylogenetic significance of chaetal arrangement and chaetogenesis in Maldanidae (Annelida)”. In: *Zoomorphology* 134.3 (2015), pp. 383–401.
- [307] P. Timmins and J. Wall. “Bone Water.” In: *Calcified Tissue Research* 23 (1977), pp 1–5.
- [308] M. S. Tite, V. Kilikoglou, and G. Vekinis. “Strength, toughness and thermal shock resistance of ancient ceramics, and their influence on technological choice”. In: *Archaeometry* 43.3 (2001), pp. 301–324.
- [309] M. S. Tite and Y. Maniatis. “Examination of Ancient Pottery using the Scanning Electron Microscope”. In: *Nature* 227 (1975).

- [310] Y. Tohno, S. Tohno, M. Utsumi, T. Minami, M. Ichii, Y. Okazaki, F. Nishiwaki, Y. Moriwake, T. Naganuma, M. Yamada, and T. Araki. “Age-Independent Constancy of Mineral Contents in Human Vertebra and Auditory Ossicle.” In: *Biological Trace Element Research* 59 (1997), pp. 167–175.
- [311] G. Totten, M. Howes, and T. Inoue, eds. *Handbook of Residual Stress and Deformation of Steel*. ASM International, Materials Park, OH, 2002.
- [312] K. Traoré and P. Blanchart. “Structural transformation of a kaolinite and calcite mixture to gehlenite and anorthite”. In: *Journal of Materials Research* 18.2 (2002), pp. 475–481.
- [313] K. Traoré, T. S. Kabré, and P. Blanchart. “Gehlenite and anorthite crystallisation from kaolinite and calcite mix”. In: *Ceramics International* 29 (2003), pp. 377–383.
- [314] V. Turov, V. Gun’ko, V. Zarko, R. Leboda, M. Jablonski, M. Gorzelak, and E. Jagiello-Wojtowicz. “Weakly and strongly associated nonfreezable water bound in bones.” In: *Colloids and Surfaces B: Interfaces* 48 (2006), pp. 167–175.
- [315] B. Tymrak, M. Kreiger, and J. Pearce. “Mechanical properties of components fabricated with open-source 3-D printers under realistic environmental conditions”. In: *Materials & Design* 58 (June 2014), pp. 242–246. doi: 10.1016/j.matdes.2014.02.038.
- [316] G. Tzschichholz, G. Steinborn, M. P. Hentschel, A. Lange, and P. Klobes. “Characterisation of porous titania yttrium oxide compounds by mercury intrusion porosimetry and X-ray refractometry”. In: *Journal of Porous Materials* 18 (2011), pp. 83–88.
- [317] F.-J. Ulm, M. Vandamme, C. Bobko, J. Ortega, K. Tai, and C. Ortiz. “Statistical indentation techniques for hydrated nanocomposites: concrete, bone, and shale”. In: *Journal of the American Ceramic Society* 90 (2007), pp. 2677–2692.
- [318] M. J. Urist, R. J. DeLange, and G. Finerman. “Bone cell differentiation and growth factors”. In: *Science* 220 (1983), pp. 680–686.
- [319] A. Valentinitich, J. M. Patsch, A. J. Burghardt, T. M. Link, S. Majumdar, L. Fischer, C. Schueller-Weidekamm, H. Resch, F. Kainberger, and G. Langs. “Computational identification and quantification of trabecular microarchitecture classes by 3-D texture analysis-based clustering.” In: *Bone* 54 (2013), pp. 133–140.
- [320] L. J. Vandeperre, J. Wang, and W. J. Clegg. “Effects of porosity on the measured fracture energy of brittle materials”. In: *Philosophical Magazine* (2004).
- [321] V. Vass, C. Morin, S. Scheiner, and C. Hellmich. “Review of “Universal” Rules Governing Bone Composition, Organization, and Elasticity Across Organizational Hierarchies.” In: *Multiscale Mechanobiology of Bone Remodeling and Adaptation*. Ed. by P. Pivonka. Vol. 578. CISM International Centre for Mechanical Sciences (Courses and Lectures). Springer Nature, June 2018, pp. 175–229.
- [322] M. Viana, P. Jouannin, C. Pontier, and D. Chulia. “About pycnometric density measurements”. In: *Talanta* 57 (2002), pp. 583–593.
- [323] A. Viani, R. Ševčík, M.-S. Appavou, and A. Radulescu. “Evolution of fine microstructure during firing of extruded clays: A small angle neutron scattering study”. In: *Applied Clay Science* 166 (2018), pp. 1–8.

- [324] C. Vitale-Brovarone, E. Verné, L. Robiglio, P. Appendino, F. Bassi, G. Martinasso, G. Muzio, and R. Canuto. “Development of glass–ceramic scaffolds for bone tissue engineering: Characterisation, proliferation of human osteoblasts and nodule formation.” In: *Acta Biomaterialia* 3 (2007), pp. 199–208.
- [325] J. Vuong and C. Hellmich. “Bone fibrillogenesis and mineralization: Quantitative analysis and implications for tissue elasticity.” In: *Journal of Theoretical Biology* 287 (2011), pp. 115–130.
- [326] G. Wagner and M. Laubichler. “Rupert Riedl and the re-synthesis of evolutionary and developmental biology: Body plans and evolvability.” In: *Journal of Experimental Zoology* 302B (2004), pp. 92–102.
- [327] X. Wang, X. Yang, Z. Guo, Y. Zhou, and H. Song. “Nanoindentation Characterization of Mechanical Properties of Ferrite and Austenite in Duplex Stainless Steel”. In: *Advanced Materials Research* 26-28 (2007), pp. 1165–1170.
- [328] Y. Wang, S. Von Euw, F. M. Fernandes, S. Cassaignon, M. Selmane, G. Laurent, G. Pehau-Arnaudet, C. Coelho, L. Bonhomme-Coury, M.-M. Giraud-Guille, F. Babonneau, T. Azaïs, and N. Nassif. “Water-mediated structuring of bone apatite.” In: *Nature Materials*. 12 (2013), pp. 1144–1153.
- [329] S. Weiner and H. Wagner. “The material bone: Structure-Mechanical Function Relations”. In: *Annual Review of Materials Science* 28 (1998), pp. 271–298.
- [330] R. Weiss and W. N. “Studies on the biology of fish bone. III. Ultrastructure of osteogenesis and resorption in osteocytic (cellular) and anosteocytic (acellular) bones.” In: *Calcified Tissue International* 28 (1979), pp. 43–56.
- [331] W. Weißbach. *Werkstoffkunde: Strukturen, Eigenschaften, Prüfung [Materials Science: Structures, Properties, Testing]*. 18th. In German. Vieweg+Teubner, Wiesbaden, 2012.
- [332] U. Wolfram, W. H. J., and P. Zysset. “Rehydration of vertebral trabecular bone: influences on its anisotropy, its stiffness and the indentation work with a view to age, gender and vertebral level.” In: *Bone* 46 (2010), pp. 348–354.
- [333] D. Zahn and O. Hochrein. “Computational study of interfaces between hydroxyapatite and water.” In: *Physical Chemistry Chemical Physics*. 5 (2003), pp. 4004–4007.
- [334] A. Zaoui. “Continuum micromechanics: survey”. In: *Journal of Engineering Mechanics (ASCE)* 128.8 (2002), pp. 808–816.
- [335] L. Zelaya-Lainez, H. Kariem, W. Nischkauer, A. Limbeck, and C. Hellmich. ““Variances” and “in-variances” in hierarchical porosity and composition, across femoral tissues from cow, horse, ostrich, emu, pig, rabbit, and frog”. In: *Materials Science and Engineering: C* 117 (Dec. 2020), p. 111234. doi: 10.1016/j.msec.2020.111234.
- [336] D. Zhang, S. Weinbaum, and S. Cowin. “Estimates of the Peak Pressures in Bone Pore Water”. In: *Journal of Biomechanical Engineering* 120 (1998), pp. 697–703.
- [337] J. Zhou, G. Ye, and K. van Breugel. “Characterization of pore structure in cement-based materials using pressurization–depressurization cycling mercury intrusion porosimetry (PDC-MIP)”. In: *Cement and Concrete Research* 40 (2010), pp. 1120–1128. doi: 10.1016/j.cemconres.2010.02.011. URL: <http://dx.doi.org/10.1016/j.cemconres.2010.02.011>.

- [338] L. Zhu, B. Xu, H. Wang, and C. Wang. “Measurement of residual stress in quenched 1045 steel by the nanoindentation method”. In: *Materials Characterization* 61 (2010), pp. 1359–1362.
- [339] W. Zhu, J. Hughes, and C. Bicanic N.and Pearce. “Nanoindentation mapping of mechanical properties of cement paste and natural rocks”. In: *Materials Characterization* 58 (2007), pp. 1189–1198.
- [340] T. Zubkova, I. Yakovleva, L. Kar’kina, and I. Veretennikova. “Study of the Hardness and Elastic Modulus of Cementite in the Structure of Granular Pearlite by the Nano-Indentation Method”. In: *Metal Science and Heat Treatment* 56 (2014), pp. 330–335.

# Chapter 7

## Curriculum Vitae

---

### Personal Information

Name: **Luis Zelaya-Lainez**  
Date of birth: July 31<sup>st</sup>, 1987  
Nationality: Honduras  
Current address: Brünner Straße 55/3/309, 1210 Vienna, Austria

### Education

Enrolled: Doctor of Philosophy (Ph.D.) program **since 2016**  
Institute for Mechanics of Materials and Structures  
Vienna University of Technology (TU WIEN)  
Vienna, Austria.

Master in Science (MSc.) **2013-2016**  
Master's Degree in Biomedical Engineering<sup>1</sup>  
Vienna University of Technology (TU WIEN)  
Vienna, Austria.

Master in Science (MSc.) **2010-2012**  
Master's Degree in Occupational safety and health<sup>2</sup>  
Polytechnic University of Valencia (UPV)  
Valencia, Spain.

---

<sup>1</sup>Thesis: "Allocation of Bone Fluid Throughout the Hierarchical Structure of Bone: Multi-Technique Analysis on Bovine Femur." Submitted at the Institute for Mechanics of Materials and Structures.

<sup>2</sup>Thesis: "Dosimetric analysis and investigation of shielding of a radioisotope laboratory using the Monte Carlo based code MCNP5. Application to occupational risk assessment." Submitted at the Department of Chemical and Nuclear engineering.

- Enrolled: Master in Science (MSc.) program **2010-**  
 Master's Degree Program in Electronic Engineer  
 Polytechnic University of Valencia (UPV)  
 Valencia, Spain.
- Bachelor in Science (BSc.) **2005-2009**  
 Licentiate degree in Industrial Engineering<sup>3</sup>  
 Central American Technological University  
 (UNITEC)  
 Tegucigalpa, Honduras.
- High School Diploma **1992-2005**  
 La Estancia School  
 Tegucigalpa, Honduras.

## Awards

- Young Researcher Award **2016**  
 33rd Danubia Adria Symposium on Advances  
 in Experimental Mechanics  
 Portorož, Eslovenia
- Committee Award **2003**  
 Proceedings of the Organization of American  
 States  
 Harvard Association Cultivating Inter-  
 American Democracy (HACIA Democracy)<sup>4</sup>  
 Summit of the Americas  
 Guatemala City, Guatemala

## Work Experience

- University Assistant **since 2016**  
 Institute for Mechanics of Materials and Structures  
 Vienna University of Technology (TU WIEN)  
 Vienna, Austria

<sup>3</sup>Five years engineering degree with a mechanical orientation.

<sup>4</sup>Organization based at Harvard University, Cambridge, USA.

Student Assistant **2011-2012**  
 IBERTEL Project  
 Polytechnic University of Valencia (UPV)  
 Valencia, Spain

## Scientific Activities Abroad

ERICA NMR Workshop and Training School. **01/2020**  
 Engineered Calcium-Silicate-Hydrates for Applications (ERICA)<sup>5</sup>.  
 University of Surrey  
 Guildorf, UK

Short Term Scientific Mission. **01/2019**  
 ID17 - Biomedical Beamline  
 European Synchrotron Radiation Facility (ESRF)  
 Grenoble, France

Short Term Scientific Mission. **11/2018**  
 ID17 - Biomedical Beamline  
 European Synchrotron Radiation Facility (ESRF)  
 Grenoble, France

The 2<sup>nd</sup> School of Cost Action Bioneca. **10/2018**  
 Cost Action: CA16122 “Biomaterials and advanced physical techniques for regenerative cardiology and neurology”  
 Dubrovnik, Croatia

Research stay **02/2017**  
 Scientific and Technological Cooperation.  
 614852 WTZ SERBIEN<sup>6</sup>  
 University of Kragujevac  
 Kragujevac, Serbia

<sup>5</sup> A project funded by the European Union under the Horizon 2020

<sup>6</sup> Funded by the Austrian Agency for International Cooperation in Education and Research (oead)



## Scientific Dissemination

### Publications in Scientific Journals

L Zelaya-Lainez, H Kariem, W Nischkauer, A Limbeck, C Hellmich. “Variances” and “invariances” in hierarchical porosity and composition, across femoral tissues from cow, horse, ostrich, emu, pig, rabbit, and frog. *Materials Science and Engineering: C*. 117, 111234, (2020). <https://doi.org/10.1016/j.msec.2020.111234>.

L Zelaya-Lainez, G Balduzzi, O Lahayne, KN Ikeda, F Raible, C Herzig, W Nischkauer, A Limbeck, C Hellmich. Deciphering a Biological 3D Printing System: Nanoindentation on Jaws of *Platynereis Dumerilii*. *Submitted: JOM*, (2021).

V Jagsch, P Kuttke, O Lahayne, L Zelaya-Lainez, S Scheiner, C Hellmich. Multiscale and multitechnique investigation of the elasticity of grooved rail steel. *Construction and Building Materials*, 238, 117768, (2020). <https://doi.org/10.1016/j.conbuildmat.2019.117768>.

T Buchner, T Kiefer, L Zelaya-Lainez, W Gaggl, T Konegger, J Füssl. A multitechnique, quantitative characterization of the pore space of fired bricks made of five clayey raw materials used in European brick industry. *Applied Clay Science*, (2020). <https://doi.org/10.1016/j.clay.2020.105884>.

T Buchner, T Kiefer, W Gaggl, L Zelaya-Lainez, J Füssl. A complete automated quantitative and morphometrical characterization of material phases of fired bricks from five different clayey raw materials based on information from Scanning Electron Microscopy, Energy Dispersive X-ray Spectroscopy and Powder X-ray Diffraction. *Under review: Construction and Building Materials*, (2020).

G Balduzzi, L Zelaya-Lainez, G Hochreiner, C Hellmich. Dog-bone samples may not provide direct access to the longitudinal tensile strength of clear-wood. *Accepted: The Open Civil Engineering Journal*, (2020)

### Conference Papers

L Zelaya-Lainez, O Lahayne, G Balduzzi, C Hellmich. Micromechanics of Non-embedded spruce wood: Novel polishing and indentation protocol. *36th Danubia Adria Symposium on Advances in Experimental Mechanics*, (2019). ISBN: 978-802610876-4.

L Zelaya-Lainez, G Balduzzi, KN Ikeda, F Raible, C Hellmich. *Platynereis dumerilii* chaetae: Mechanical loading estimation from kinematics in larva stage. *36th Danubia Adria Symposium on Advances in Experimental Mechanics*, (2019). ISBN: 978-802610876-4.

### Conference Presentations and Posters

L Zelaya-Lainez, H Kariem, W Nischkauer, A Limbeck, C Hellmich. Average of Extracellular Bone Tissue Composition is Invariant Across Mammalian Femora Tissues. *Oral presentation at the Biennial Meeting ViCEM - Vienna Center for Engineering in Medicine in Vienna, Austria, (2019)*

L Zelaya-Lainez, G Balduzzi, O Lahayne, C Hellmich. Micromechanics of Non-Embedded Spruce Wood: Novel Polishing and Indentation Protocol. *Poster presentation at the 36th Danubia-Adria Symposium on Advanced in Experimental Mechanics in Plzen, Czech Republic, (2019).*

L Zelaya-Lainez, G Balduzzi, O Lahayne, KN Ikeda, F Raible, C Hellmich. Platynereis Dumerilii Chaetae: Mechanical Loading Estimation from Kinematics in Larva Stage. *Poster presentation at the 36th Danubia-Adria Symposium on Advanced in Experimental Mechanics in Plzen, Czech Republic, (2019).*

KN Ikeda, L Zelaya-Lainez, G Balduzzi, C Hellmich, F Raible. Genetic and Cell Biological Control of 3D Printing in the Marine Organism Platynereis Dumerilii. *Poster presentation at the 25th Congress of the European Society of Biomechanics (ESB 2019) in Vienna, Austria, (2019).*

L Zelaya-Lainez, H Kariem, W Nischkauer, A Limbeck, C Hellmich. Variances and In-Variances in Hierarchical Porosity and Composition, Across Different Femoral Tissues. *Oral presentation at the 25th Congress of the European Society of Biomechanics (ESB 2019) in Vienna, Austria, (2019).*

L Zelaya-Lainez, G Balduzzi, O Lahayne, KN Ikeda, F Raible, C Hellmich. Deciphering the Mechanical Function of the Bristles from Platynereis Dumerilii Larvae: A Kinematic Approach. *Oral presentation at the Engineering Mechanics Institute 2019 Conference at the California Institute of Technology (CALTECH) in Pasadena, USA, (2019).*

L Zelaya-Lainez. Experimental Determination of Chemical, Mechanical, and Micro-Structural Properties of Biomaterials, by Example of Bone and Chitin. *Oral presentation at the biomaterials and advanced physical techniques for regenerative cardiology and neurology COST Action in Dubrovnik, Croatia, (2018).*

L Zelaya-Lainez, H Kariem, W Nischkauer, A Limbeck, C Hellmich. Average of Extracellular Bone Tissue Composition is Invariant Across Mammalian Femora Tissues. *Poster presentation at the 8th World Congress of Biomechanics in Dublin, Ireland, (2018).*

L Zelaya-Lainez, H Kariem, W Nischkauer, A Limbeck, C Hellmich. Variances and In-Variances in Composition and Micro-Structure, Across Femoral Tissues from Cow, Horse, Emu, Frog, Ostrich, Pig, and Rabbit. *Oral presentation at the Engineering Mechanics Institute Conference 2018 at the Massachusetts Institute of Technology (MIT), in Cambridge, USA, (2018).*

L Zelaya-Lainez, A Kurfürst, T Sustersic, A Vulović, N Filipovic, C Hellmich. Modelling of innovative hearing implant devices using bone conduction sound. *Oral presentation at the University of Kragujevac in Kragujevac, Serbia, (2017).*

L Zelaya-Lainez, H Kariem, W Nischkauer, A Limbeck, C Hellmich. The Allocation of Bone Fluid in Bovine Cortical Bone Utilizing a Multi-Technique Analysis. *Poster presentation at the 33rd Danubia Adria Symposium on Advances in Experimental Mechanics in Portorož, Eslovenia, (2016).*

L Zelaya-Lainez. Committee participation at the Proceedings of the Organization of American States from the Harvard Association Cultivating Inter-American Democracy (HACIA Democracy) Summit of the Americas in Guatemala City, Guatemala, (2003).